

Primer on nuclear effects in neutrino interactions

**Artur M. Ankowski
SLAC National Accelerator Laboratory**

Fermilab, November 7, 2017

Outline

1) **Introduction**

- Neutrino interactions in a nutshell
- Accurate neutrino-energy reconstruction requires an accurate modeling of nuclear effects

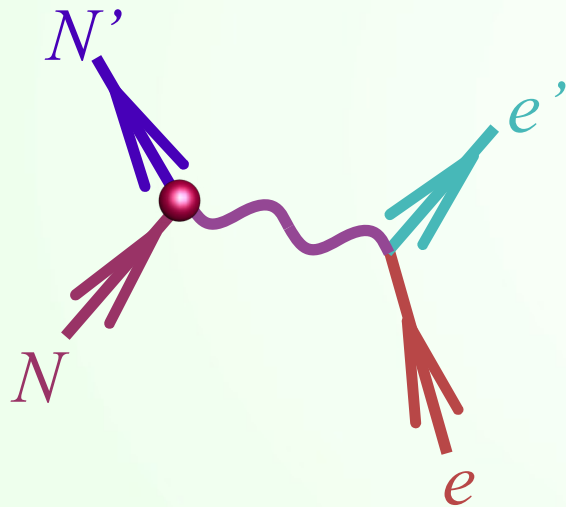
2) **Impulse approximation**

- Why to test nuclear models using electron scattering data
- Fermi gas model
- Shell model
- Spectral function approach
- Final-state interactions in the spectral function approach

3) **Summary**

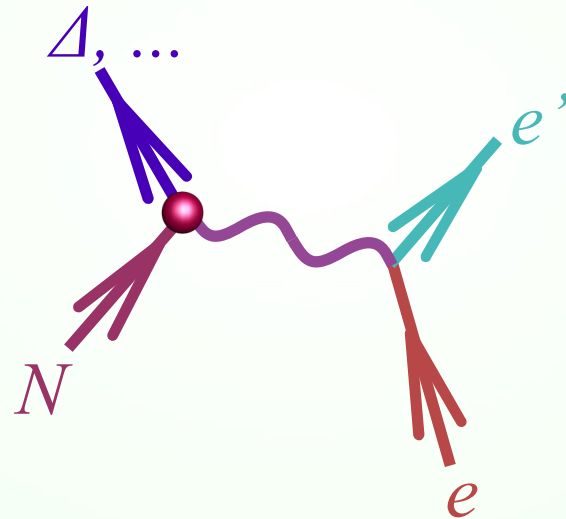
Electron scattering on a free nucleon

elastic
scattering



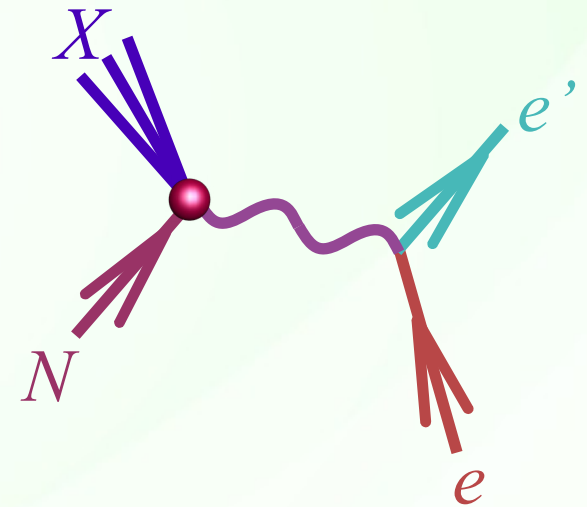
$$x=1$$

resonance
excitation



energy transfer
 ~ 300 MeV

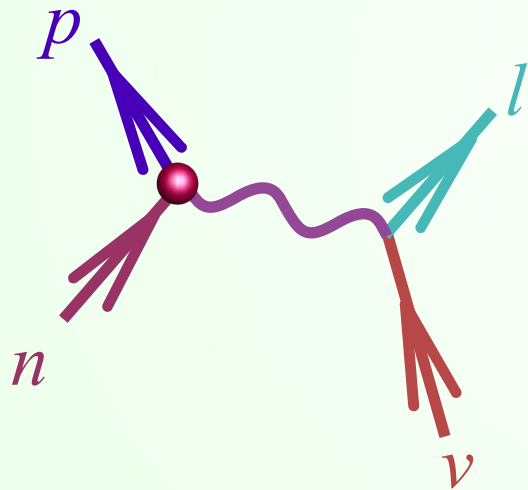
deep inelastic
scattering



$$x \ll 1$$

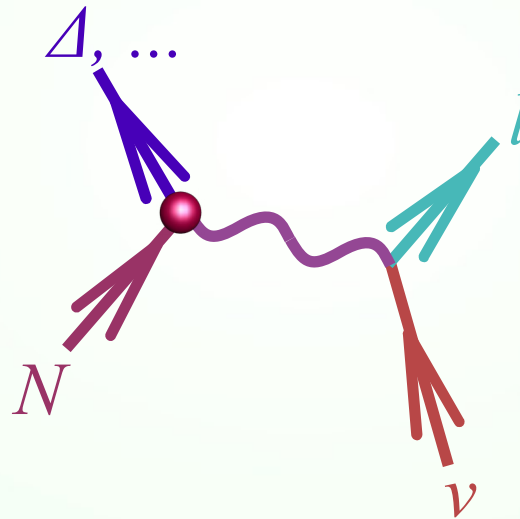
Neutrino CC scattering on a free nucleon

quasielastic scattering



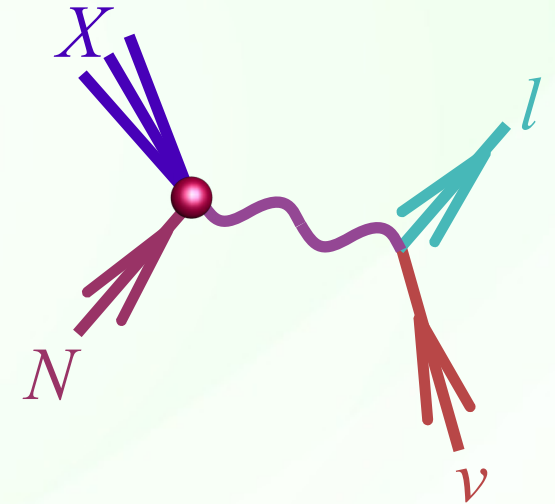
$$x=1$$

resonance excitation



energy transfer
 ~ 300 MeV

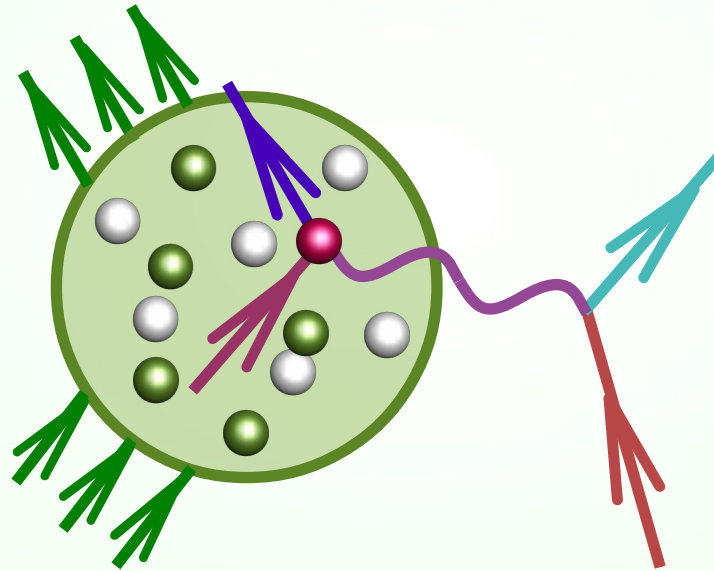
deep inelastic scattering



$$x \ll 1$$

Terminology difference

The processes $\nu + N \rightarrow \nu' + N'$ and $e + N \rightarrow e' + N'$ for bound nucleons are called



elastic scattering
[neutrino physics]

quasielastic scattering
[nuclear physics & (e,e')]

(Quasi)elastic scattering

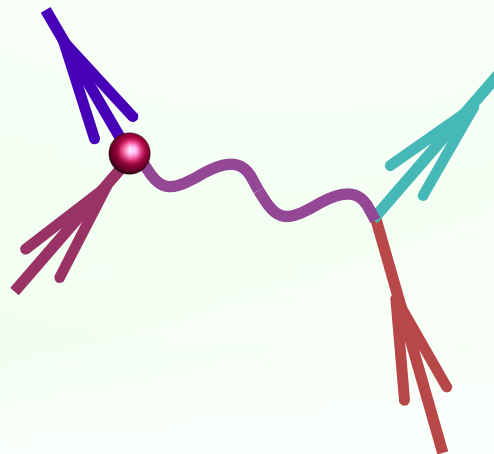
In $e + N \rightarrow e + N'$ and $\nu + n \rightarrow l + p$ on **free nucleons** for a fixed beam energy, given scattering angle θ corresponds to a single value of energy transfer ω .

(Quasi)elastic condition

$$Q^2 = 2 M \omega$$

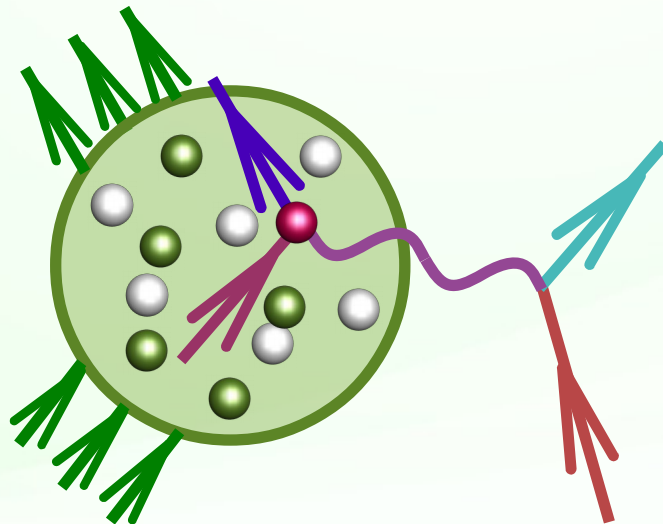
Lepton kinematics ($m=0$)

$$Q^2 = 2 E (E - \omega) (1 - \cos \theta)$$



(Quasi)elastic scattering

In a **nucleus**, nucleons have an energy distribution and undergo Fermi motion. Even for a fixed beam energy, given scattering angle corresponds to a range of energy transfers.



- **Free nucleon**

$$E_p'^2 - \mathbf{p}'^2 = M^2$$

$$(M + \omega)^2 - \mathbf{q}^2 = M^2$$

$$2 M \omega = Q^2$$

$$Q^2 / (2 M \omega) = 1$$

- **Bound nucleon**

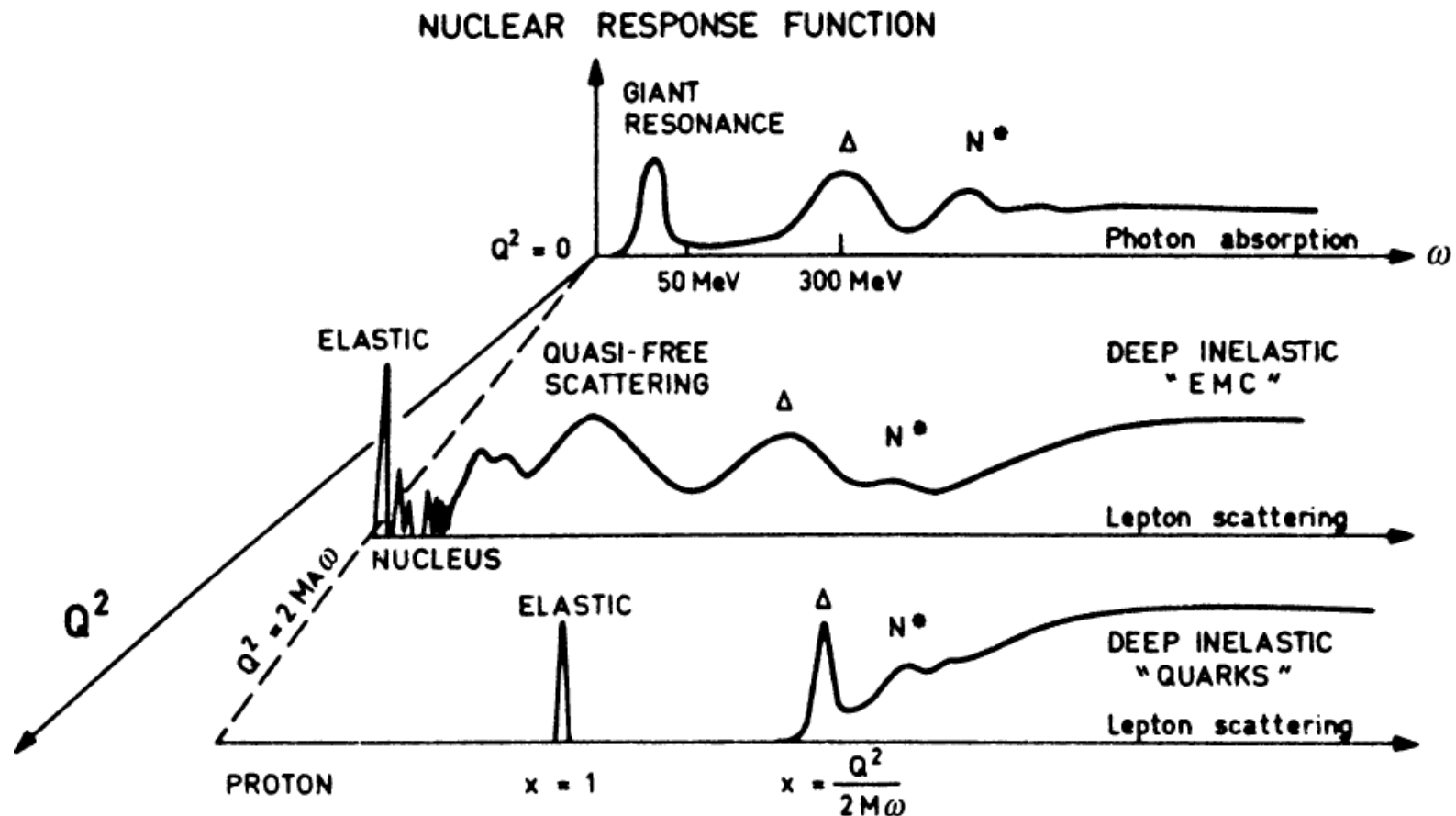
$$E_p'^2 - \mathbf{p}'^2 = M^2$$

$$(M - E + \omega)^2 - (\mathbf{p} + \mathbf{q})^2 = M^2$$

$$2 M \omega + E [E - 2(\omega + M)] - \mathbf{p}(\mathbf{p} + 2\mathbf{q}) = Q^2$$

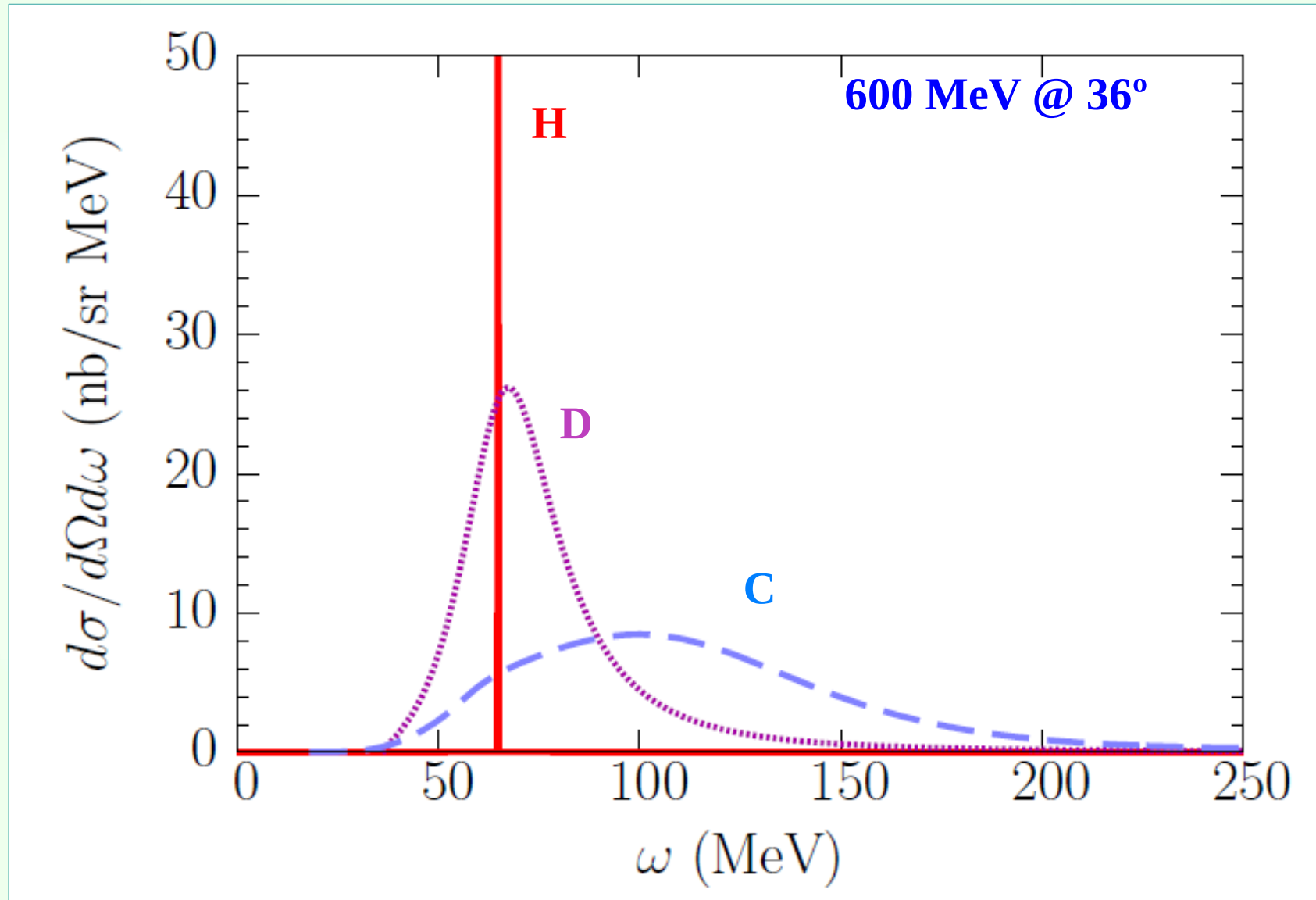
$$Q^2 / (2 M \omega) = 1 + \frac{E}{M} (\dots) + \frac{\mathbf{p}}{M} (\dots)$$

Free nucleon vs. bound nucleon



Frois, NP 434, 57c (1985)

Target dependence

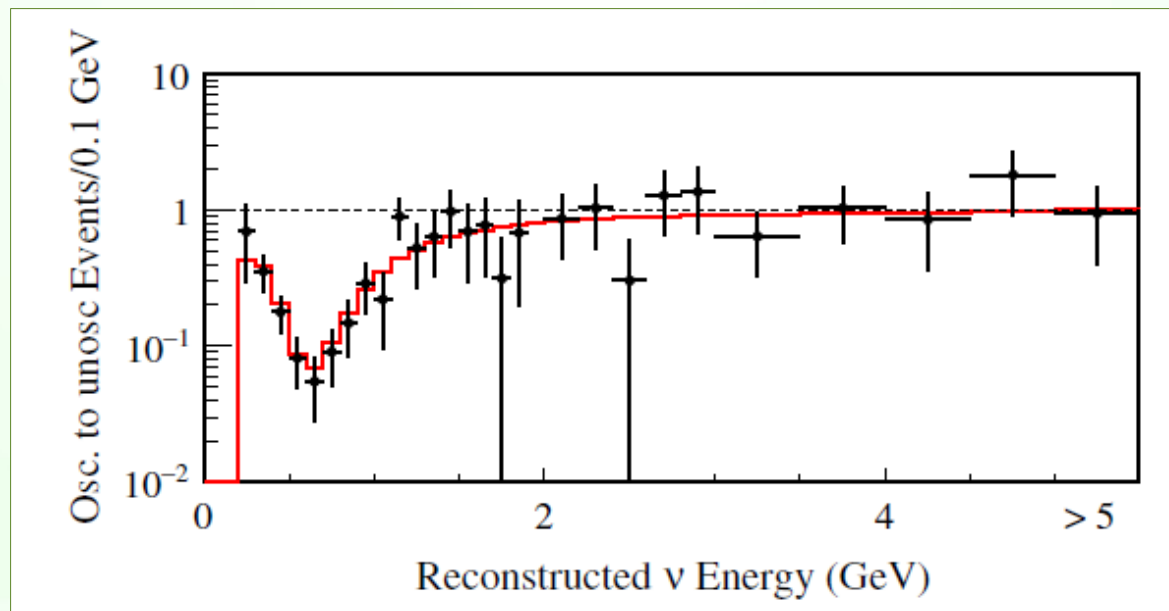


Neutrino oscillations in a nutshell

In the simplest case of 2 flavors

$$P(\nu_\alpha \rightarrow \nu_\alpha) = 1 - \sin^2 2\theta \sin^2 \left(\frac{\Delta m^2 L}{4E_\nu} \right)$$

Example [K. Abe *et al.* (T2K Collaboration), PRD 91, 072010 (2015)]

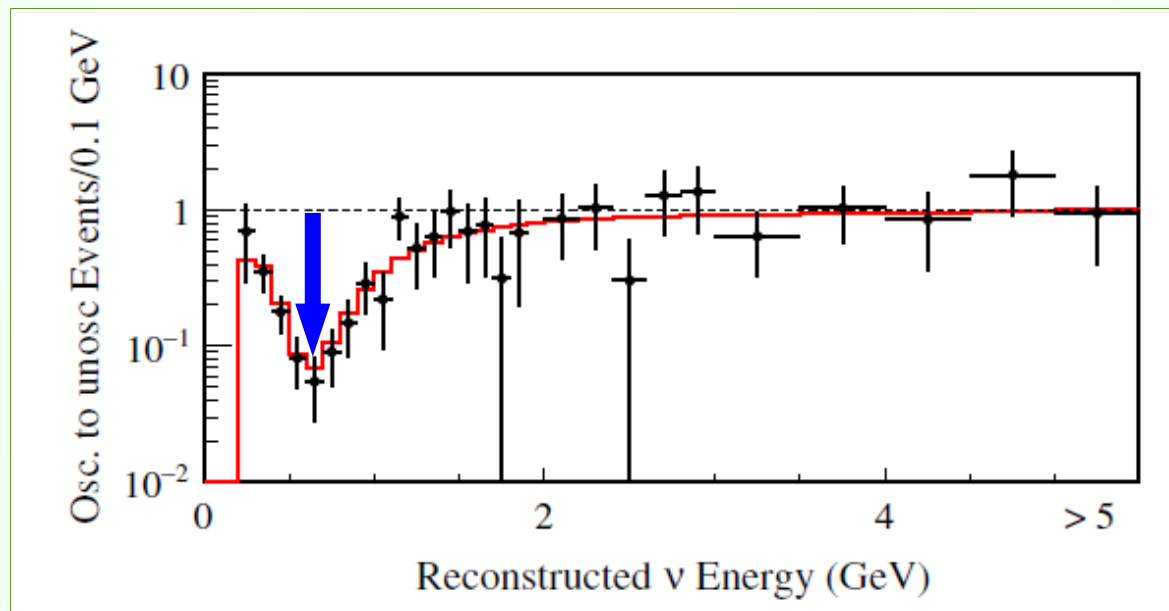


Neutrino oscillations in a nutshell

In the simplest case of 2 flavors

$$P(\nu_\alpha \rightarrow \nu_\alpha) = 1 - \boxed{\sin^2 2\theta} \sin^2 \left(\frac{\Delta m^2 L}{4E_\nu} \right)$$

Example [K. Abe *et al.* (T2K Collaboration), PRD 91, 072010 (2015)]

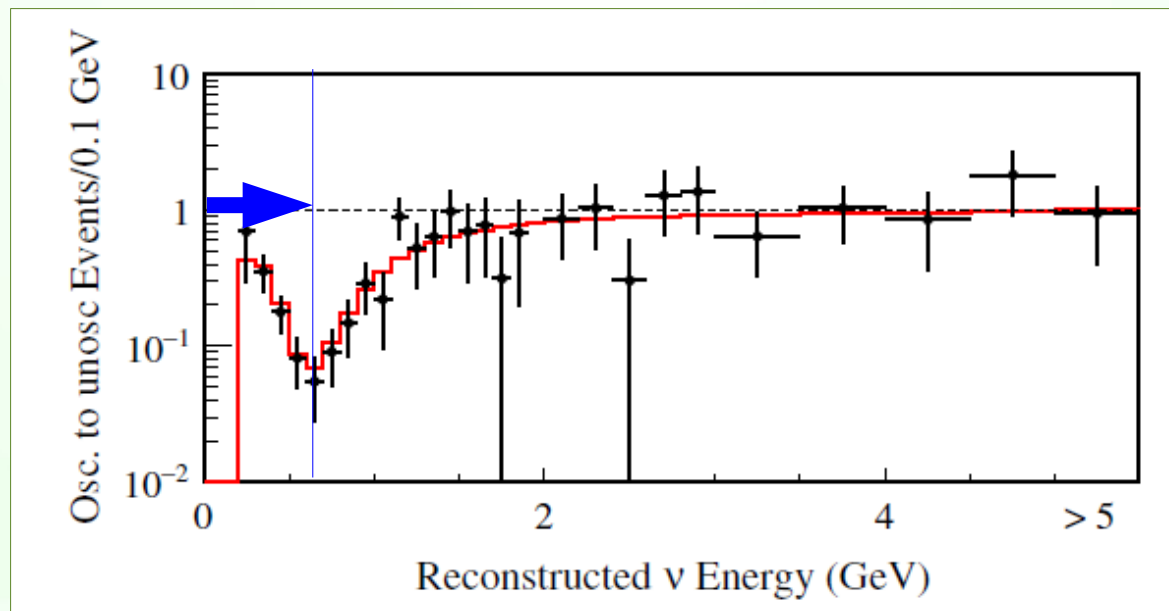


Neutrino oscillations in a nutshell

In the simplest case of 2 flavors

$$P(\nu_\alpha \rightarrow \nu_\alpha) = 1 - \sin^2 2\theta \sin^2 \left(\frac{\Delta m^2 L}{4E_\nu} \right)$$

Example [K. Abe *et al.* (T2K Collaboration), PRD 91, 072010 (2015)]



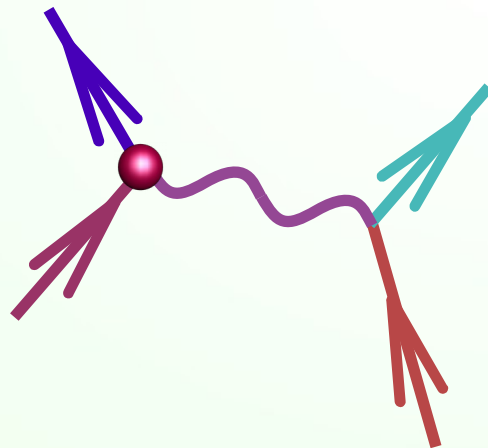


Energy reconstruction

Kinematic reconstruction

In quasielastic scattering off **free nucleons**, $\bar{\nu} + p \rightarrow l + n$ and $\nu + n \rightarrow l + p$, we can deduce the neutrino energy from the charged lepton's kinematics.

No need to reconstruct the nucleon kinematics.

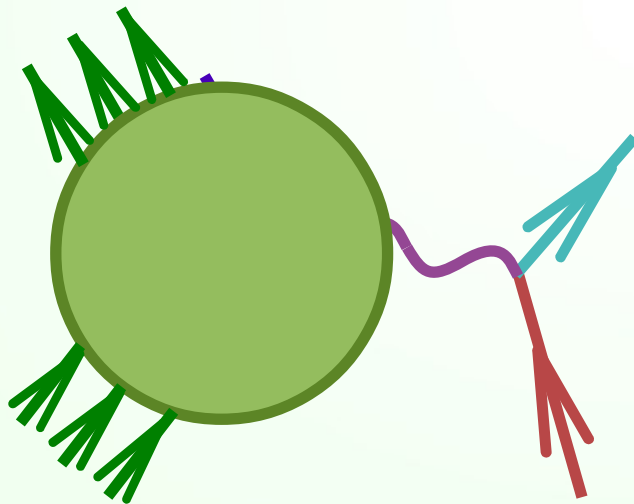


E' and θ known

$$E = \frac{ME' + \text{const}}{M - E' + |\mathbf{k}'| \cos \theta}$$

Kinematic reconstruction

In **nuclei** the reconstruction becomes an approximation due to the binding energy, Fermi motion, final-state interactions, two-body interactions etc.



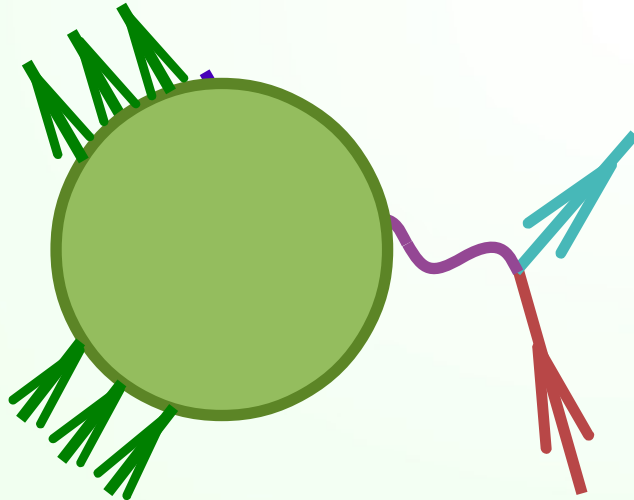
E' and θ known

$$E \simeq \frac{(M - \epsilon) E' + \text{const}}{M - \epsilon - E' + |\mathbf{k}'| \cos \theta}$$

Unknown monochromatic beam

Consider the simplest (unrealistic) case:

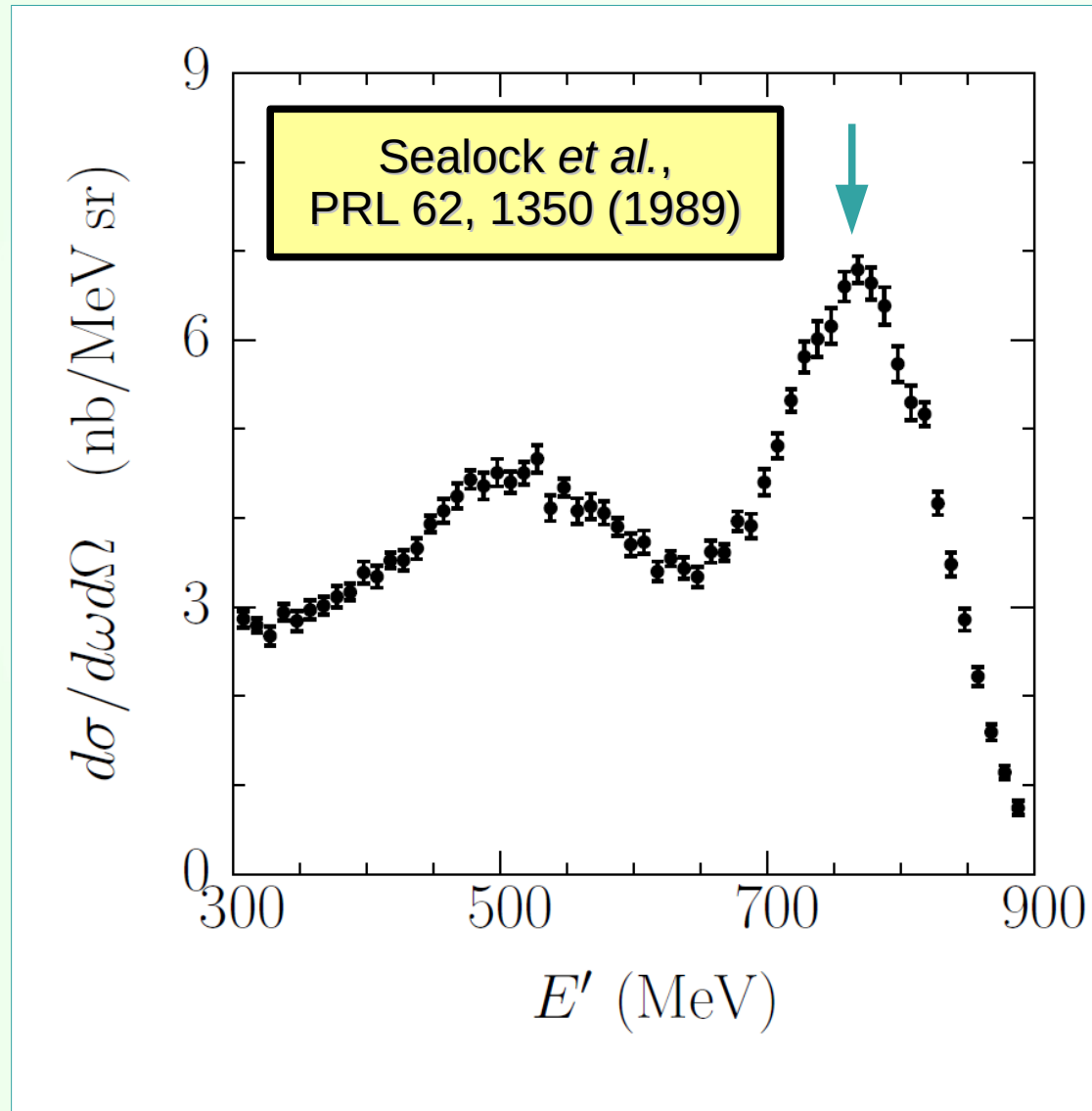
the beam is **monochromatic** but its energy is **unknown** and has to be reconstructed



E' and θ known

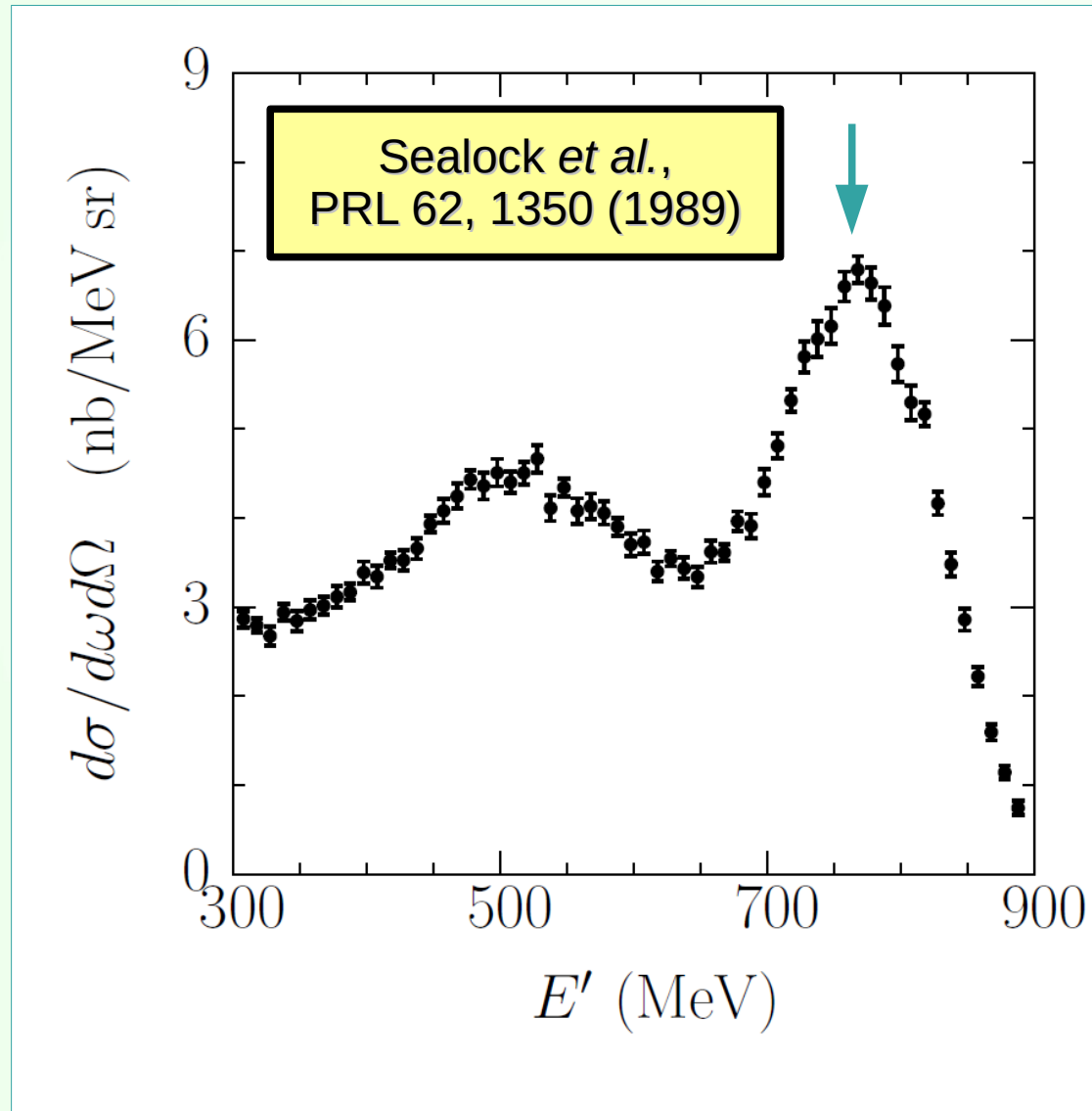
$E = ?$

“Unknown” monochromatic e^- beam



$E' = 768$ MeV
 $\theta = 37.5$ deg
 $\Delta E' = 5$ MeV

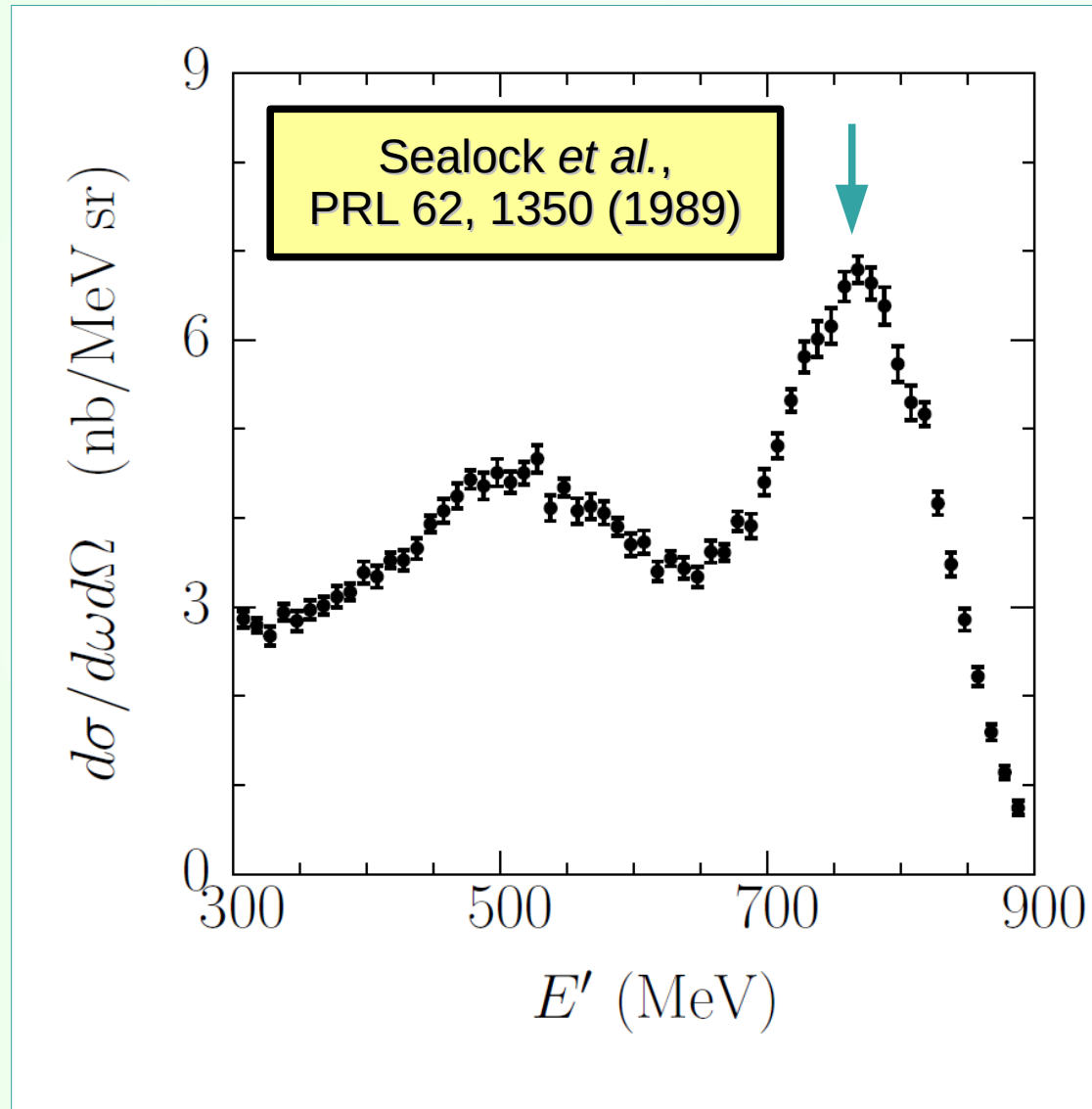
“Unknown” monochromatic e^- beam



$$\begin{aligned} E' &= 768 \text{ MeV} \\ \theta &= 37.5 \text{ deg} \\ \Delta E' &= 5 \text{ MeV} \end{aligned}$$

$$\begin{aligned} \text{for } \epsilon &= 25 \text{ MeV} \\ E &= 960 \text{ MeV} \\ \Delta E &= 7 \text{ MeV} \end{aligned}$$

“Unknown” monochromatic e^- beam



$E' = 768$ MeV
 $\theta = 37.5$ deg
 $\Delta E' = 5$ MeV

for $\epsilon = 25$ MeV
 $E = 960$ MeV
 $\Delta E = 7$ MeV

true value
 $E = 961$ MeV

“Unknown” monochromatic e^- beam

θ (deg)	37.5	37.5	37.1	36.0	36.0
E' (MeV)	976	768	615	487.5	287.5
$\Delta E'$ (MeV)	5	5	5	5	2.5

Assuming $\epsilon = 25$ MeV

rec. E	1285 ± 8	960 ± 7	741 ± 7	571 ± 6	333 ± 3
true E	1299	961	730	560	320

“Unknown” monochromatic e^- beam

θ (deg)	37.5	37.5	37.1	36.0	36.0
E' (MeV)	976	768	615	487.5	287.5
$\Delta E'$ (MeV)	5	5	5	5	2.5

Appropriate ϵ value?

true E	1299	961	730	560	320
ϵ	33 ± 5	26 ± 5	16 ± 5	16 ± 3	13 ± 3

Sealock et al.,
PRL 62, 1350
(1989)

O'Connell et al.,
PRC 35, 1063
(1987)

Barreau et al.,
NPA 402, 515
(1983)

“Unknown” monochromatic e^- beam

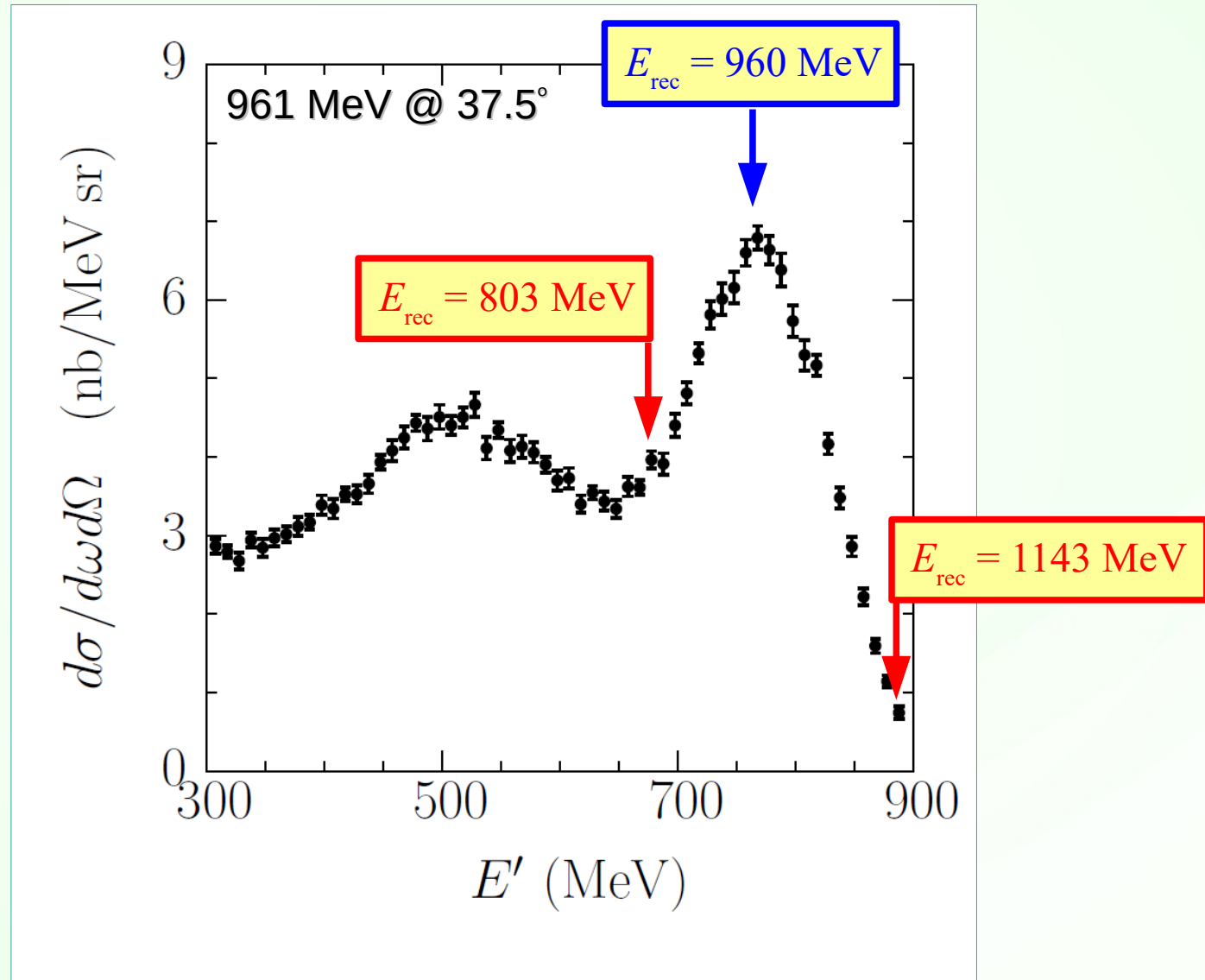
θ (deg)	37.5	37.5	37.1	36.0	36.0
E' (MeV)	976	768	615	487.5	287.5
$\Delta E'$ (MeV)	5	5	5	5	2.5

Appropriate ϵ value?

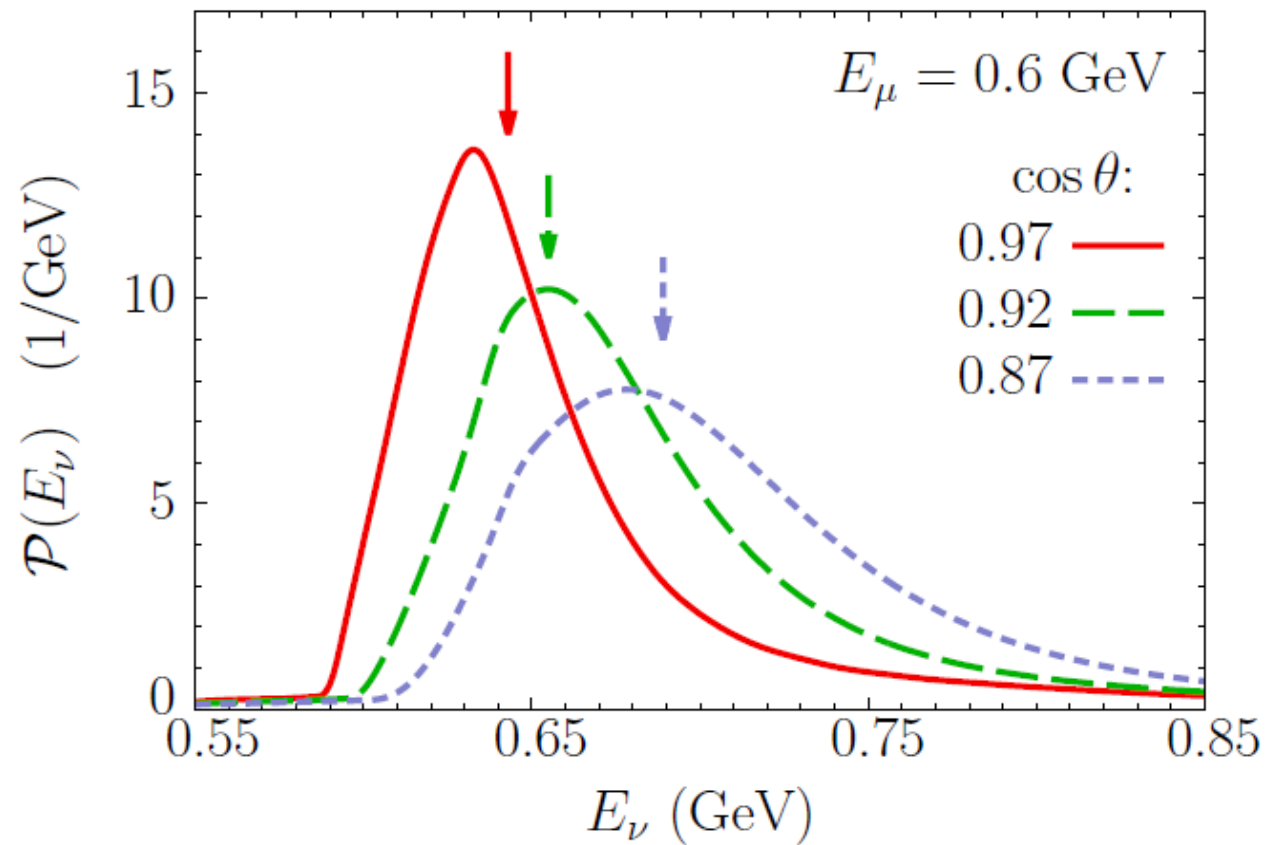
true E	1299	961	730	560	320
ϵ	33 ± 5	26 ± 5	16 ± 5	16 ± 3	13 ± 3

different $E \equiv$ different $Q^2 \equiv$ different θ
 \rightarrow different ϵ

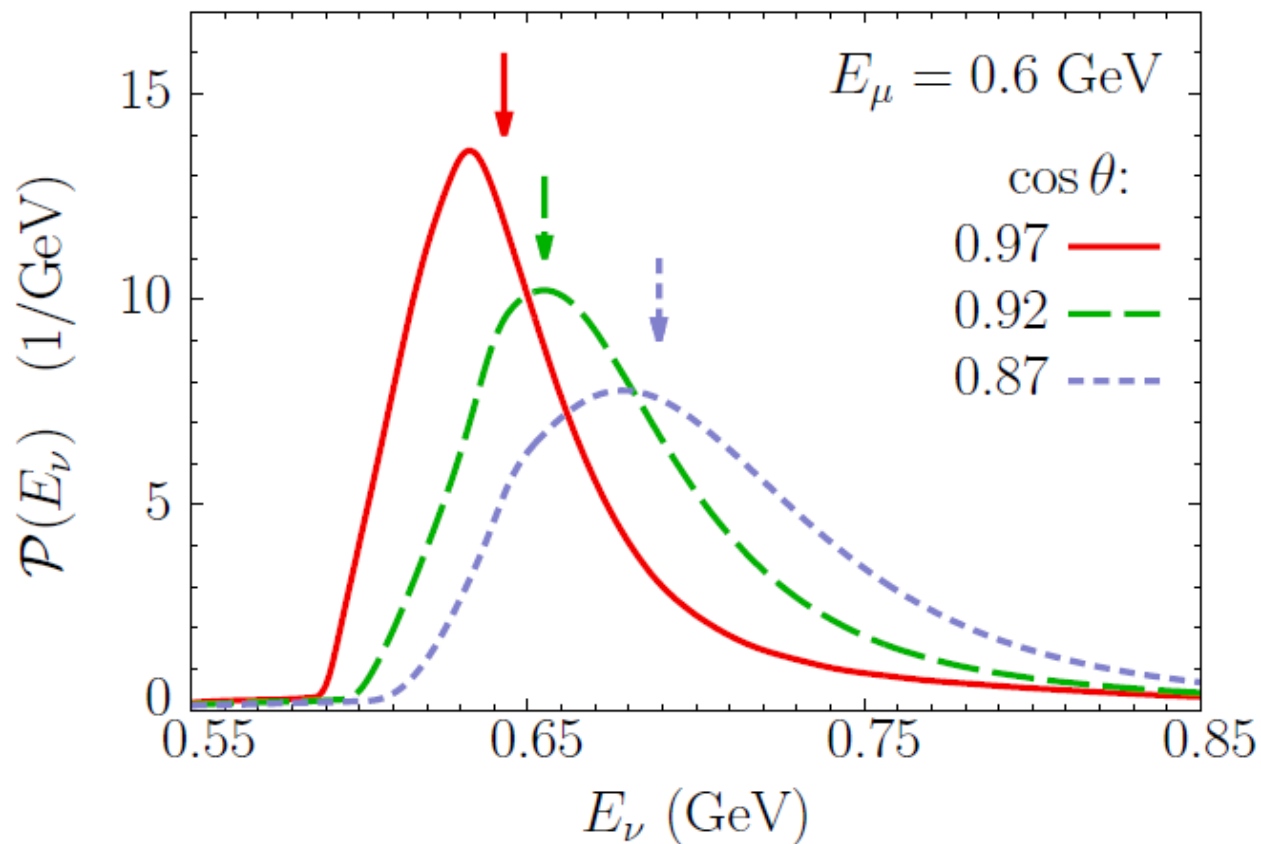
“Unknown” monochromatic e^- beam



Realistic calculations vs E_{rec}



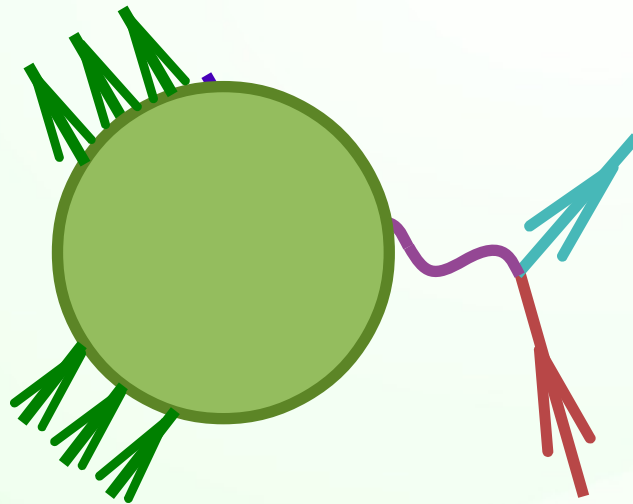
Realistic calculations vs E_{rec}



Same physics drives the QE peak position and relates the kinematics to neutrino energy

Polychromatic beam

In modern experiments, the neutrino beams are not monochromatic, and the **energy must be reconstructed** from the observables, typically E' and $\cos \theta$ under the CCQE event hypothesis.



E' and θ known

$E = ?$

CC0 π events

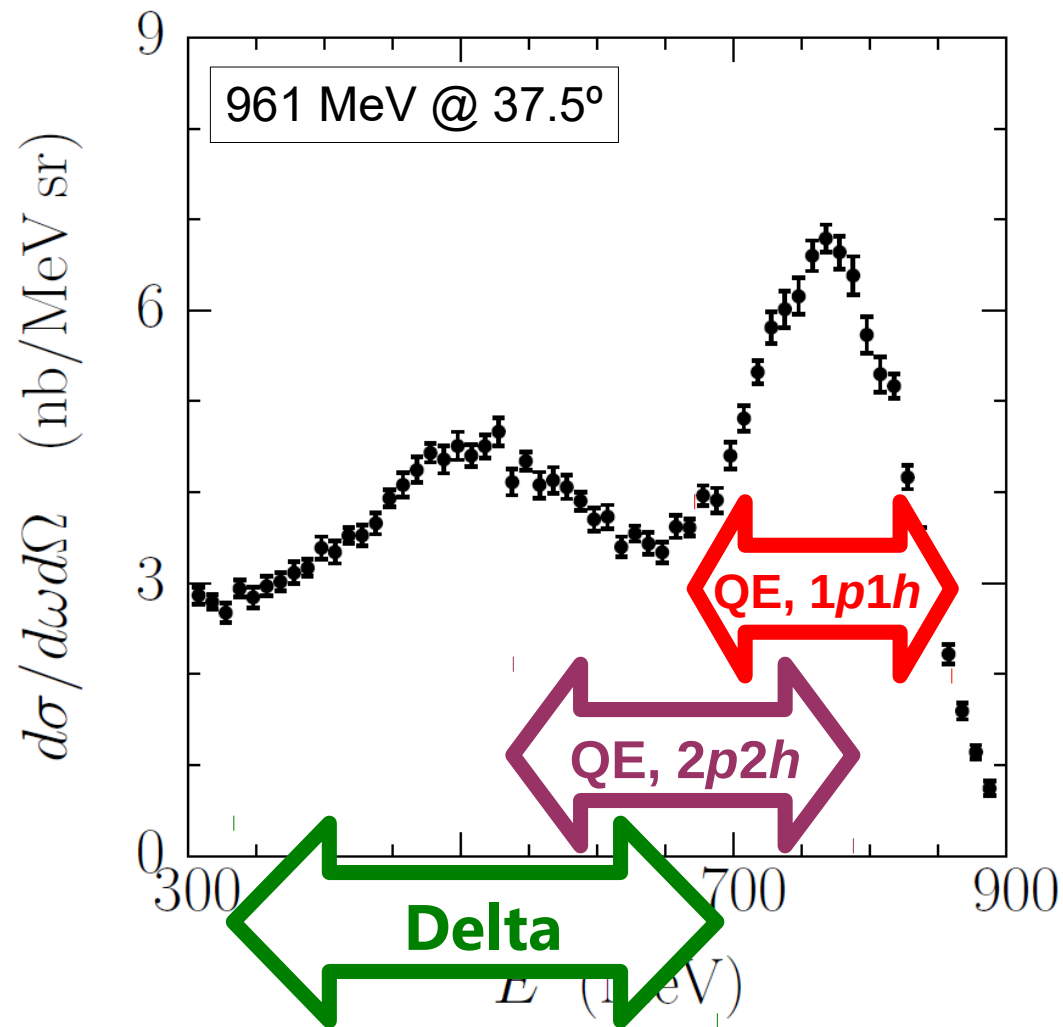
In practice, CCQE energy reconstruction is applied to all events not containing **observed pions**.

+ CCQE (any number of nucleons)
pion production and followed by absorption
undetected pions

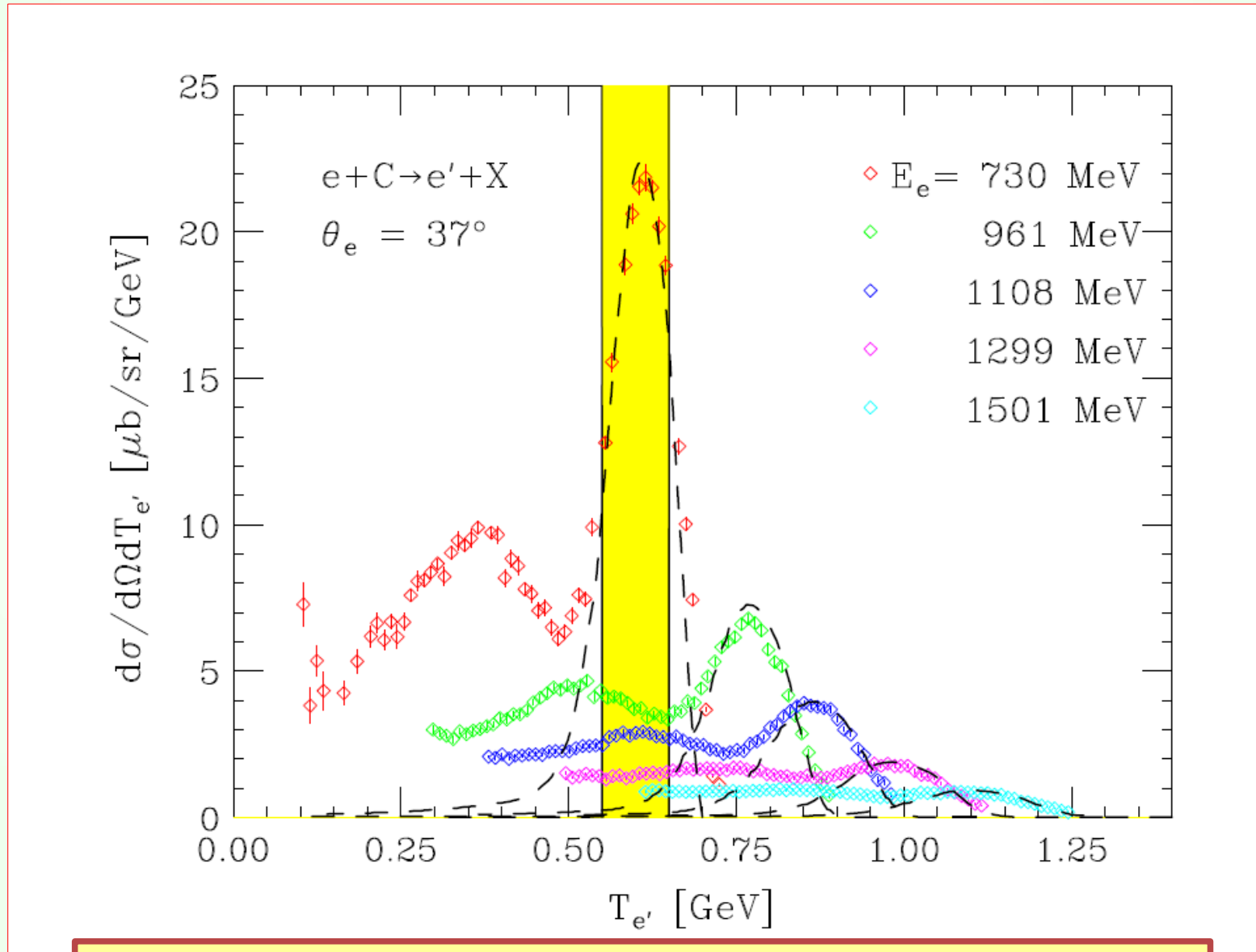
— CCQE with pions from FSI

0 π events

Recall the monochromatic-beam case



CCQE events of given l^\pm kinematics



Omar Benhar @ NuFact11, PRL 105, 132301 (2010)

CCQE events of given l^\pm kinematics

Very different **processes** and **neutrino energies** contribute to CCQE-like events of a given E' and $\cos \theta$.

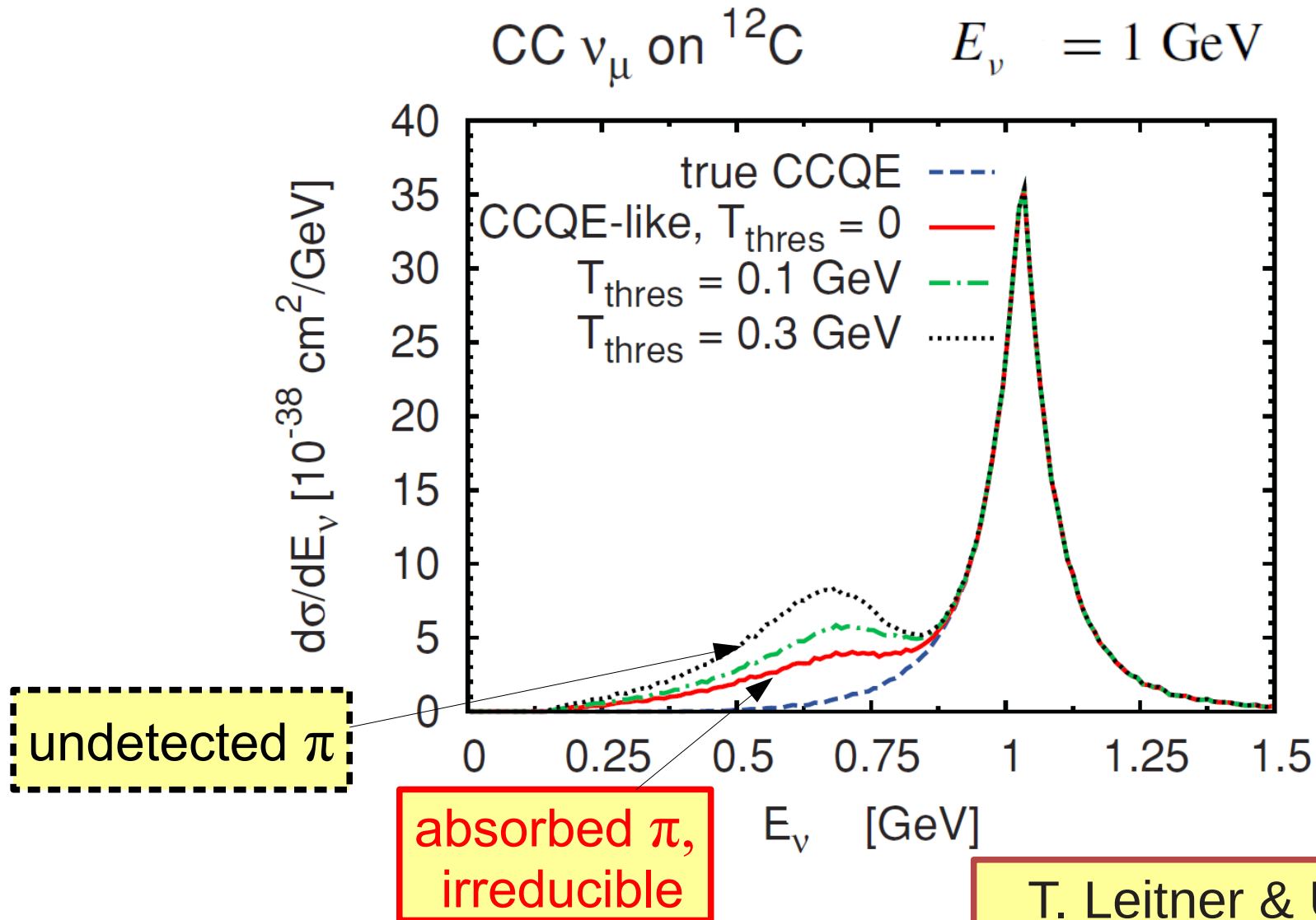
An undetected pion typically lowers the reconstructed energy by **$\sim 300\text{--}350$ MeV**.

Note that in the reconstruction formula, $M_\Delta = 1232$ MeV would be more suitable than $M' = 939$ MeV.

$$E_v^{\text{rec}} = \frac{2(M - \varepsilon)E_\ell + M'^2 - (M - \varepsilon)^2 - m_\ell^2}{2(M - \varepsilon - E_\ell + |\mathbf{k}_\ell| \cos \theta)}.$$

$$\frac{M_\Delta^2 - M'^2}{2M} \approx 340 \text{ MeV}$$

Absorbed or undetected pions



T. Leitner & U. Mosel
PRC 81, 064614 (2010)

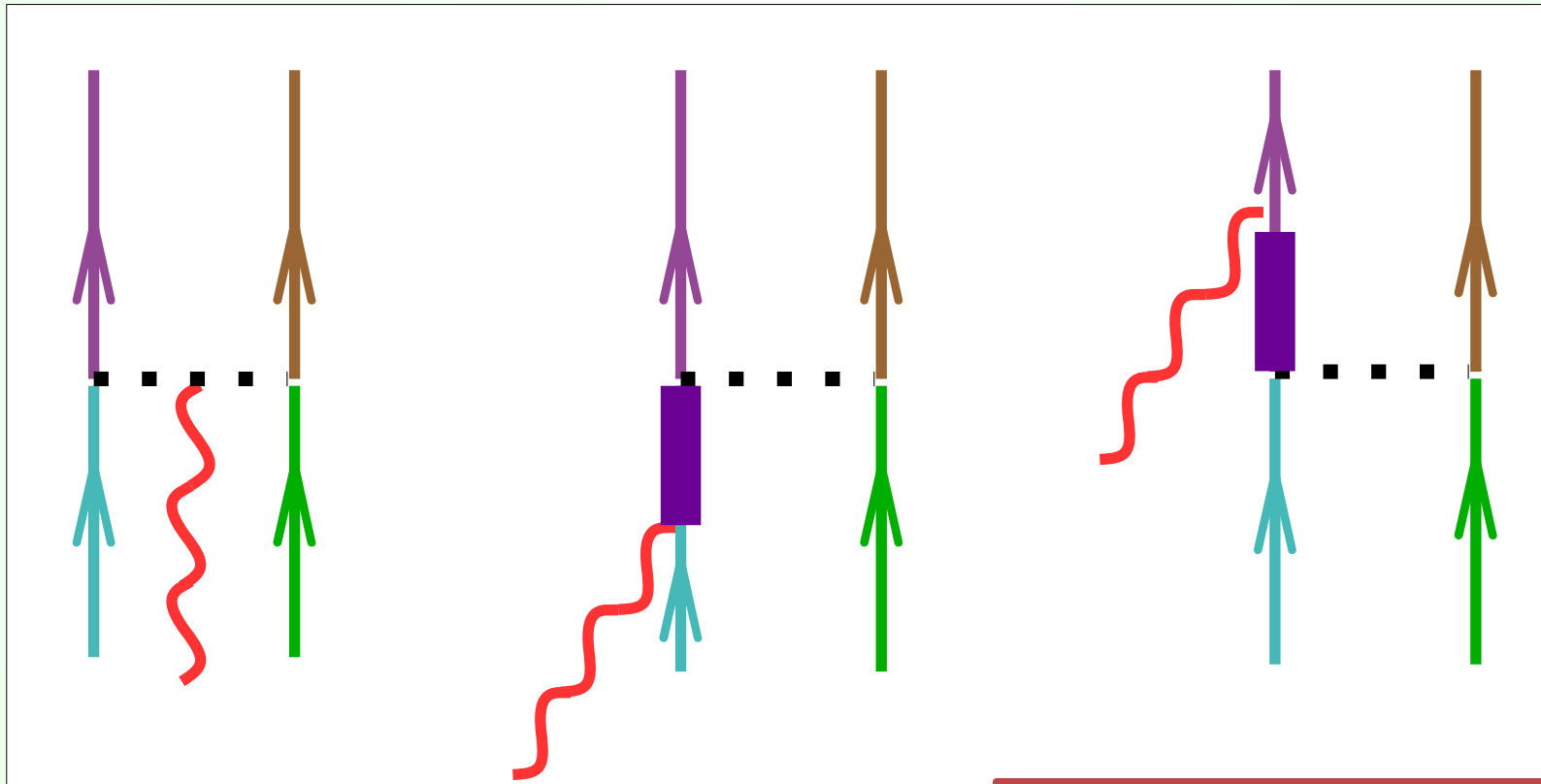
2p2h final states

Final states involving two (or more) nucleons may come from

- **initial-state correlations**: ~20% of nucleons in nucleus strongly interact, typically forming a deuteron-like np pair of high relative momentum
- **final-state interactions**
- **2-body reaction mechanisms**, such as by meson-exchange currents

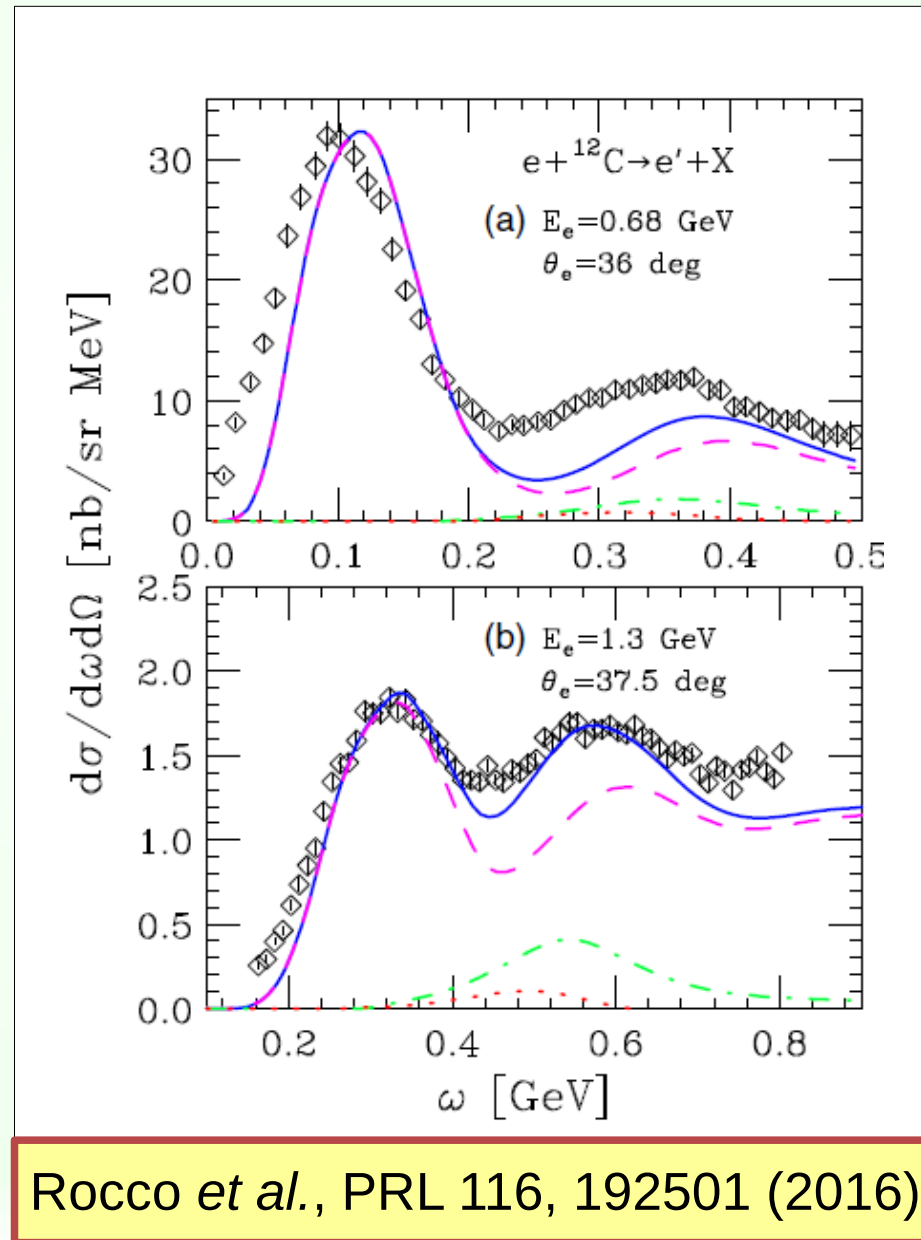
Alberico *et al.*
Ann. Phys. 154, 356 (1984)

2-body reaction mechanisms



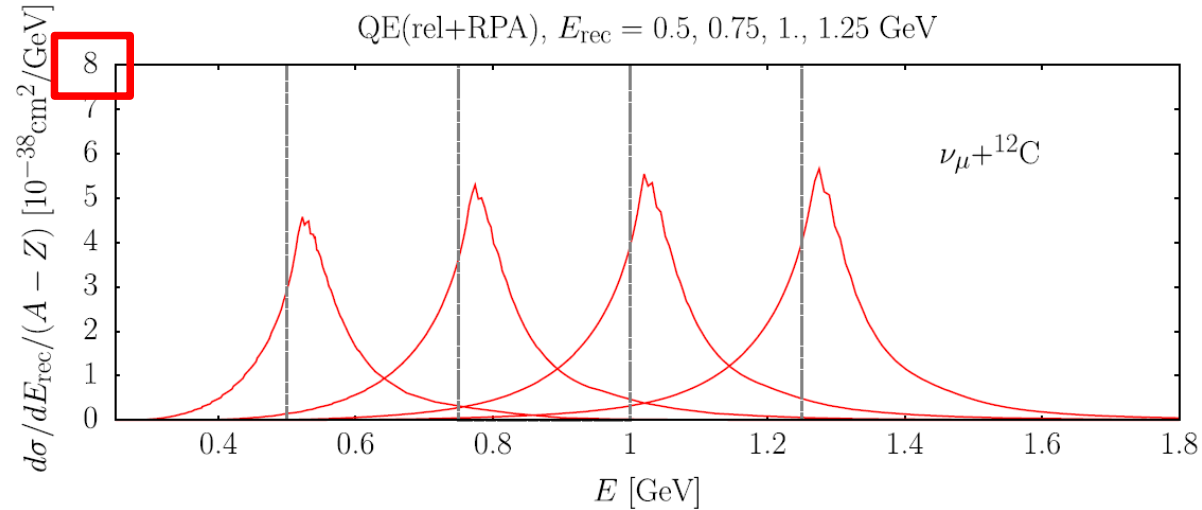
Donnelly *et al.*
PLB 76, 393 (1978)

2p2h contribution to the cross section

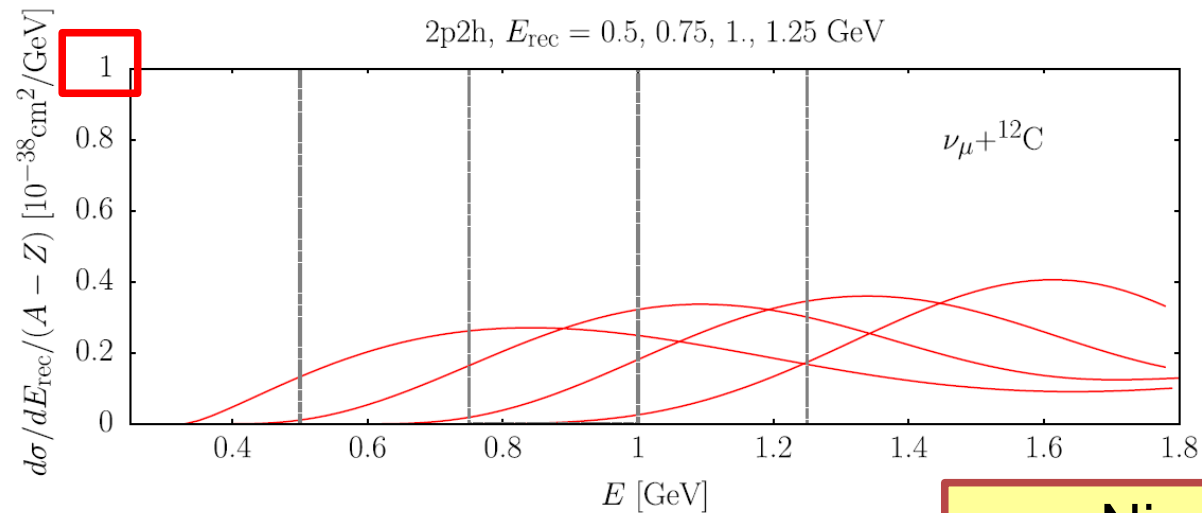


2p2h effect on energy reconstruction

1p1h

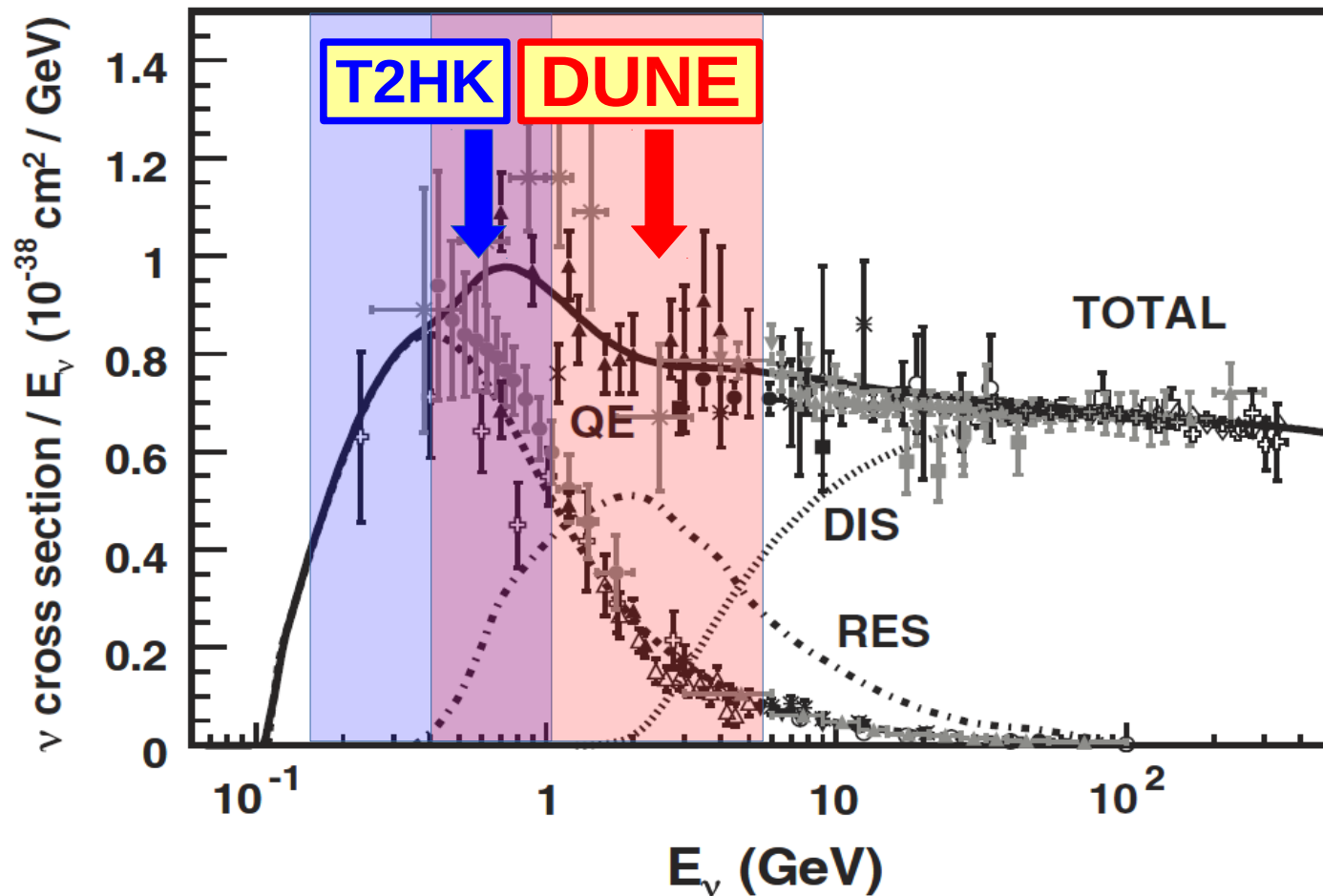


2p2h



Nieves *et al.*,
PRD 85, 113008 (2012)

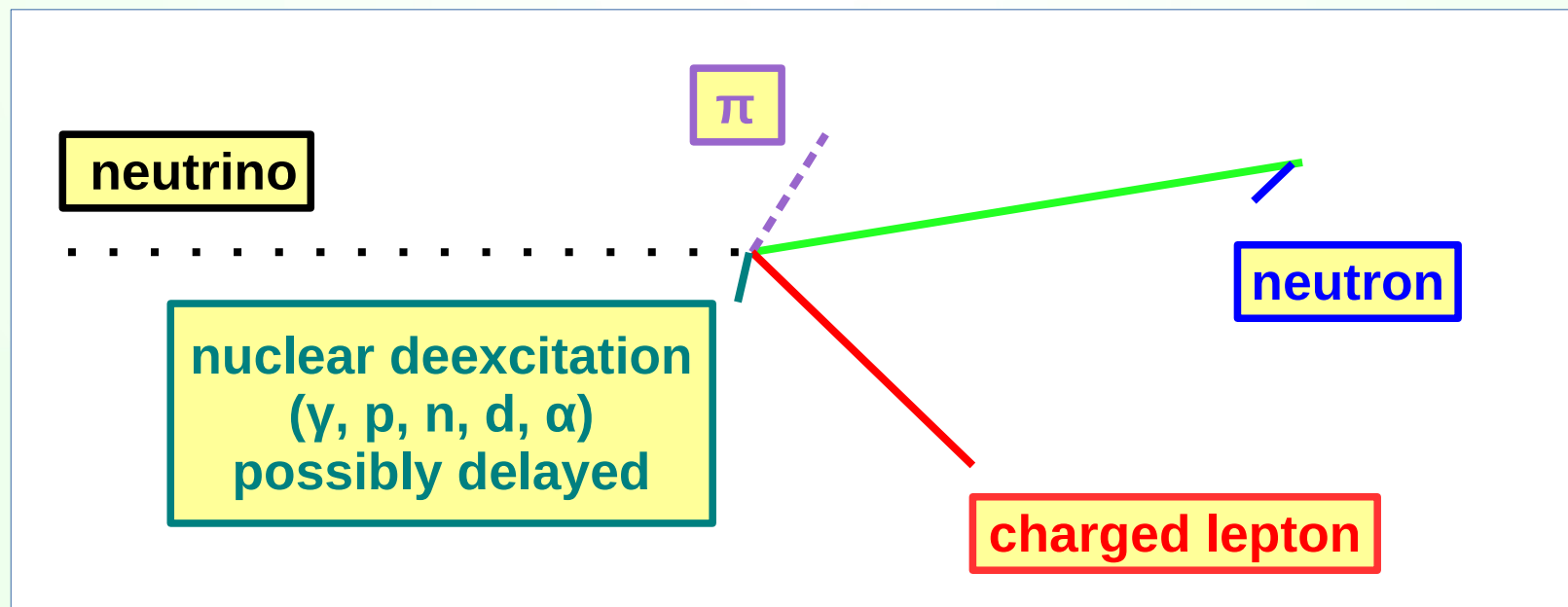
Neutrino scattering



adopted from
Formaggio & Zeller, RMP 84, 1307 (2013)

Calorimetric energy reconstruction

- Seemingly simple procedure: add all energy depositions in the detector related to the neutrino event
- Advantages: (i) applicable to any final states, (ii) in an ideal detector, the reconstruction would be exact and insensitive to nuclear effects



Calorimetric energy reconstruction

- In a real detector the method is only insensitive to nuclear effects when

missing energy \ll neutrino energy

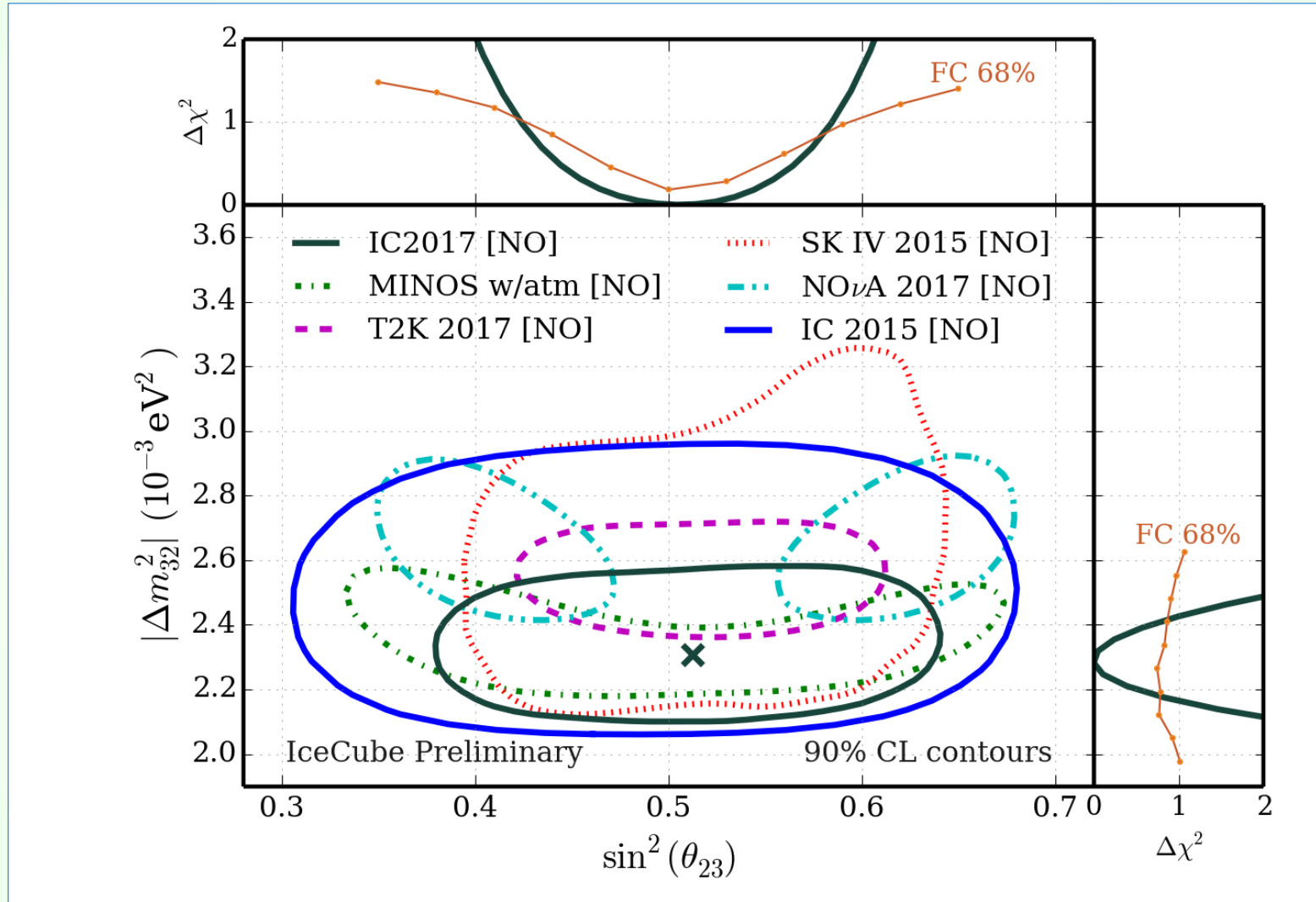
- Otherwise, requires input from nuclear models

A.M.A., arXiv:
1704.07835

- Correction for the missing energy **may be significant**:
 - undetected pion at least $m_{\pi} = 140$ MeV
 - neutrons are hard to associate with the event

To achieve ~ 25 MeV accuracy in DUNE, **accurate predictions of exclusive cross sections are required.**

What precision are we reaching?



J. Hignight (IceCube), APS April Meeting, 2017

What precision are we reaching?

At neutrino energy ~ 600 MeV (T2K kinematics),

- 10% uncertainty (current T2K), ~ 60 MeV
- 2% uncertainty (current global fits), ~ 10 MeV

At the NOvA and DUNE kinematics, values $\times 4-5$.

DUNE and **T2HK** aim at uncertainties $< 1\%$,
requiring $\sim \mathbf{25\ MeV}$ and $\sim \mathbf{5\ MeV}$ precision.

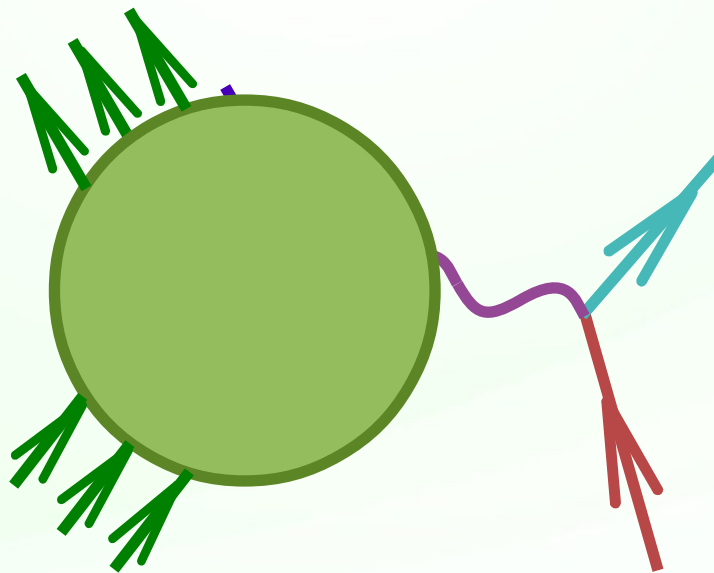
Effects considered to be “small” need to be accounted for accurately to avoid biases.



Impulse approximation

Impulse approximation

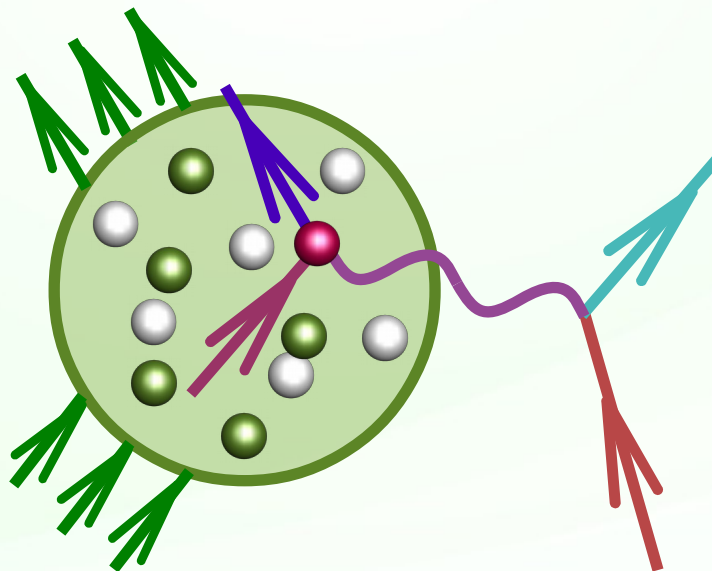
Assumption: the dominant process of lepton-nucleus interaction is **scattering off a single nucleon**, with the remaining nucleons acting as a spectator system.



Impulse approximation

Assumption: the dominant process of lepton-nucleus interaction is **scattering off a single nucleon**, with the remaining nucleons acting as a spectator system.

It is valid when the momentum transfer $|\mathbf{q}|$ is high enough, as the probe's spatial resolution is $\sim 1/|\mathbf{q}|$.



$A(e, e')$ cross section

In Born approximation

$$\frac{d^2\sigma}{d\Omega_{e'} dE_{e'}} = \frac{\alpha^2}{Q^4} \frac{E_{e'}}{E_e} L_{\mu\nu} W^{\mu\nu}$$

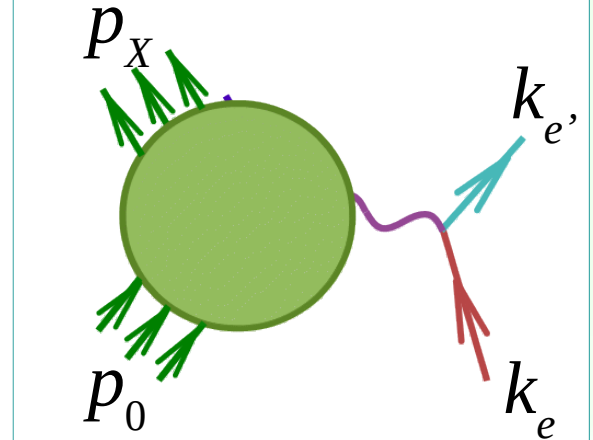
with the lepton tensor

$$L_{\mu\nu} = 2 [k_e^\mu k_{e'}^\nu + k_e^\nu k_{e'}^\mu - g^{\mu\nu} (k_e k_{e'})]$$

and the nuclear tensor

$$W^{\mu\nu} = \sum_X \langle 0 | J^\mu | X \rangle \langle X | J^\nu | 0 \rangle \delta^{(4)}(p_0 + q - p_X)$$

$$W^{\mu\nu} = W_1 \left(-g^{\mu\nu} + \frac{q^\mu q^\nu}{q^2} \right) + \frac{W_2}{m^2} \left(p_0^\mu - \frac{(p_0 q)}{q^2} q^\mu \right) \left(p_0^\nu - \frac{(p_0 q)}{q^2} q^\nu \right)$$



Impulse approximation

The current reduces to a sum of 1-body currents

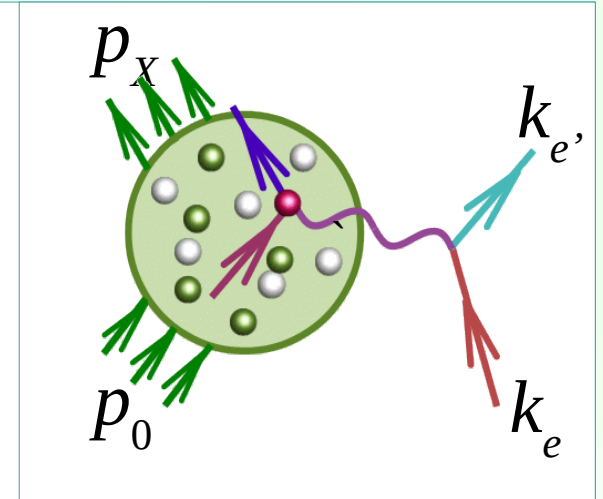
$$J^\mu \rightarrow \sum_i j_i^\mu$$

and the final state separates to

$$|X\rangle \rightarrow |x, \mathbf{p}_x\rangle \otimes |\mathcal{R}, \mathbf{p}_\mathcal{R}\rangle$$

leading to the nuclear current

$$\langle 0 | J^\mu | X \rangle = \left(\frac{M}{\sqrt{|\mathbf{p}_\mathcal{R}|^2 + M^2}} \right)^{1/2} \langle 0 | \mathcal{R}, \mathbf{p}_\mathcal{R}; N, -\mathbf{p}_\mathcal{R} \rangle \sum_i \langle -\mathbf{p}_\mathcal{R}, N | j_i^\mu | x, \mathbf{p}_x \rangle$$



Impulse approximation

The nuclear tensor

$$W^{\mu\nu} = \sum_X \langle 0 | J^\mu | X \rangle \langle X | J^\nu | 0 \rangle \delta^{(4)}(p_0 + q - p_X)$$

becomes in the impulse approximation

$$\begin{aligned} W^{\mu\nu} &= \sum_{x, \mathcal{R}} \int d^3 p_{\mathcal{R}} d^3 p_x |\langle 0 | \mathcal{R}, \mathbf{p}_{\mathcal{R}}; N, -\mathbf{p}_{\mathcal{R}} \rangle|^2 \\ &\times \frac{M}{E_{\mathcal{R}}} \sum_i \langle -\mathbf{p}_{\mathcal{R}}, N | j_i^\mu | x, \mathbf{p}_x \rangle \langle \mathbf{p}_x, x | j_i^\nu | N, -\mathbf{p}_{\mathcal{R}} \rangle \\ &\times \delta^{(3)}(\mathbf{q} - \mathbf{p}_{\mathcal{R}} - \mathbf{p}_x) \delta(\omega + E_0 - E_{\mathcal{R}} - E_x), \end{aligned}$$

Impulse approximation

$$W^{\mu\nu}(\mathbf{q}, \omega) = \int d^3p \, dE \, \frac{M}{E_{\mathbf{p}}} [Z S_p(\mathbf{p}, E) w_p^{\mu\nu} + (A - Z) S_n(\mathbf{p}, E) w_n^{\mu\nu}]$$

where

$$S_N(\mathbf{p}, E) = \sum_{\mathcal{R}} |\langle 0 | \mathcal{R}, -\mathbf{p}; N, \mathbf{p} \rangle|^2 \delta(E - M + E_0 - E_{\mathcal{R}})$$

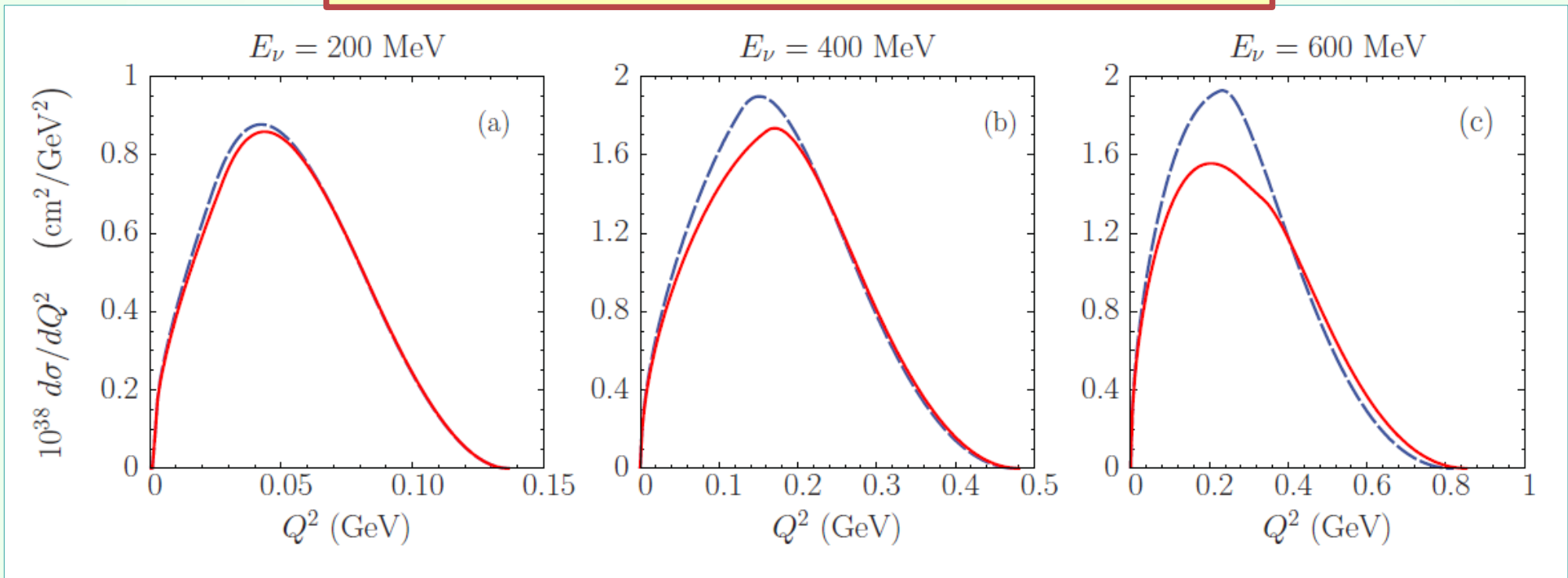
$$w_N^{\mu\nu} = \sum_x \langle \mathbf{p}, N | j_N^\mu | x, \mathbf{p} + \mathbf{q} \rangle \langle \mathbf{p} + \mathbf{q}, x | j_N^\nu | N, \mathbf{p} \rangle \delta(\tilde{\omega} + E_{\mathbf{p}} - E_x)$$

and

$$\tilde{\omega} + E_{\mathbf{p}} = E_x = \omega + E_0 - E_{\mathcal{R}} = \omega + M - E$$

Importance of relativistic kinematics

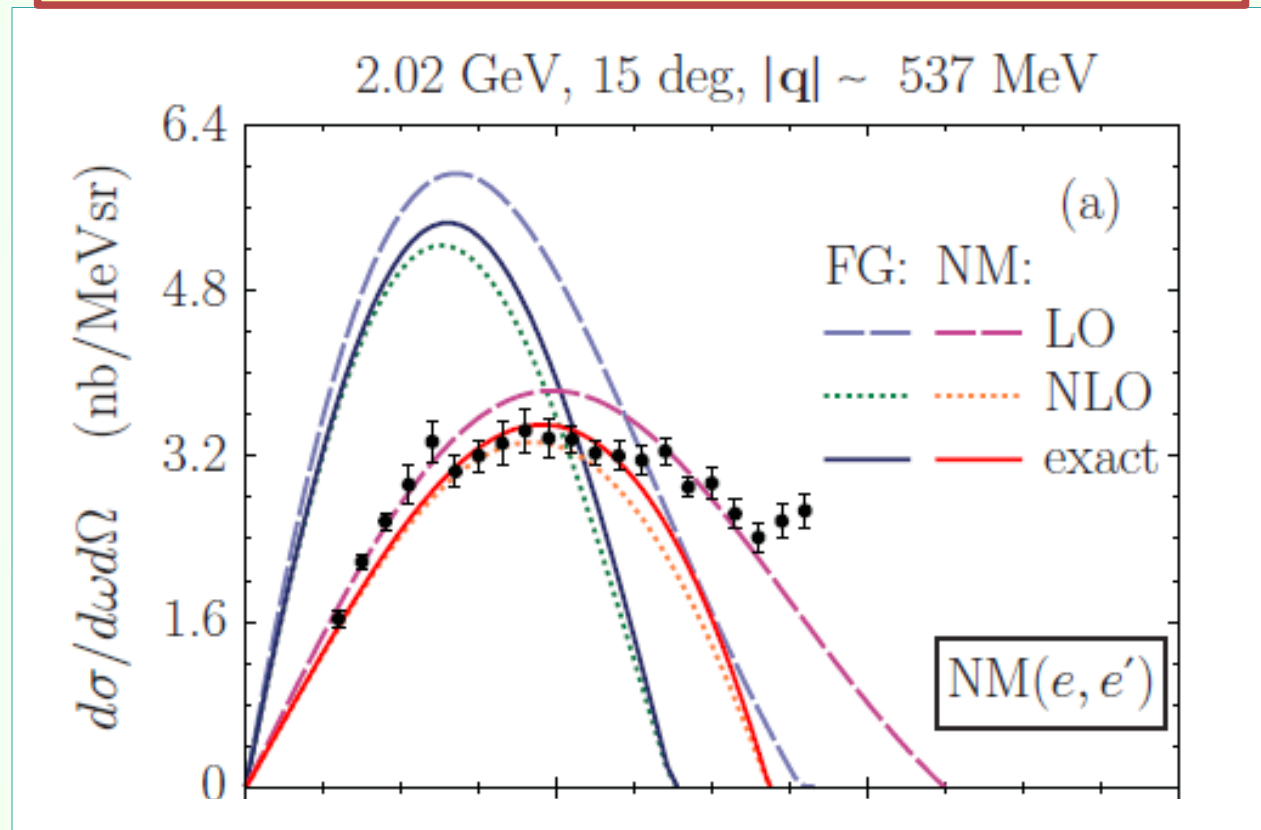
A.M.A. & O. Benhar, PRC 83, 054616 (2011)



Sizable differences between the **relativistic** and **nonrelativistic** results at neutrino energies ~ 500 MeV.

Importance of relativistic kinematics

A.M.A. & O. Benhar, PRC 83, 054616 (2011)



At $|q| \sim 540$ MeV, semi-relativistic result is **5% lower** than the exact cross section.

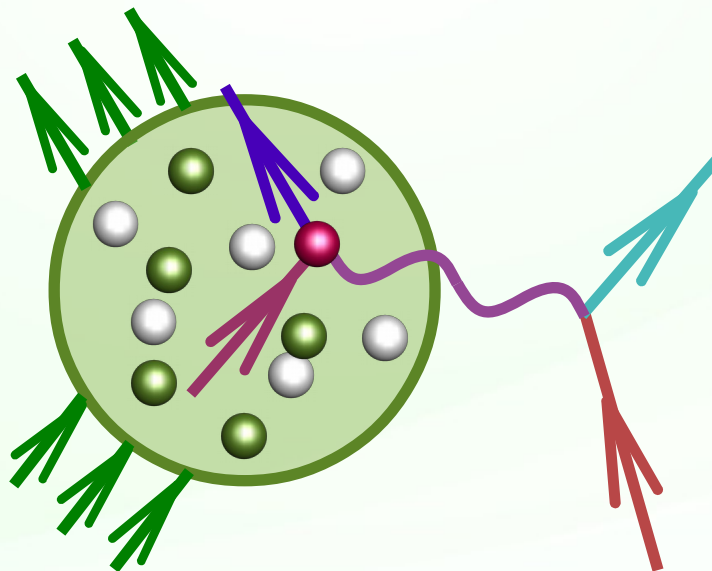
Impulse approximation

$$\frac{d\sigma_{eA}}{d\omega d\Omega} = \sum_N \int d\omega' d^3p dE \underbrace{P_{\text{hole}}^N(\mathbf{p}, E)}_{\text{Hole spectral function}} \underbrace{\frac{M}{E_p} \frac{d\sigma_{eN}^{\text{elem}}}{d\omega' d\Omega}}_{\text{Elementary cross section}} \underbrace{P_{\text{part}}^N(\mathbf{p}', \mathcal{T}', \omega')}_{\text{Particle spectral function}}$$

Hole spectral function

Particle spectral function

Elementary cross section



Impulse approximation

For scattering in a given angle, neutrinos and electrons differ only due to **the elementary cross section**.

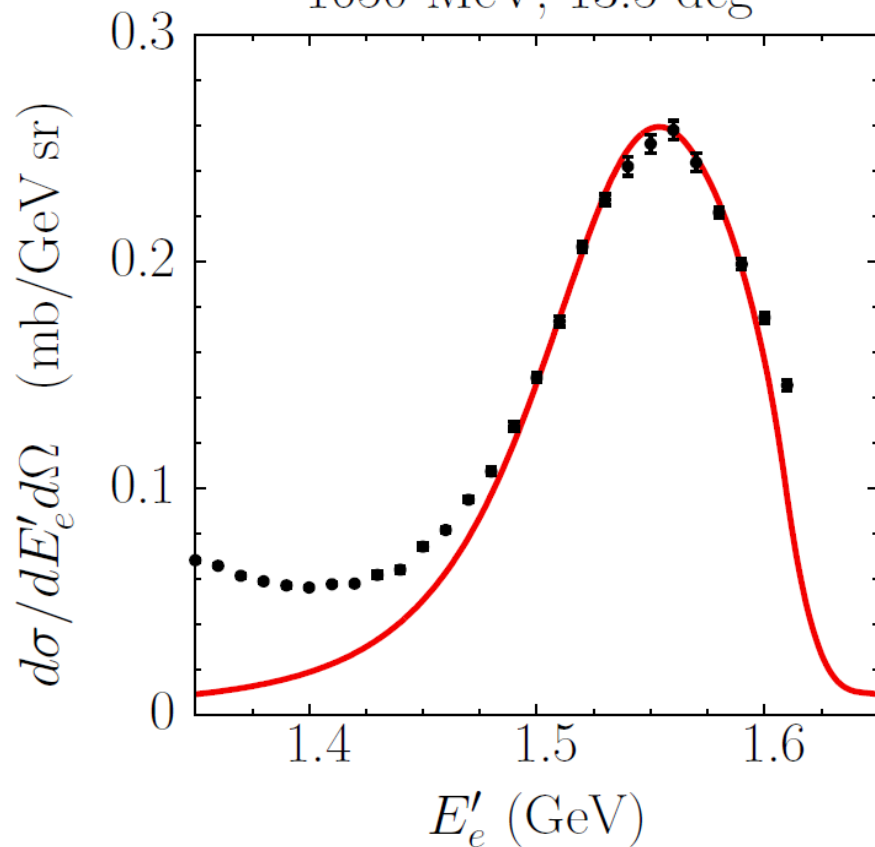
In neutrino scattering, uncertainties come from (i) interaction dynamics and (ii) **nuclear effects**.

It is **highly improbable** that theoretical approaches unable to reproduce (e,e') data would describe nuclear effects in neutrino interactions at similar kinematics.

Much more than the vector part...

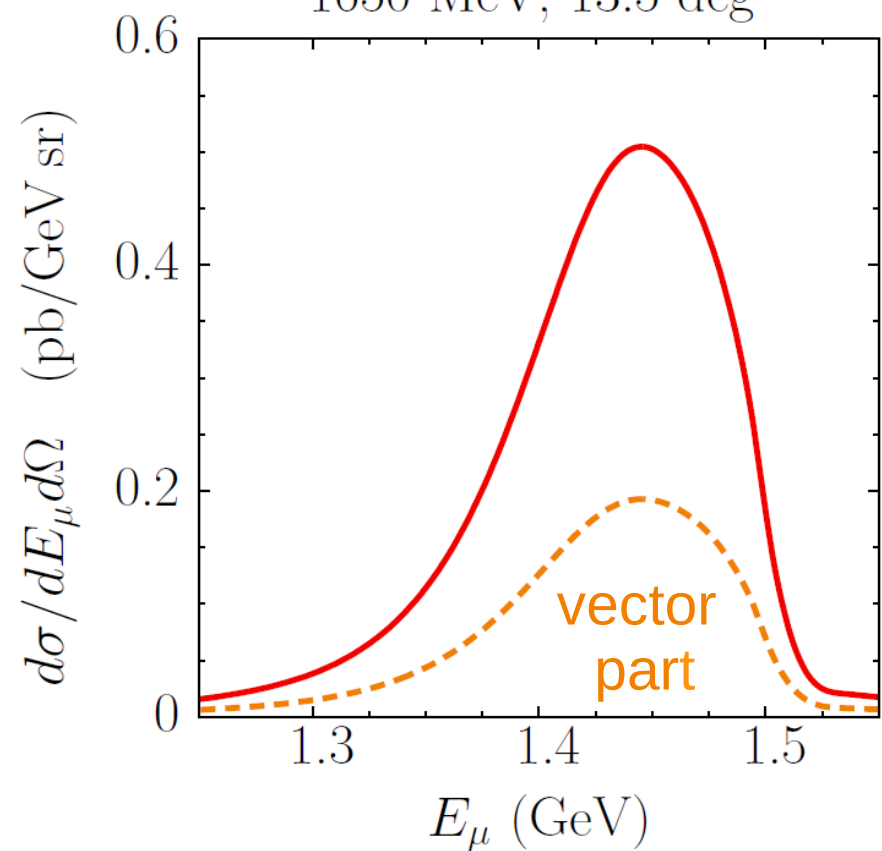
electrons

1650 MeV, 13.5 deg



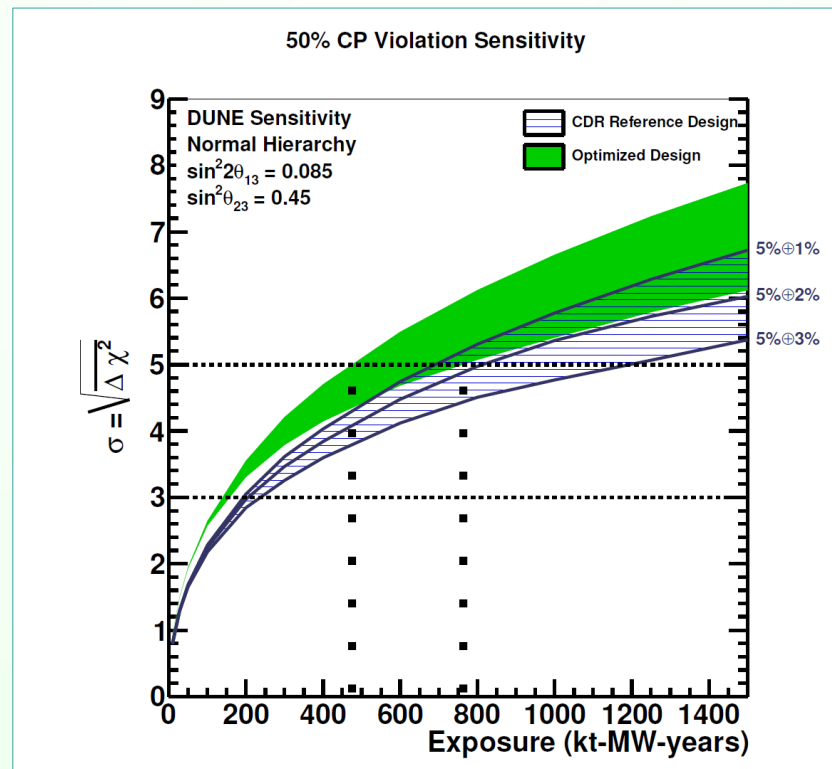
muon neutrinos

1650 MeV, 13.5 deg



How relevant is the precision?

Expected sensitivity of DUNE to CP violation as a function of exposure for a ν_e signal normalization uncertainties between 5% + 1% and 5% + 3%.



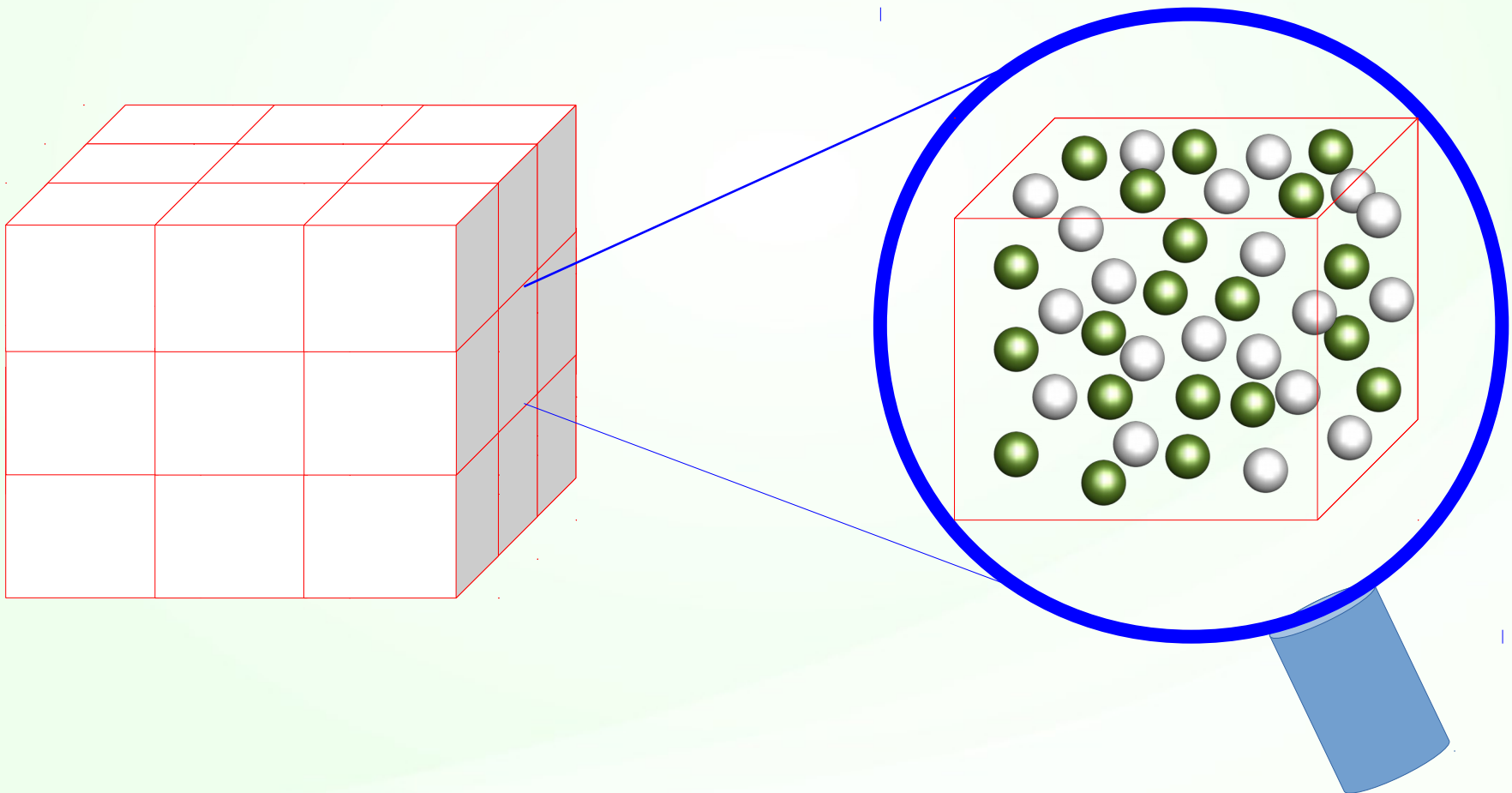
Acciari *et al.*, arXiv:1512.06148



Fermi gas model

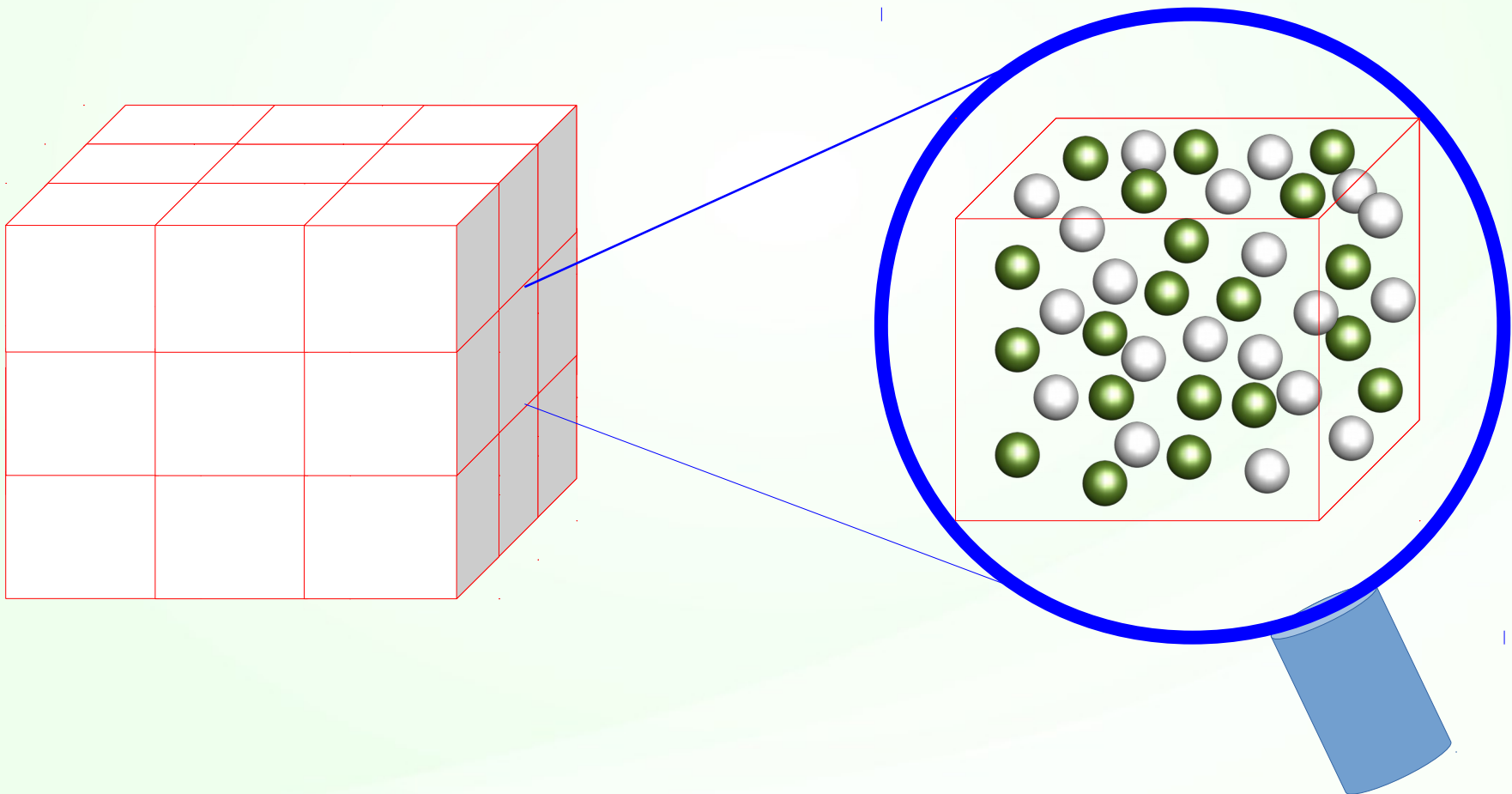
Fermi gas model

Imagine an infinite space filled uniformly with nucleons



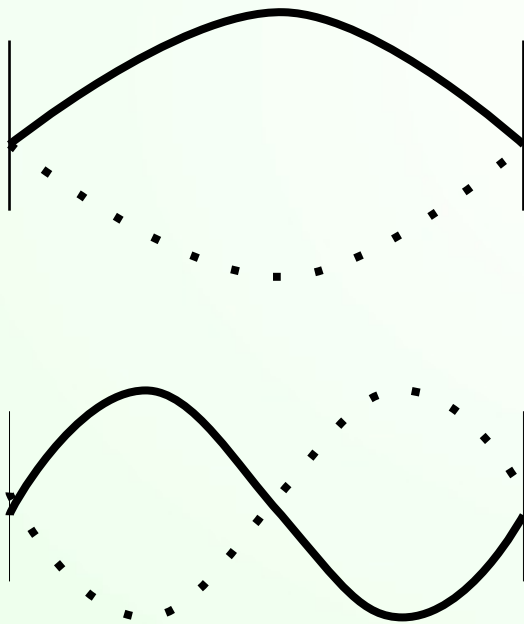
Fermi gas model

Due to the translational invariance, the eigenstates can be labeled using momentum, $\psi(x) = C e^{-ipx}$.



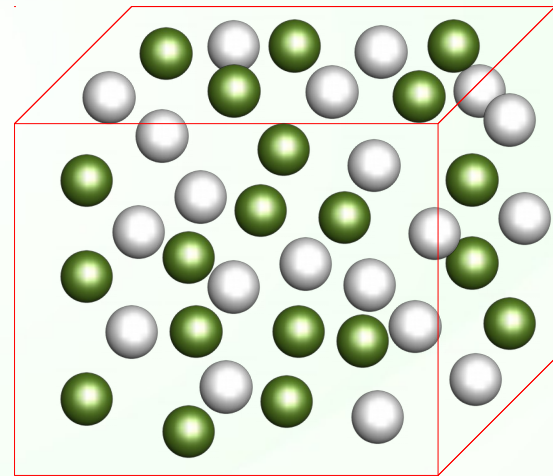
Fermi gas model

Due to the boundary conditions, $p_i \frac{L}{2} = \frac{\pi}{2} + n\pi$
every state occupies $(2\pi/L)^3$ in the momentum space



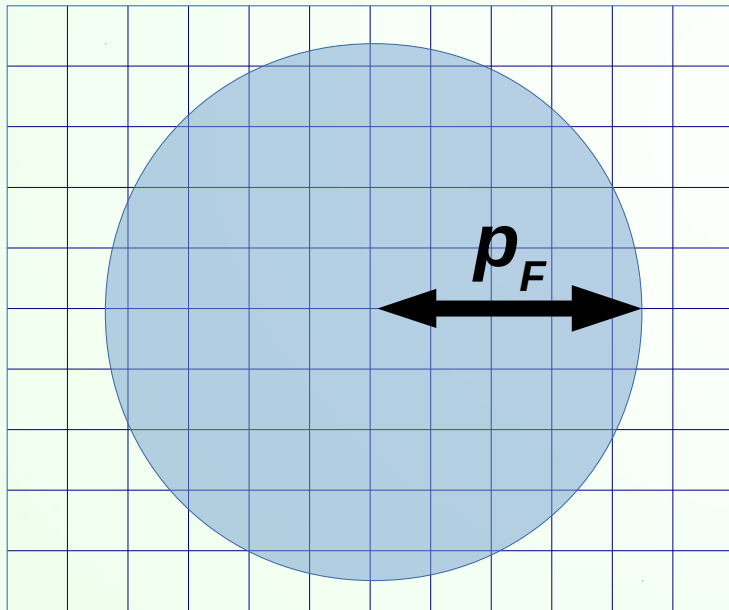
-L/2

+L/2

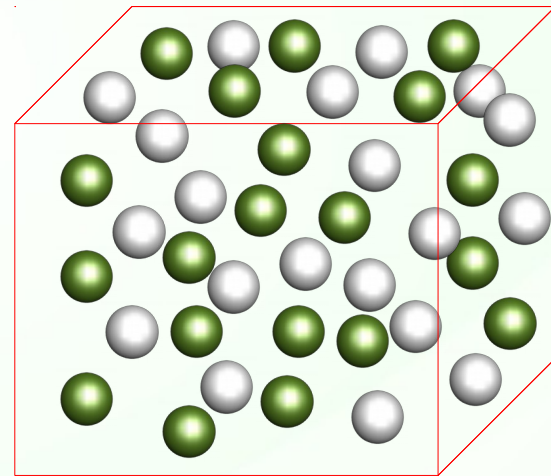


Fermi gas model

Due to the boundary conditions, $p_i \frac{L}{2} = \frac{\pi}{2} + n\pi$
every state occupies $(2\pi/L)^3$ in the momentum space

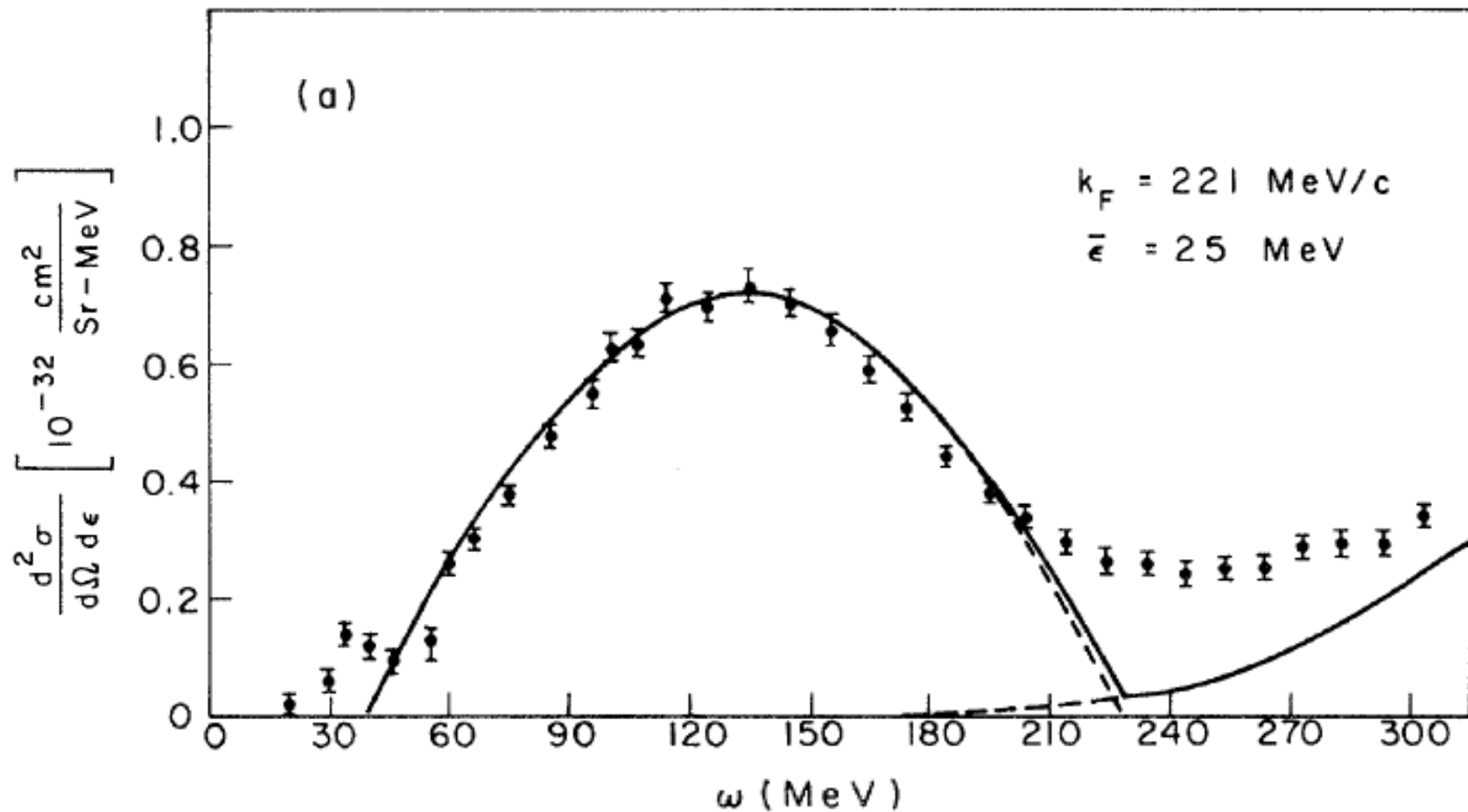


Momentum space



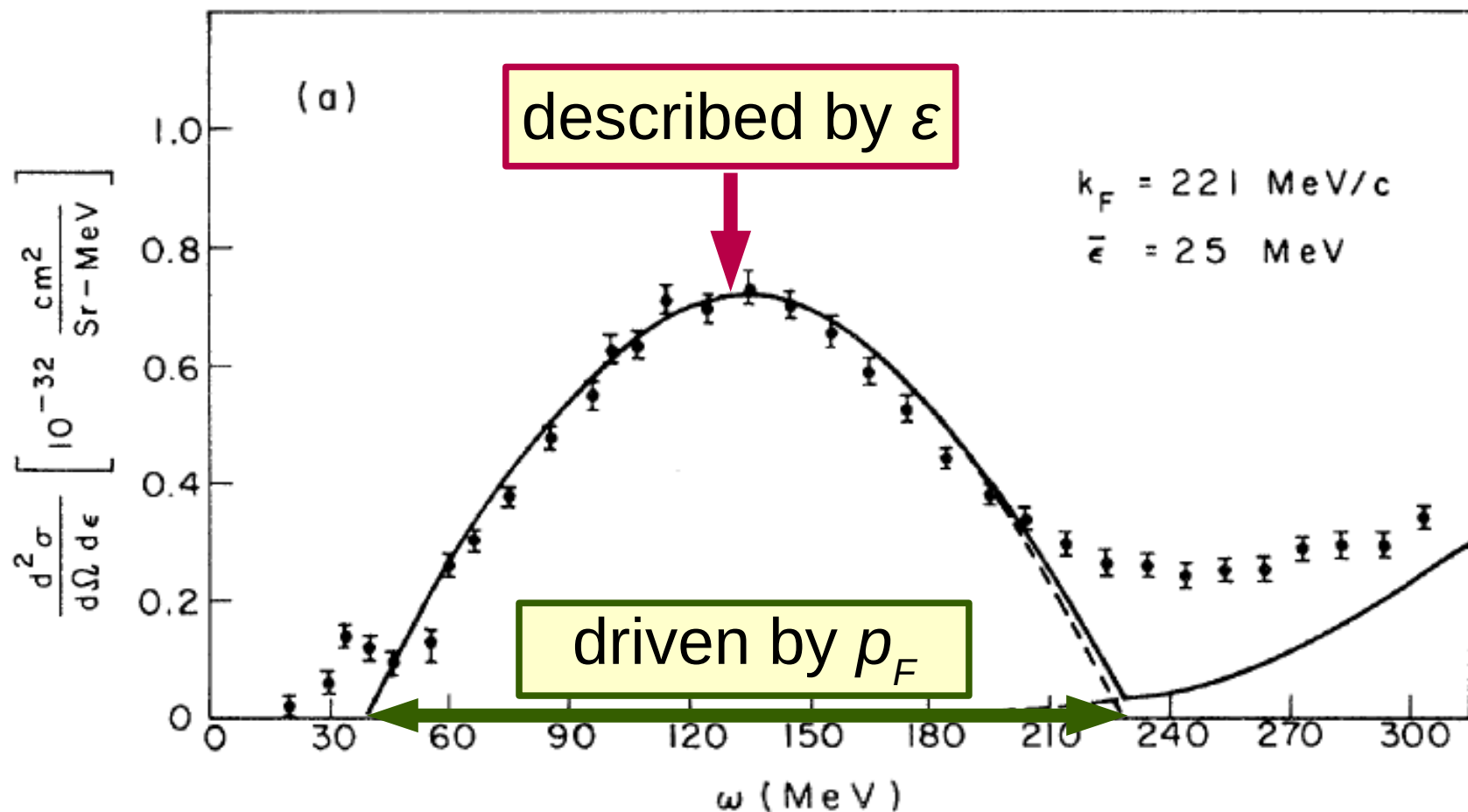
Coordinate space

Electron scattering off carbon, 500 MeV, 60 deg



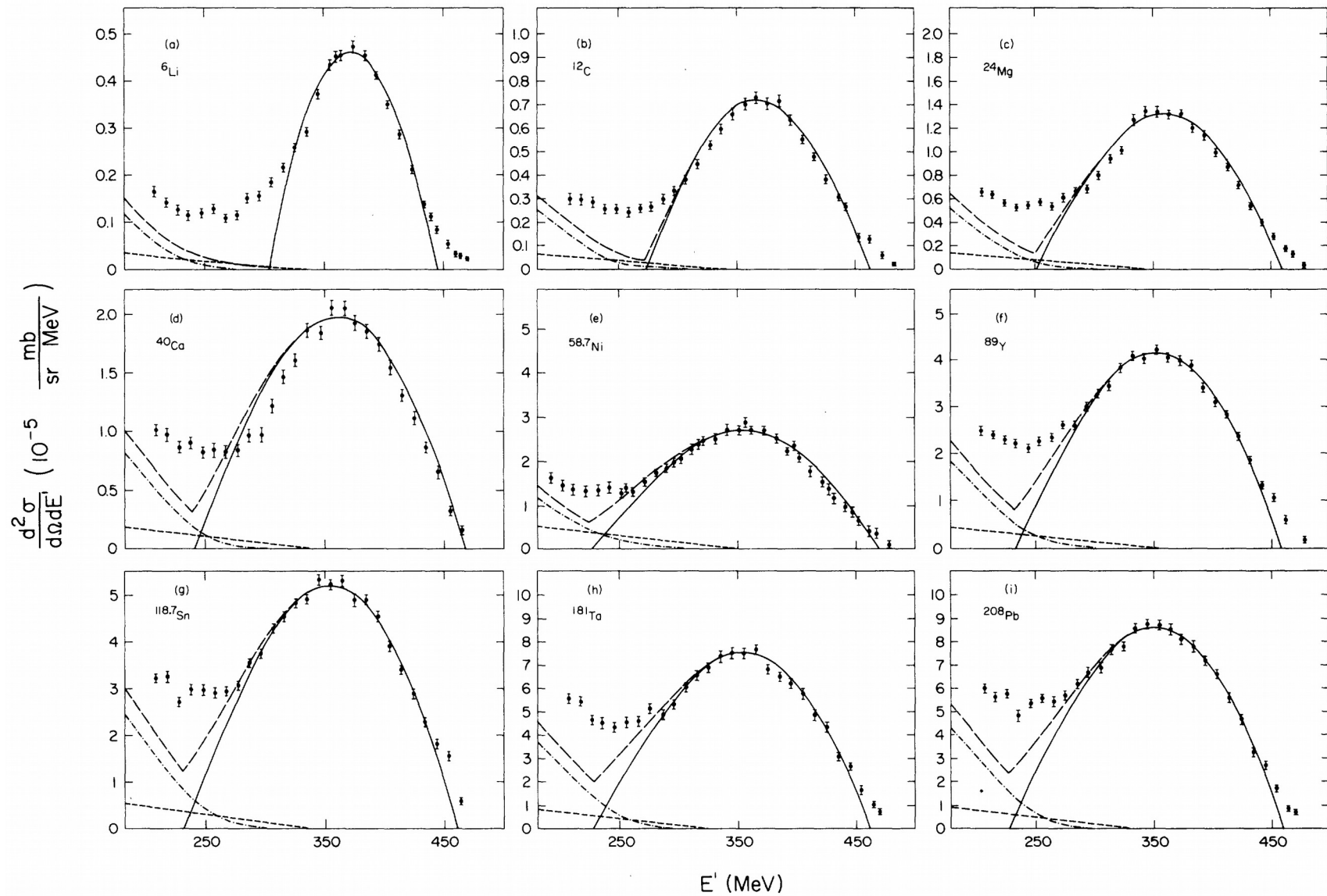
Moniz *et al.*, PRL 26, 445 (1971)

Electron scattering off carbon, 500 MeV, 60 deg



Moniz *et al.*, PRL 26, 445 (1971)

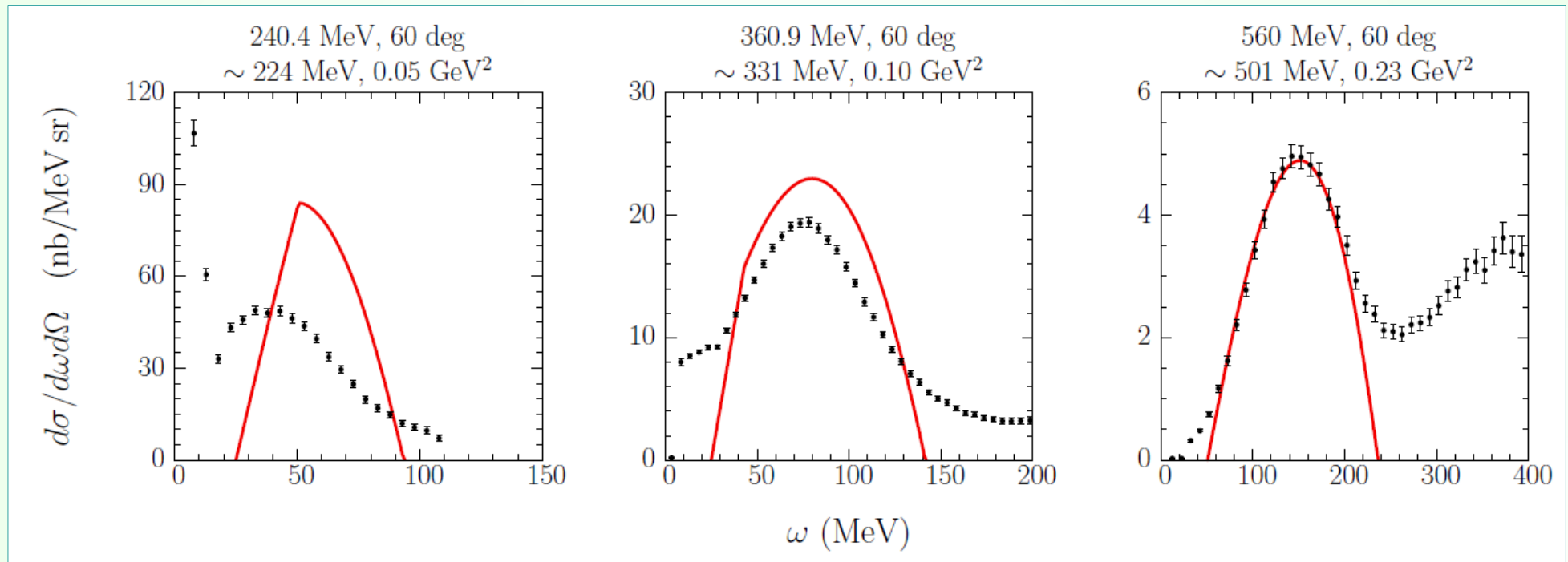
Fermi gas model



Whitney *et al.*, PRC 9, 2230 (1974)

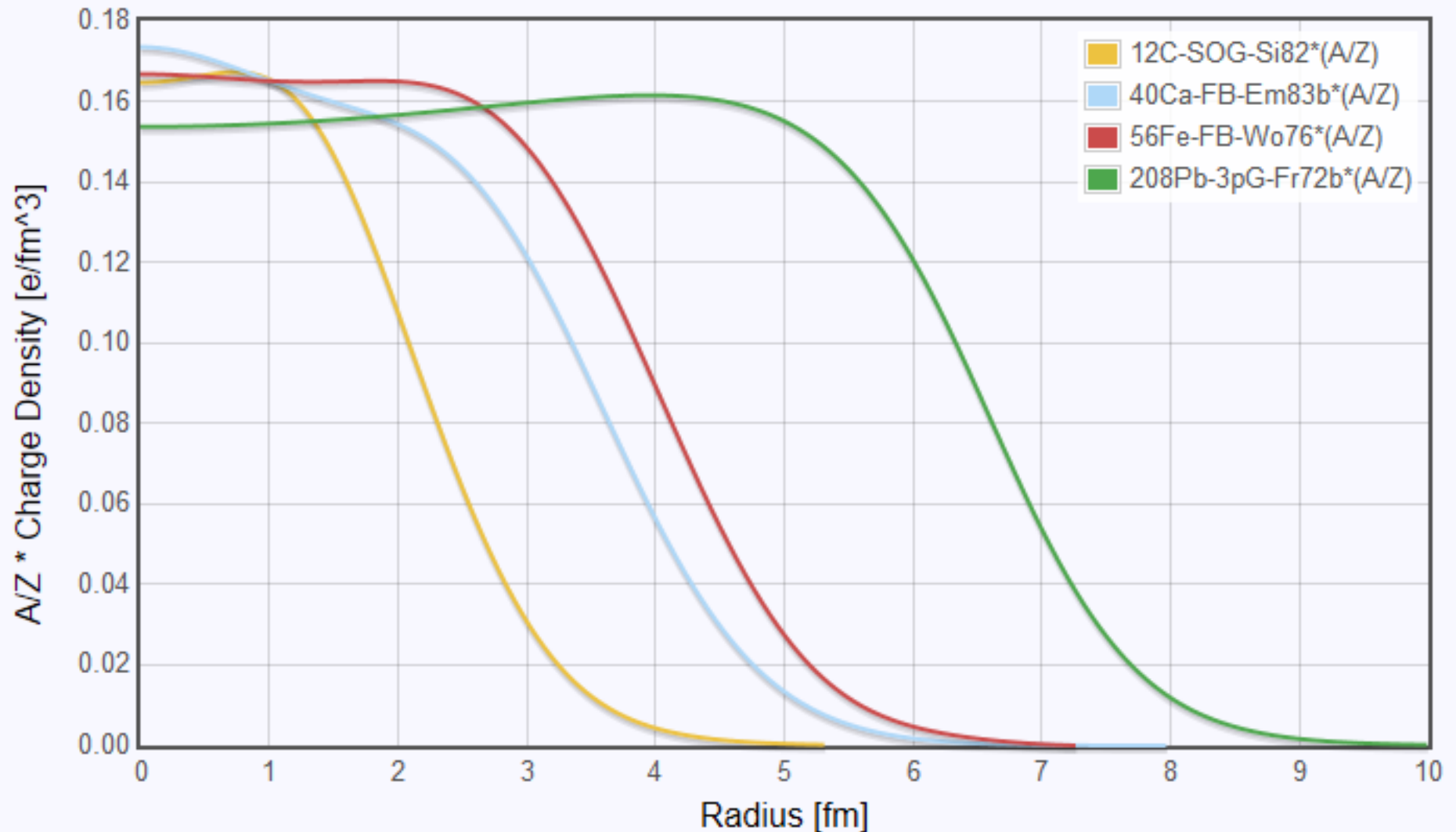
Fermi gas model

What happens at kinematics other than 500 MeV, 60 deg?



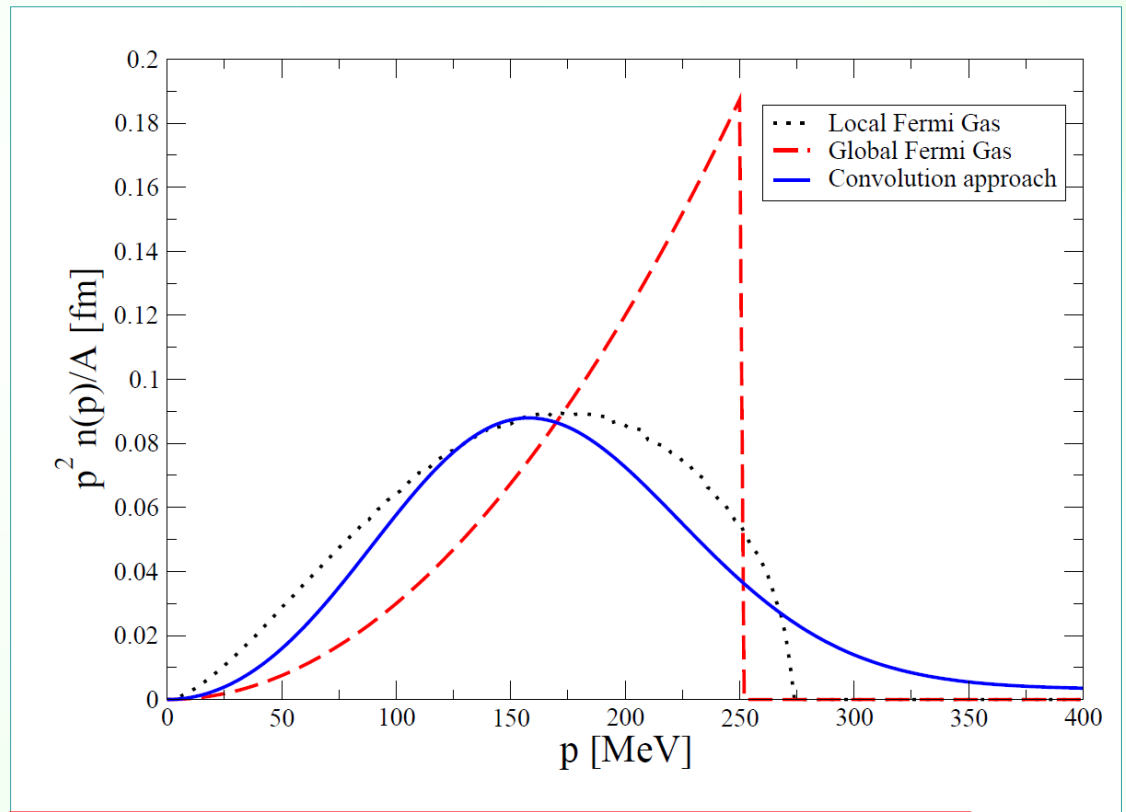
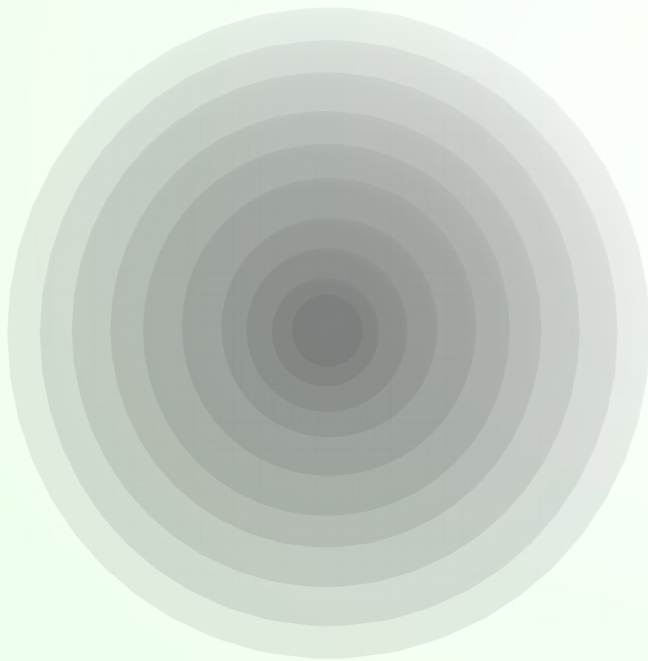
Barreau *et al.*, NPA 402, 515 (1983)

Charge-density in nuclei



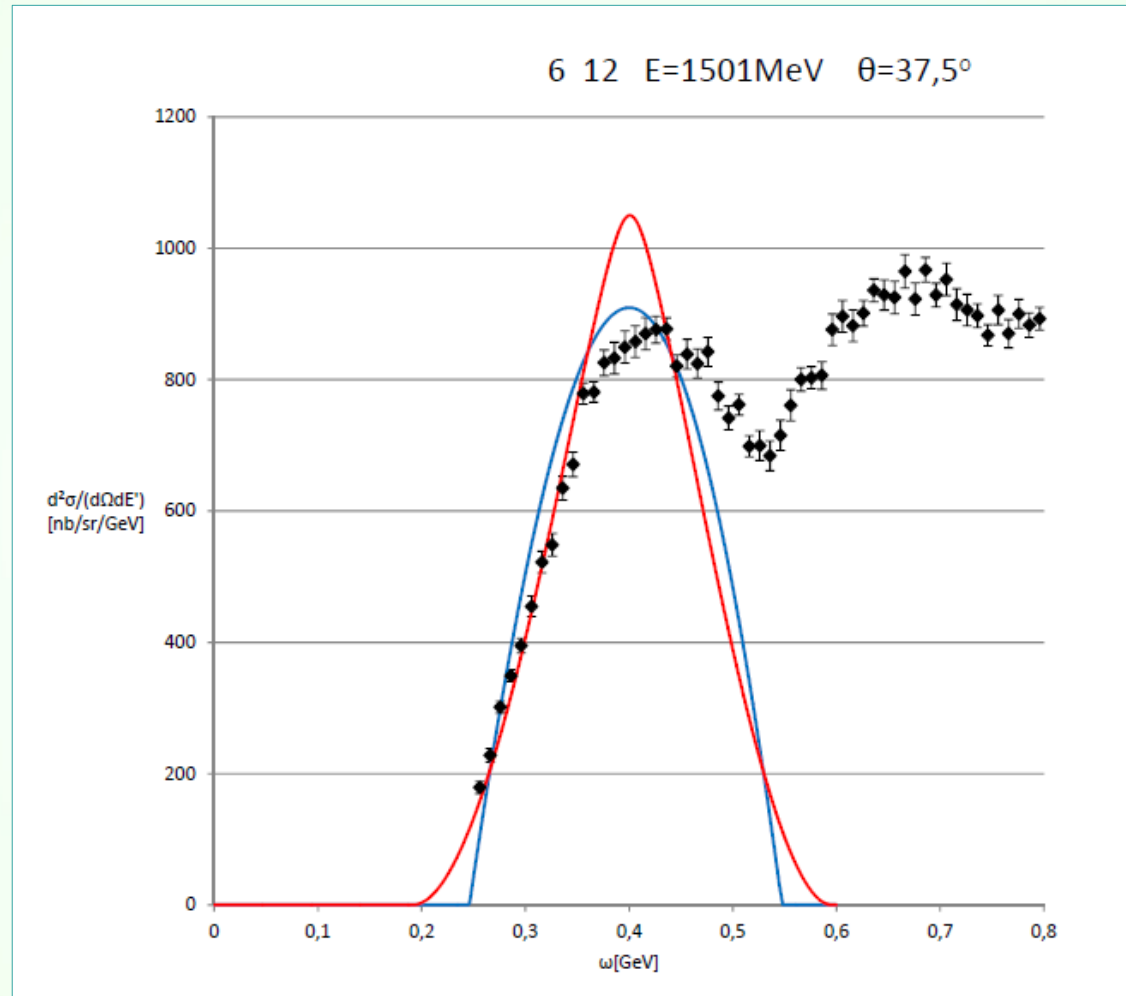
Local Fermi gas model

A spherically symmetric nucleus can be approximated by concentric spheres of a constant density.



L. Alvarez-Ruso *et al.*,
New J.Phys. 16, 075015 (2014)

Local vs. global Fermi gas models



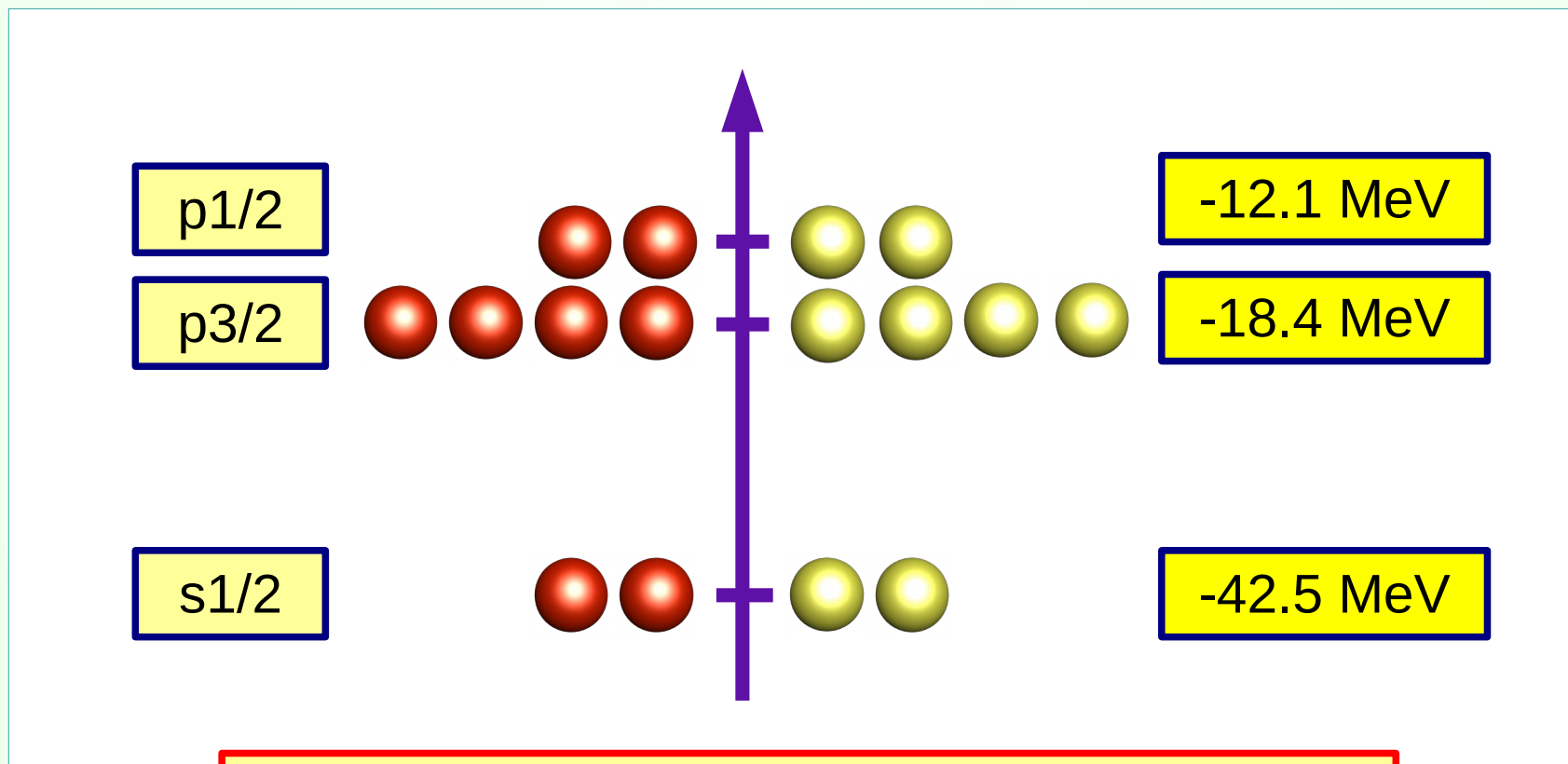
B. Kowal, M.Sc. thesis,
University of Wroclaw (2014)



Shell model

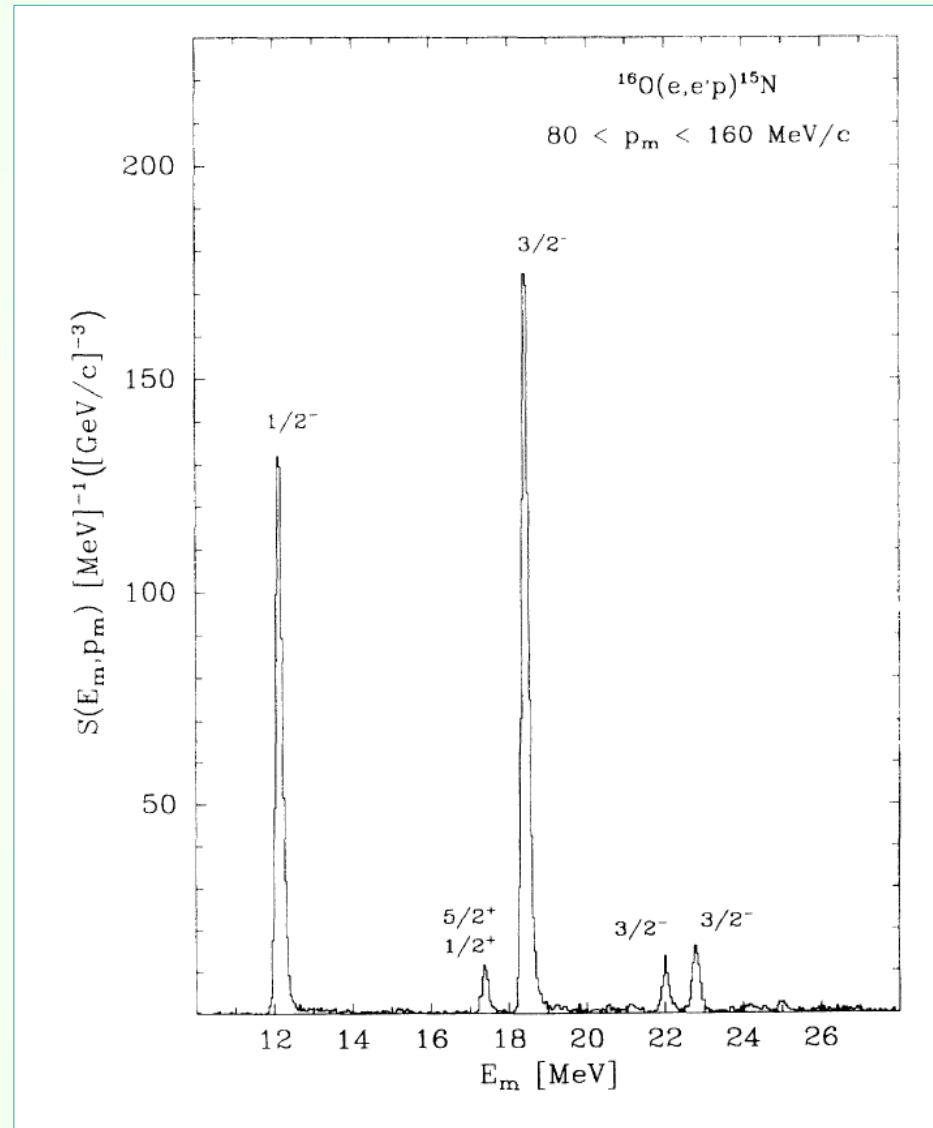
Shell model

In a spherically symmetric potential, the eigenstates can be labeled using the total angular momentum.



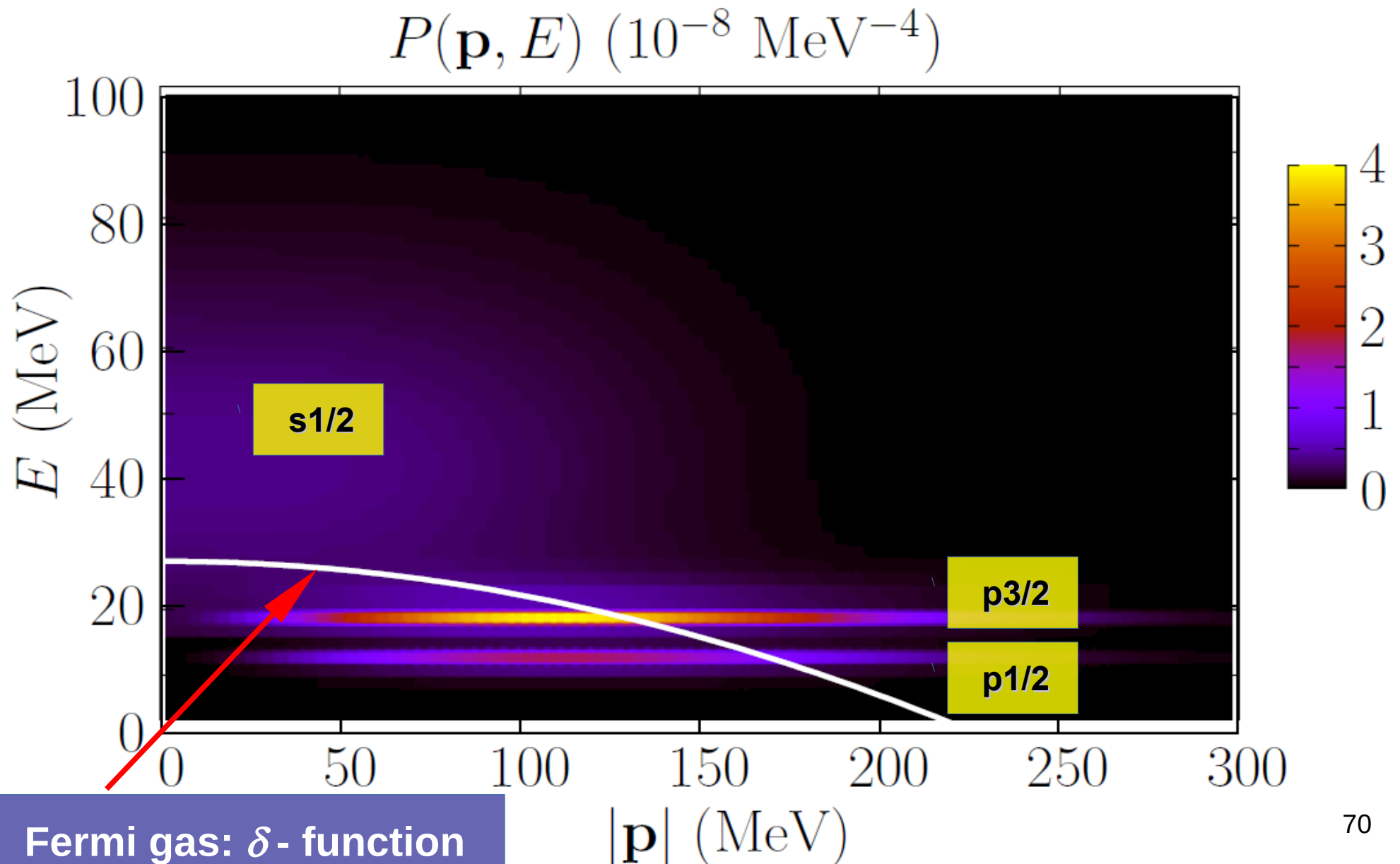
See e.g. Cohen, Concepts of Nuclear Physics, McGraw-Hill, 1971

Example: oxygen nucleus

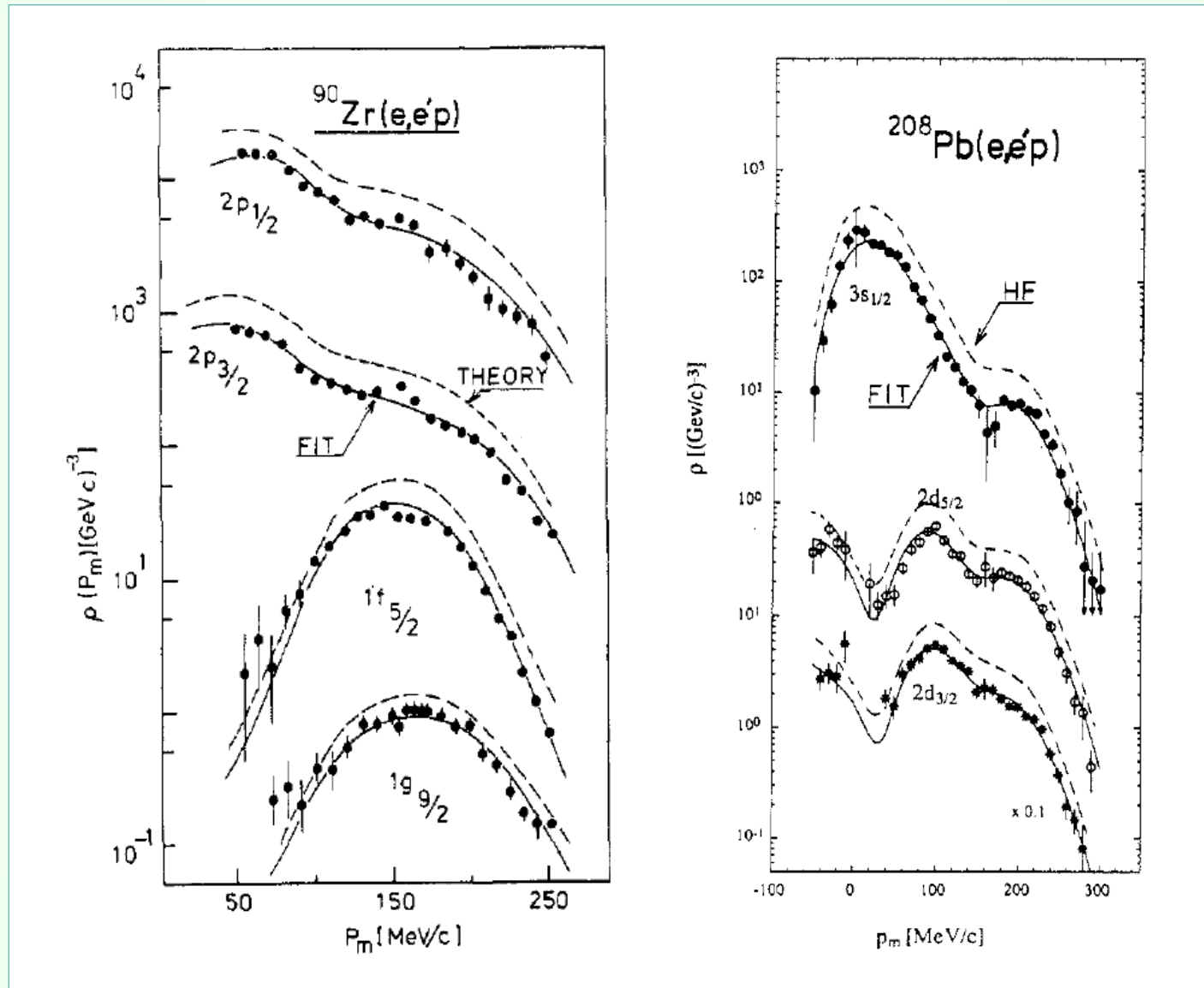


Leuschner *et al.*, PRC 49, 955 (1994)

Example: oxygen spectral function



Depletion of the shell-model states

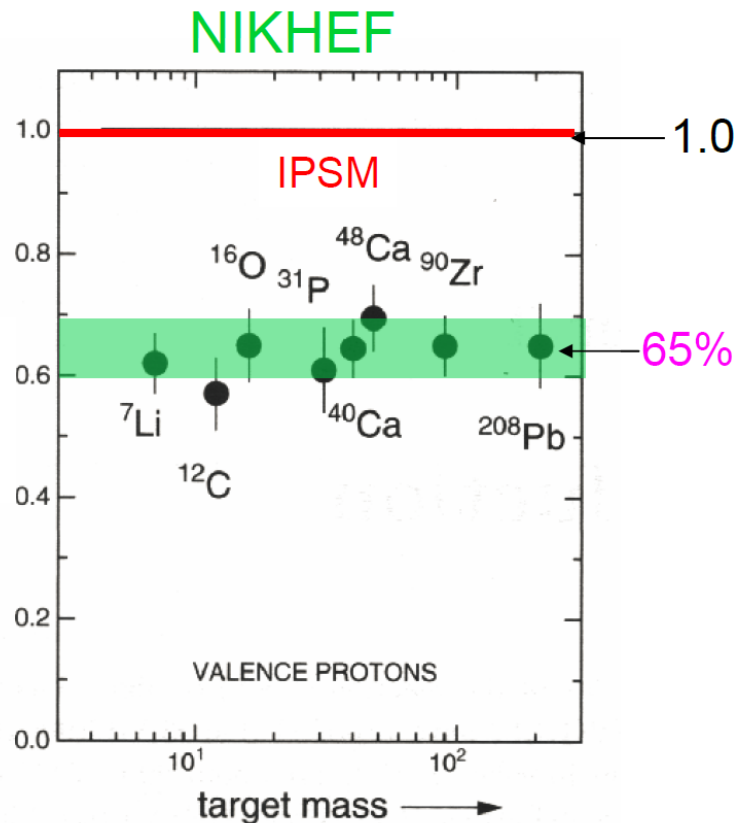


De Witt Huberts, JPG 16, 507 (1990)

Depletion of the shell-model states

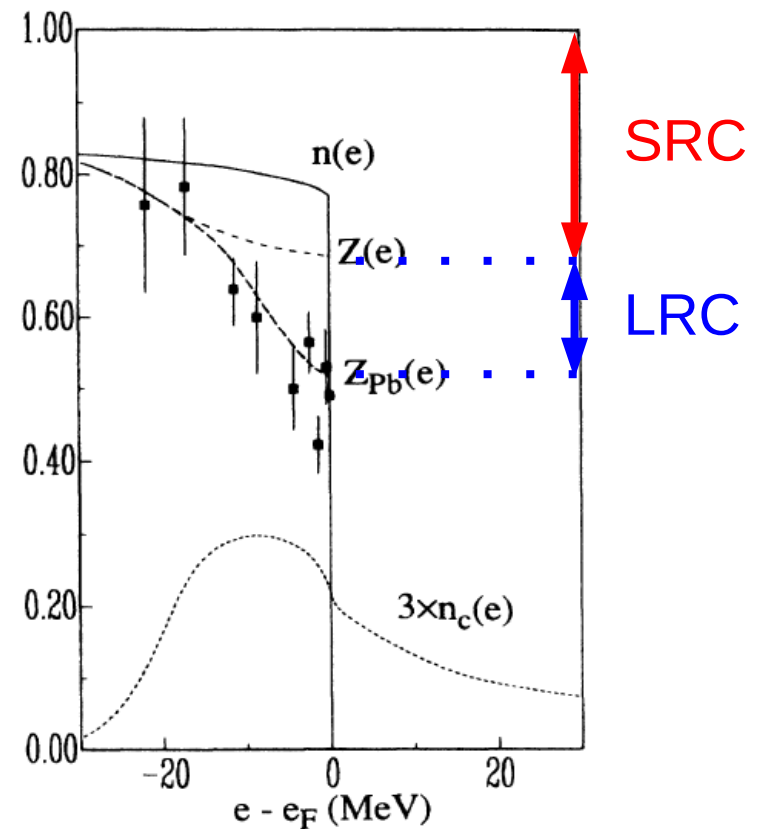
The observed depletion is $\sim 35\%$ for the valence shells (LRC and SRC) and $\sim 20\%$ when higher missing energy is probed (SRC).

Spectroscopic strengths/IPSM



D. Rohe, NuInt05

NIKHEF: $^{208}\text{Pb}(e,e'p)^{207}\text{Tl}$



Benhar et al, PRC 41, R24 (1990)

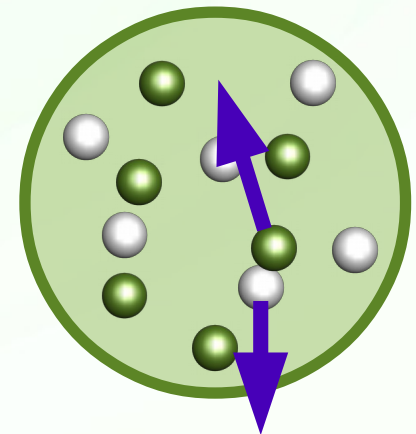


Spectral function approach

Short-range correlations


The main source of the depletion of the shell-model states at high E are **short-range nucleon-nucleon correlations**.

Yielding NN pairs (typically pn pairs) with high relative momentum, they move ~20% of nucleons to the states of high removal energies.



Short-range correlations

The hole spectral function can be expressed as

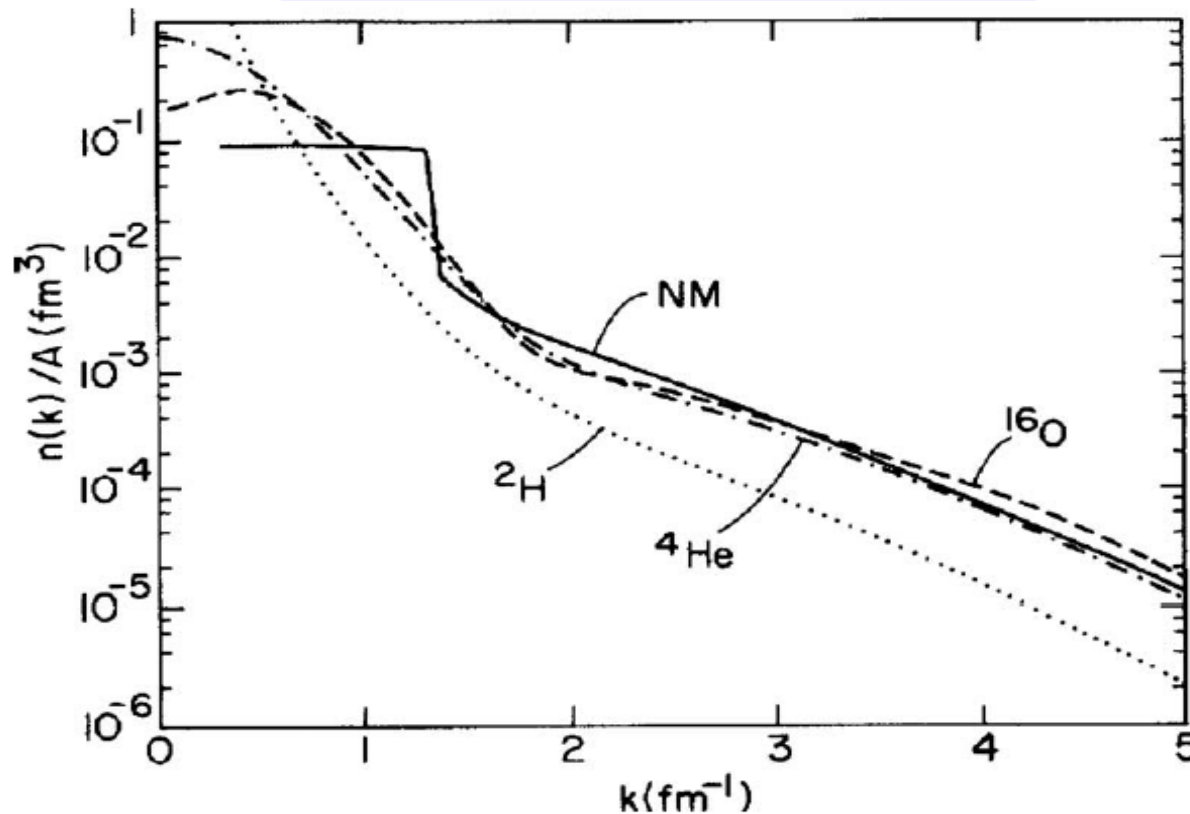
$$P_N(\mathbf{p}, E) = \sum_{\alpha} n_{\alpha} |\phi_{\alpha}|^2 f_{\alpha}(E - E_{\alpha}^N) + P_{\text{corr}}^N(\mathbf{p}, E),$$


describes the contribution
of the shell-model states,
vanishes at high $|\mathbf{p}|$ or high E

relevant only
at high $|\mathbf{p}|$ **and** E

Short-range correlations

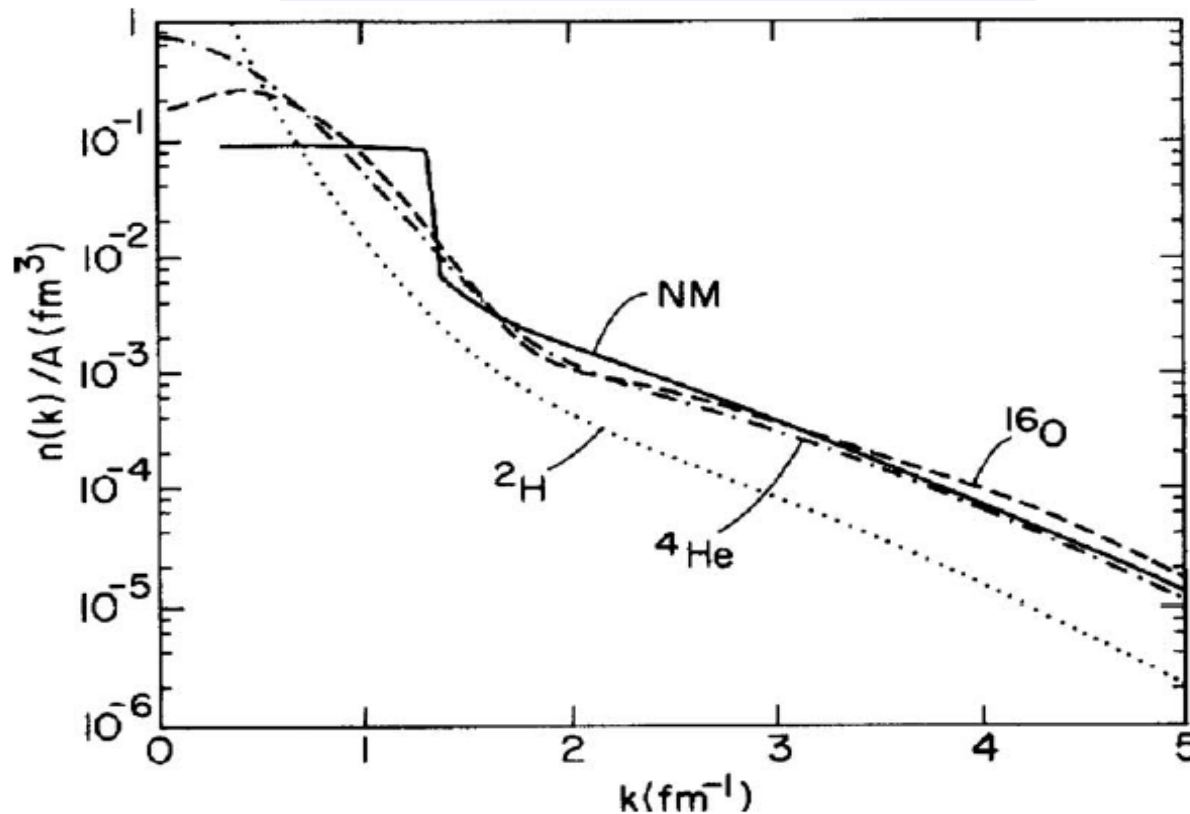
Momentum distributions



Benhar&Pandharipande, RMP 65, 817 (1993)

Short-range correlations

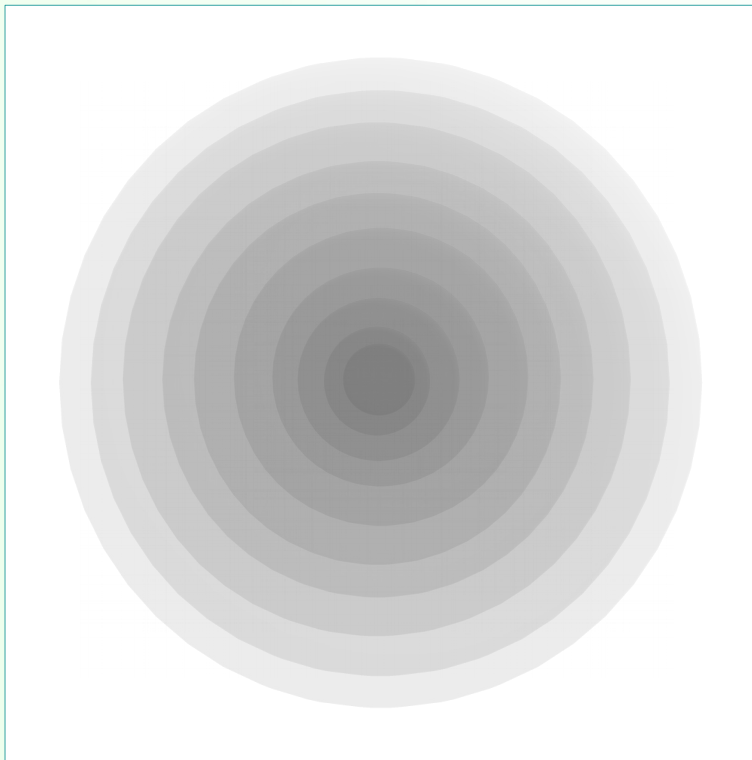
Momentum distributions



SRC don't depend on the shell structure or finite-size effects, only on the density

Local-density approximation

The correlation component in nuclei can be obtained combining the results for infinite nuclear matter obtained at different densities:

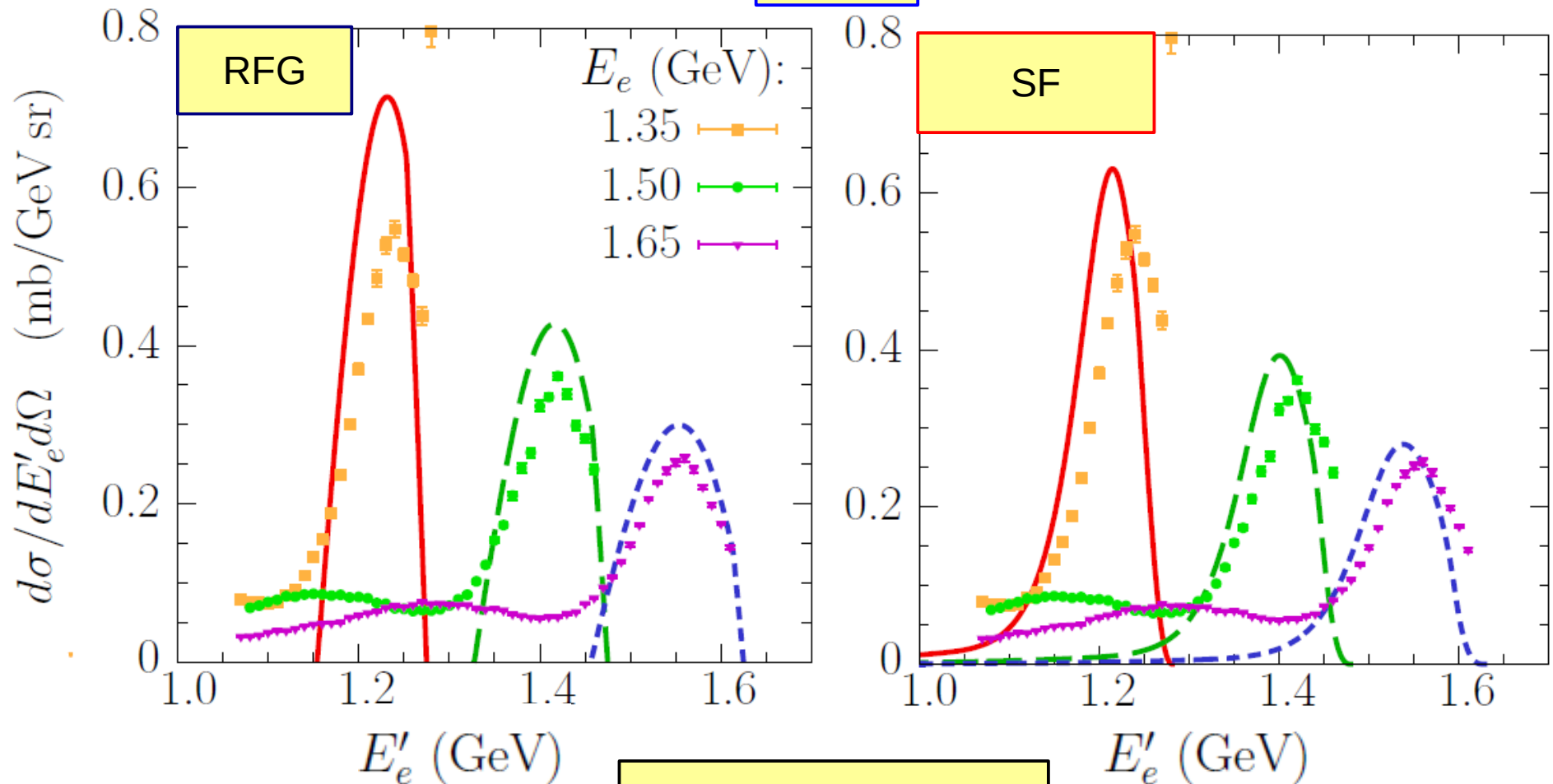


$$P_{\text{corr}}^N(\mathbf{p}, E) = \int dR \rho(R) P_{\text{corr}}^{NM,N}(\rho, \mathbf{p}, E).$$

Benhar *et al.*, NPA 579 493, (1994),
included Urbana v_{14} NN interactions
and 3N interactions
[Lagaris & Pandharipande]

Comparison to $C(e, e')$ data

13.5°



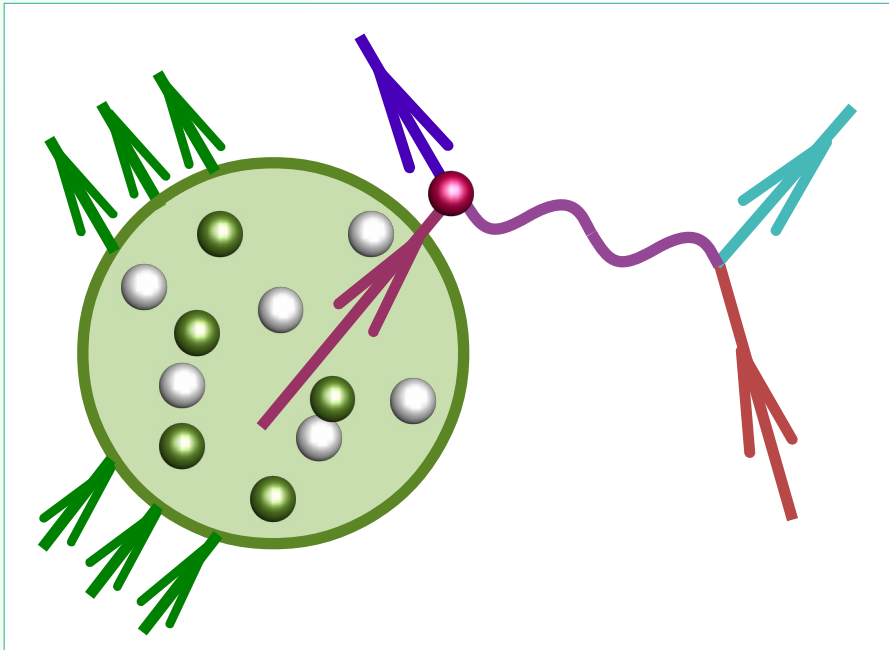
data: Baran *et al.*,
PRL 61, 400 (1988)

Energy conservation

$$E_{\mathbf{k}} + M_A = E_{\mathbf{k}'} + E_{A-1} + E_{\mathbf{p}'}$$

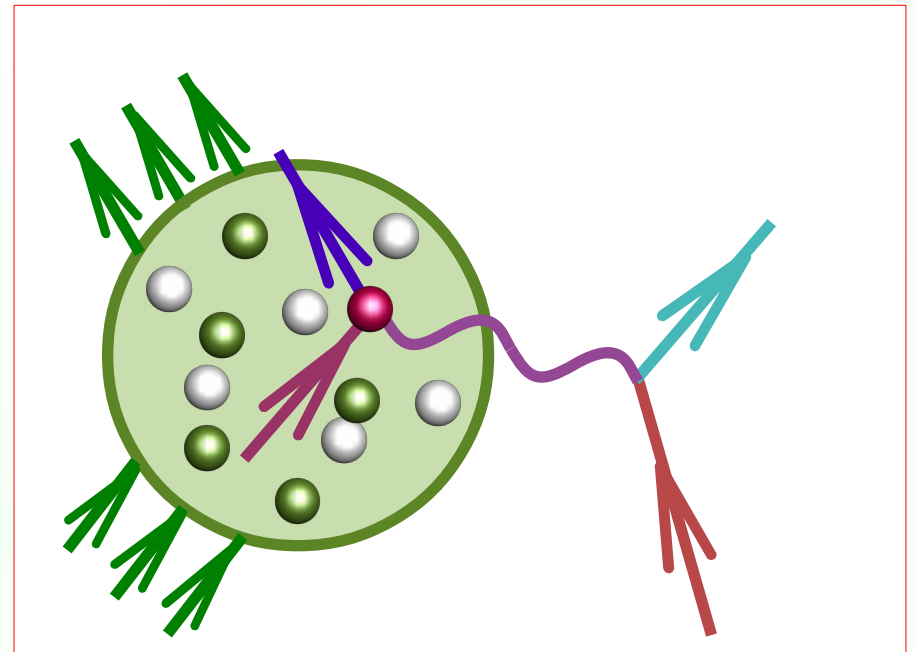
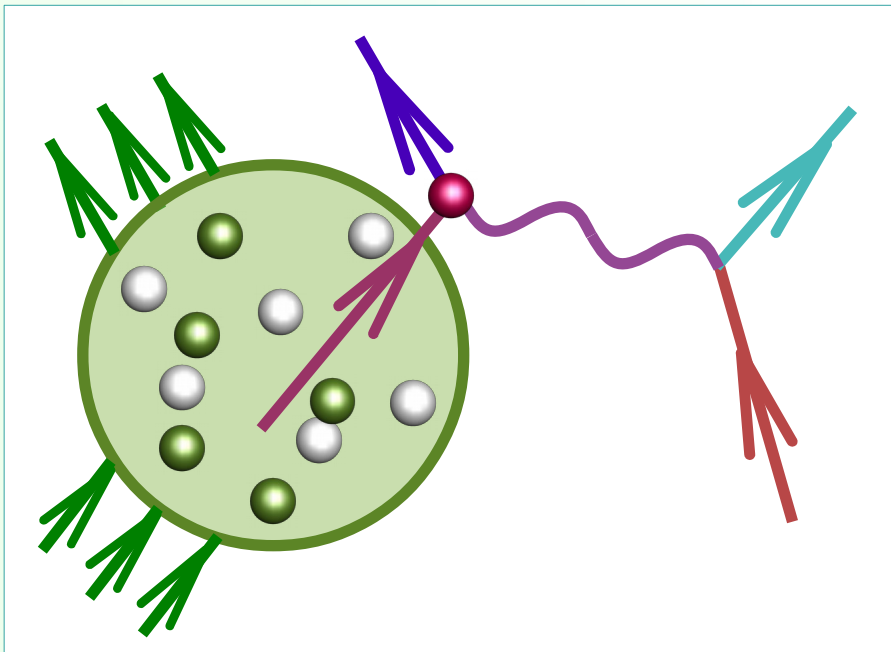
Energy conservation

$$E_{\mathbf{k}} + M_A = E_{\mathbf{k}'} + E_{A-1} + E_{\mathbf{p}'}$$



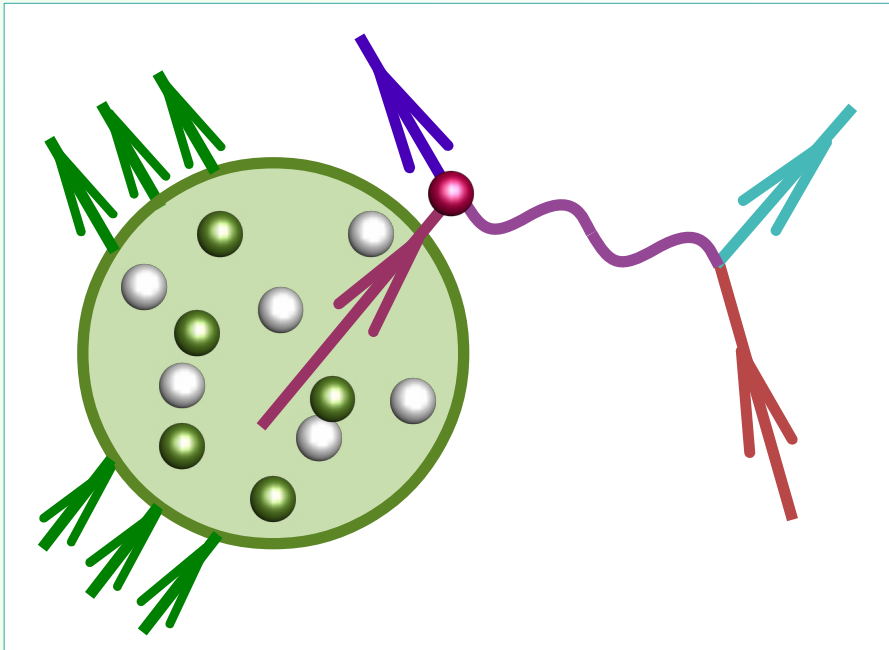
Energy conservation

$$E_{\mathbf{k}} + M_A = E_{\mathbf{k}'} + E_{A-1} + E_{\mathbf{p}'}$$

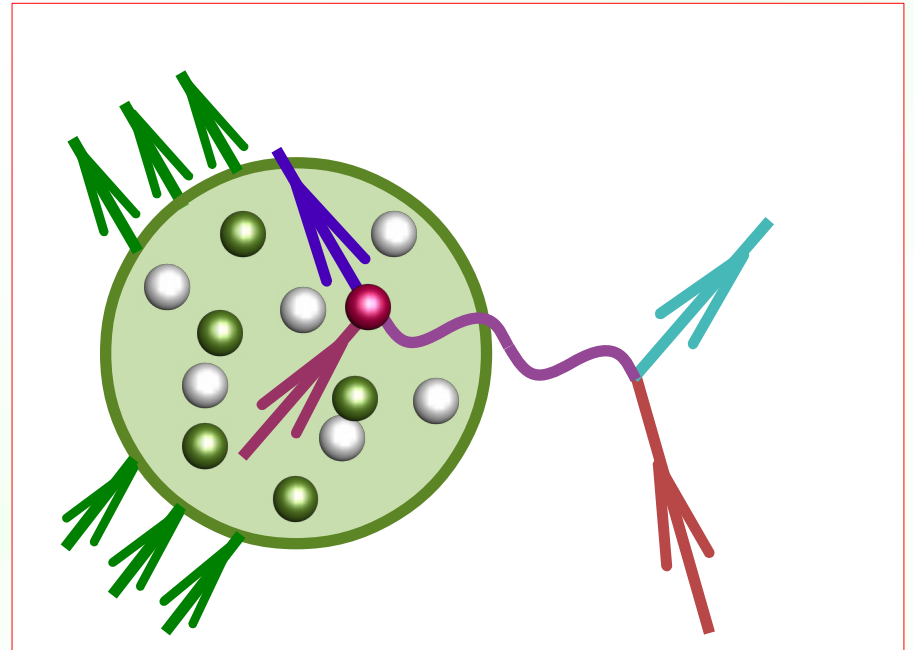


Energy conservation

$$E_{\mathbf{k}} + M_A = E_{\mathbf{k}'} + E_{A-1} + E_{\mathbf{p}'}$$

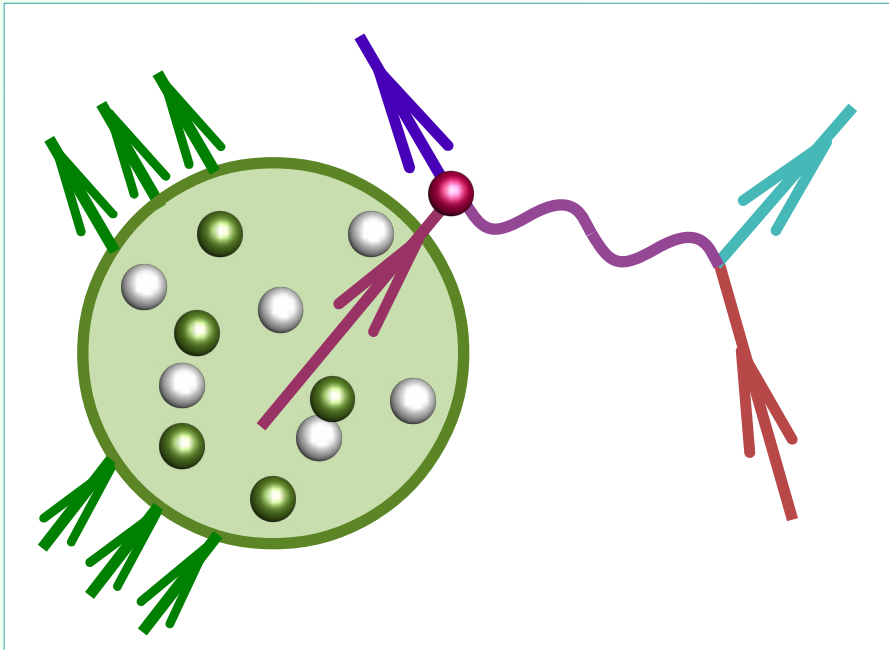


$$E_{\mathbf{k}} + M_A = E_{\mathbf{k}'} + E_{A-1} + E_{\mathbf{p}'} + U_V(\mathbf{p}')$$

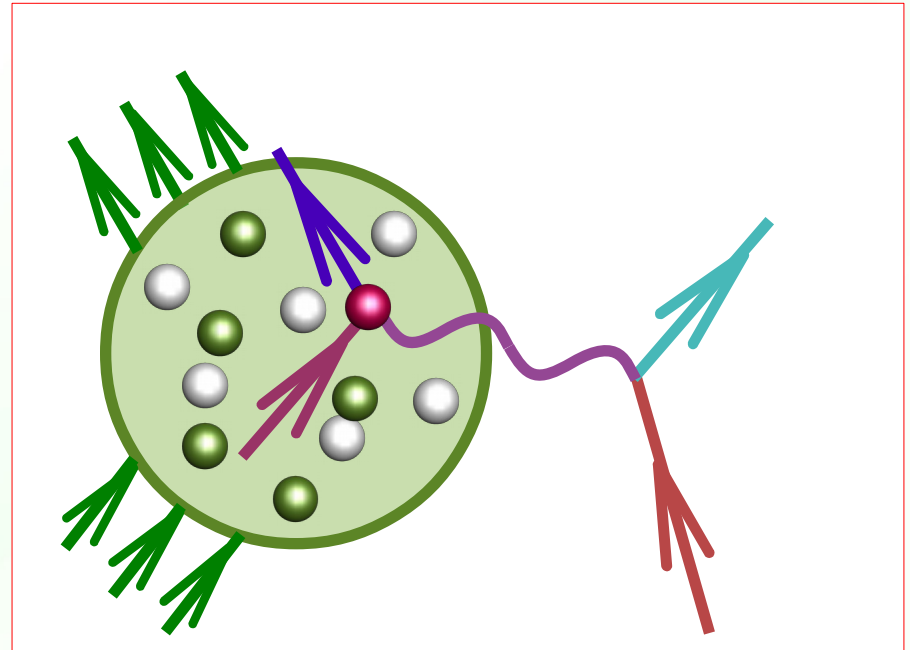


Energy conservation

$$E_{\mathbf{k}} + M_A = E_{\mathbf{k}'} + E_{A-1} + E_{\mathbf{p}'}$$



$$E_{\mathbf{k}} + M_A \approx E_{\mathbf{k}'} + E_{A-1} + E_{\mathbf{p}'} + U_V(\mathbf{p}')$$



Final-state interactions

Their effect on the cross section is easy to understand in terms of the complex optical potential:

- the **real part** modifies the struck nucleon's energy spectrum: it differs from $\sqrt{M^2 + \mathbf{p}^2}$
- the **imaginary part** reduces the single-nucleon final states and produces multinucleon final states

$$e^{i(E+U)t} = e^{i(E+U_V)t} e^{-U_W t}$$

Horikawa *et al.*, PRC 22, 1680 (1980)

Final-state interactions

In the convolution approach,

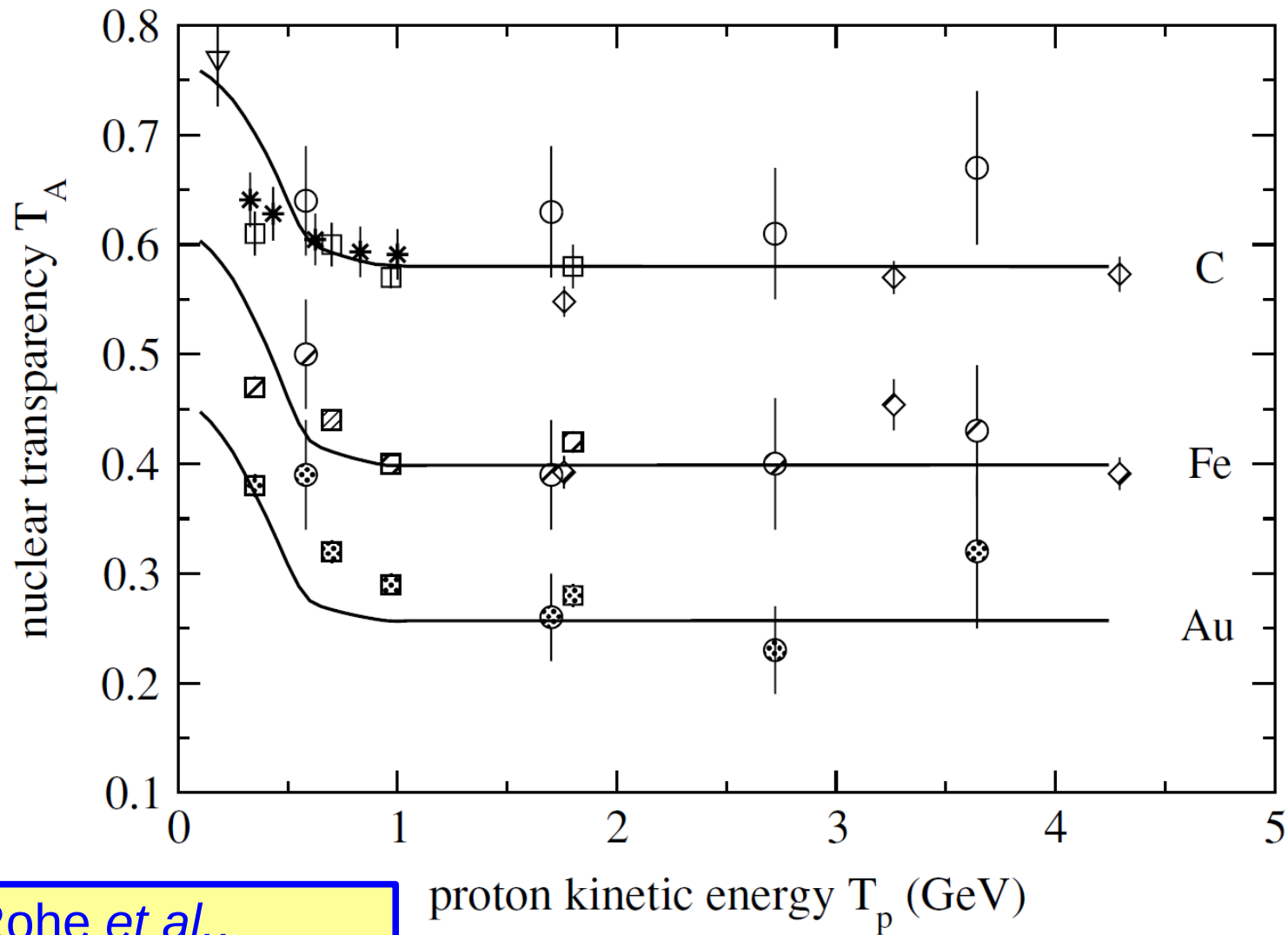
$$\frac{d\sigma^{\text{FSI}}}{d\omega d\Omega} = \int d\omega' f_{\mathbf{q}}(\omega - \omega') \frac{d\sigma^{\text{IA}}}{d\omega' d\Omega},$$

with the folding function

$$f_{\mathbf{q}}(\omega) = \delta(\omega) \sqrt{T_A} + (1 - \sqrt{T_A}) F_{\mathbf{q}}(\omega),$$

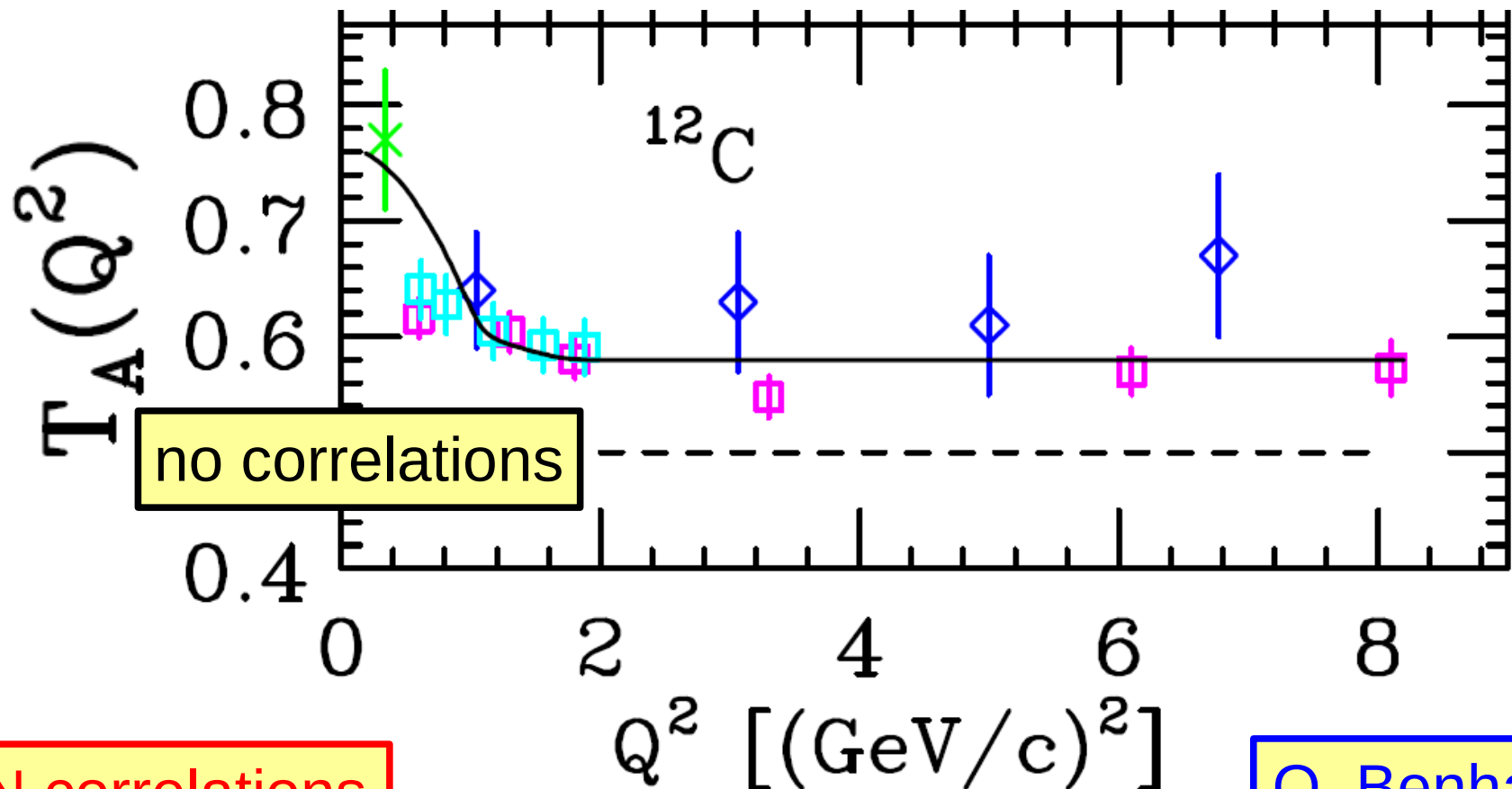
Nucl. transparency

Nuclear transparency



Rohe *et al.*,
PRC 72, 054602 (2005)

Nuclear transparency

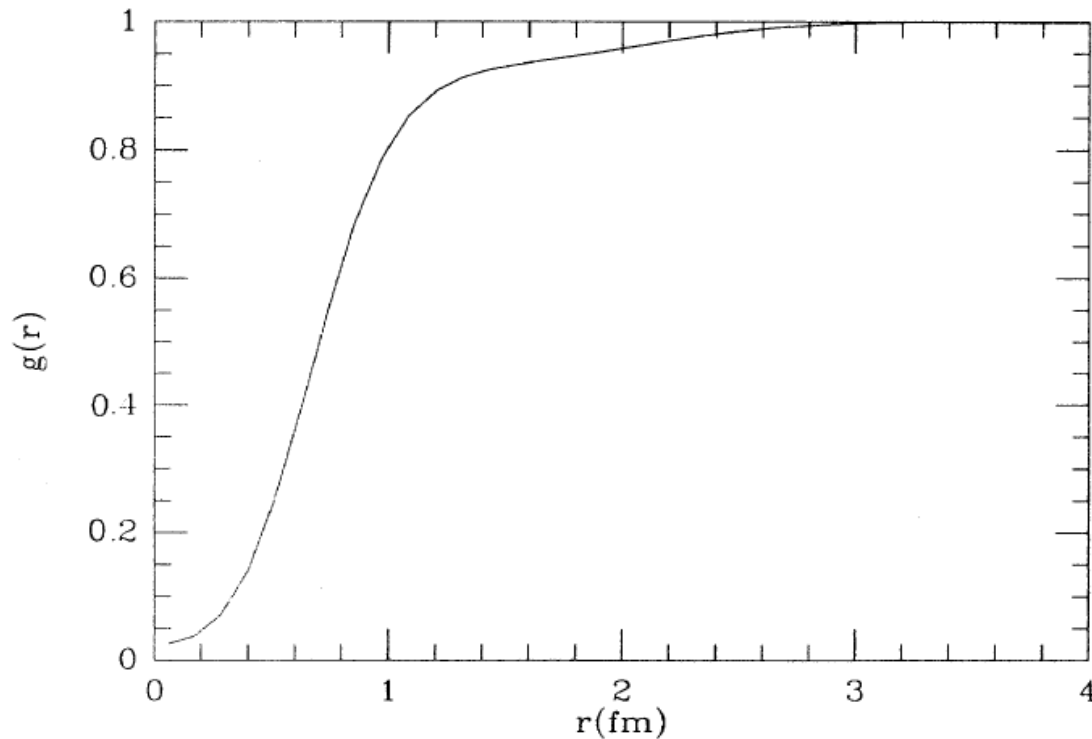


NN correlations
reduce FSI

O. Benhar
@ NuInt05

Short-range correlations

Pair distribution function of NM



Benhar *et al.*, PRC 44, 2328 (1991)

Real part of the optical potential

We account for the spectrum modification by

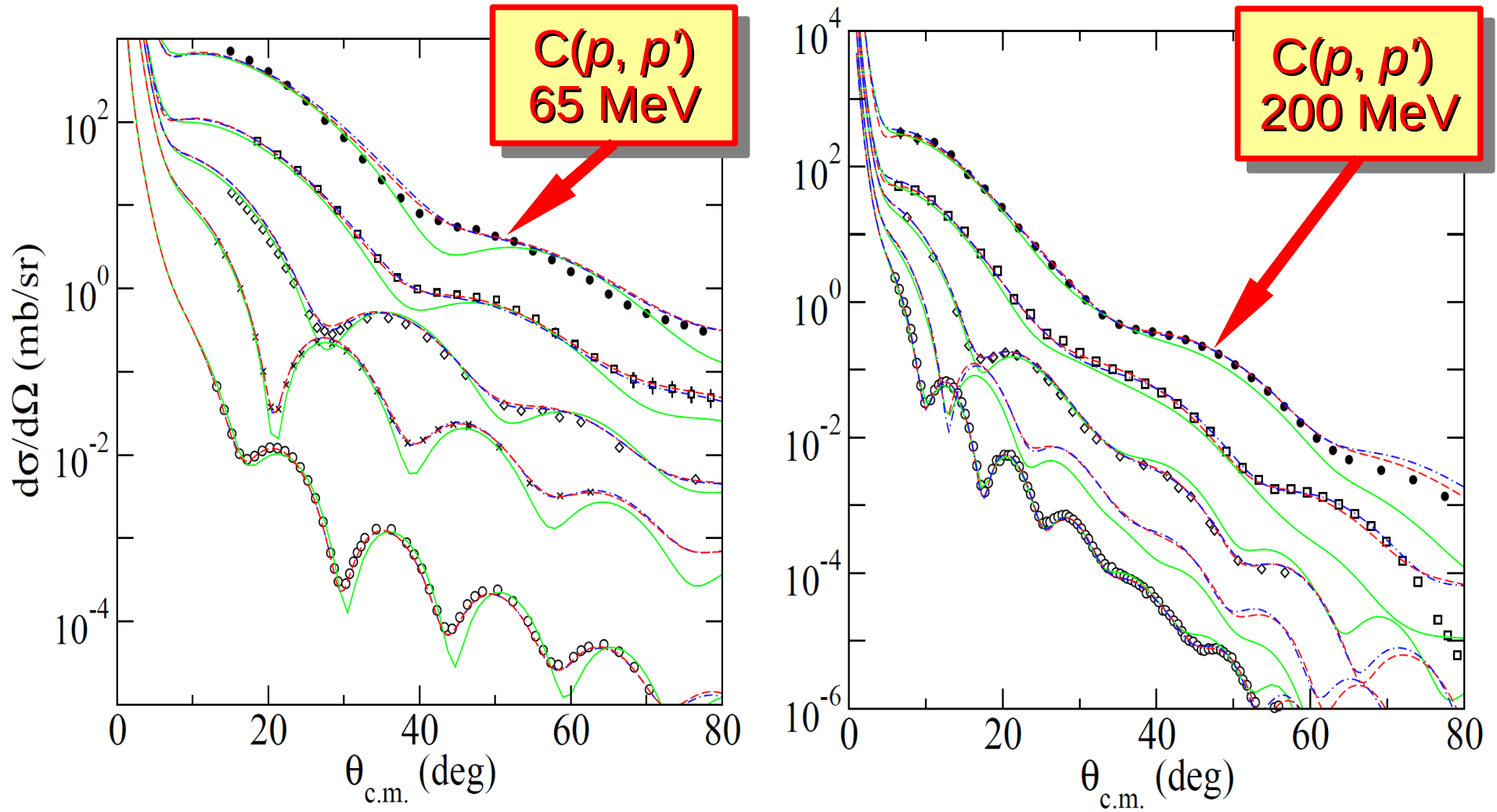
$$f_{\mathbf{q}}(\omega - \omega') \rightarrow f_{\mathbf{q}}(\omega - \omega' - U_V).$$

This procedure is similar to that from the Fermi gas model to introduce the binding energy in the argument of $\delta(\dots)$.

$$U_V = U_V(t_{\text{kin}})$$

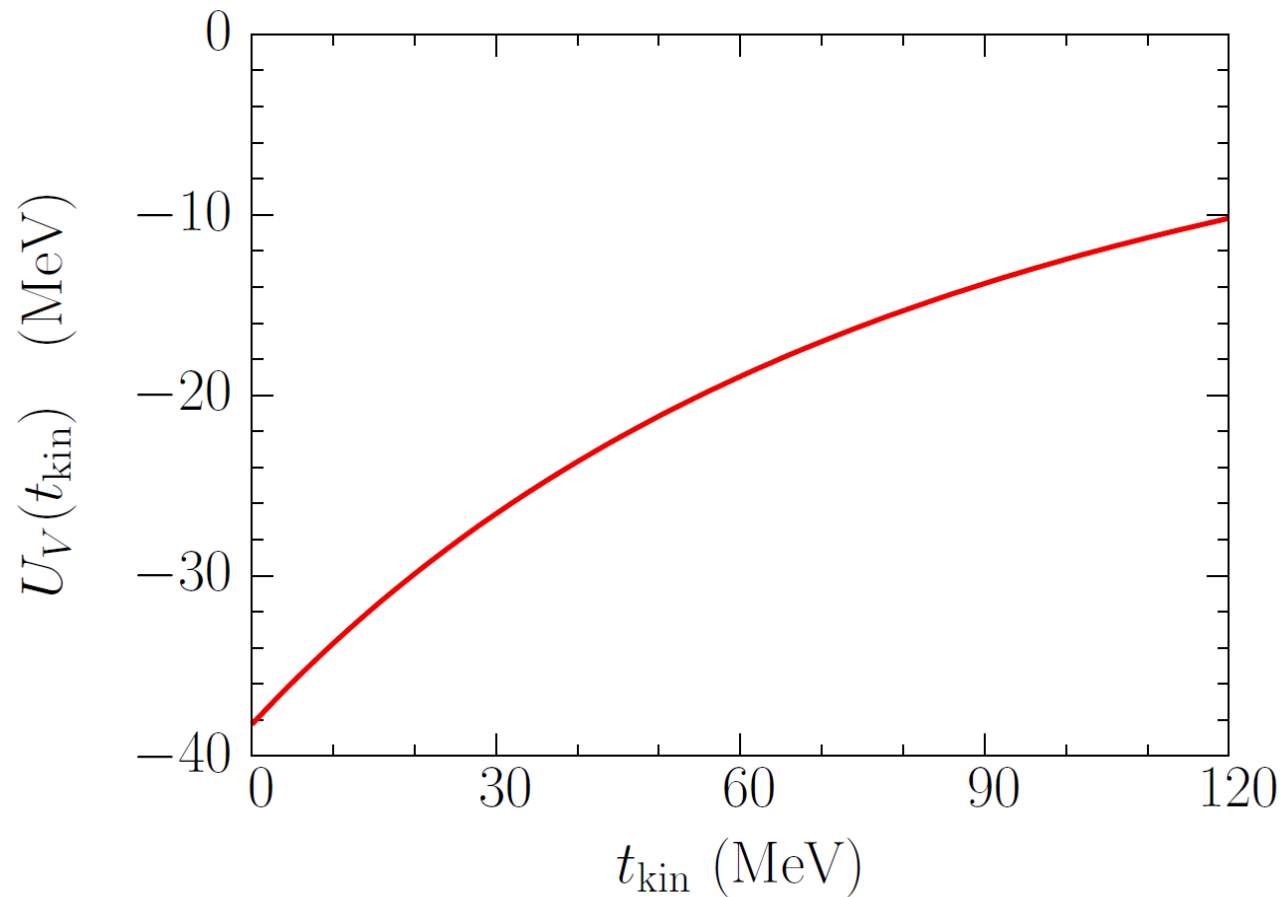
$$t_{\text{kin}} = \frac{E_{\mathbf{k}}^2(1 - \cos \theta)}{M + E_{\mathbf{k}}(1 - \cos \theta)}$$

Optical potential by Cooper *et al.*



Deb *et al.*, PRC 72, 014608 (2005)

Optical potential by Cooper *et al.*



obtained from
Cooper *et al.*, PRC 47, 297 (1993)

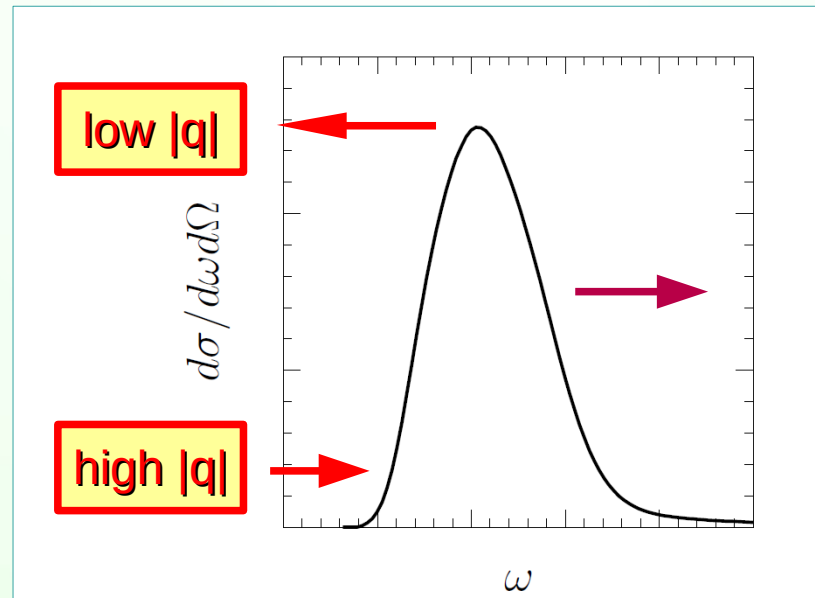
Simple comparison

Real part of the OP

- acts in the **final** state
- shifts the QE peak to **low** ω at low $|\mathbf{q}|$
(to high ω at high $|\mathbf{q}|$)

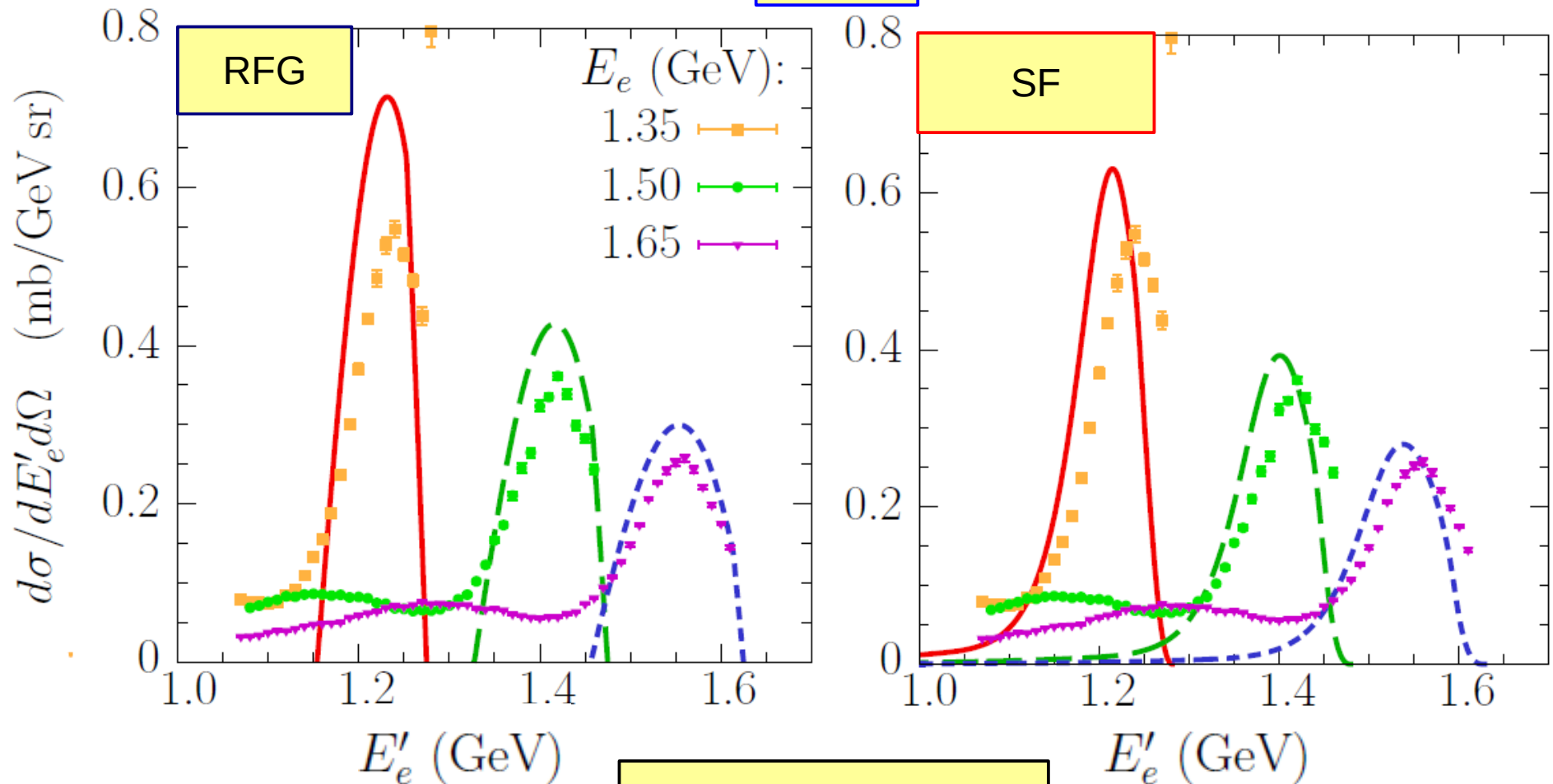
Binding energy in RFG

- acts in the **initial** state
- shifts the QE peak to **high** ω



Comparison to $C(e, e')$ data

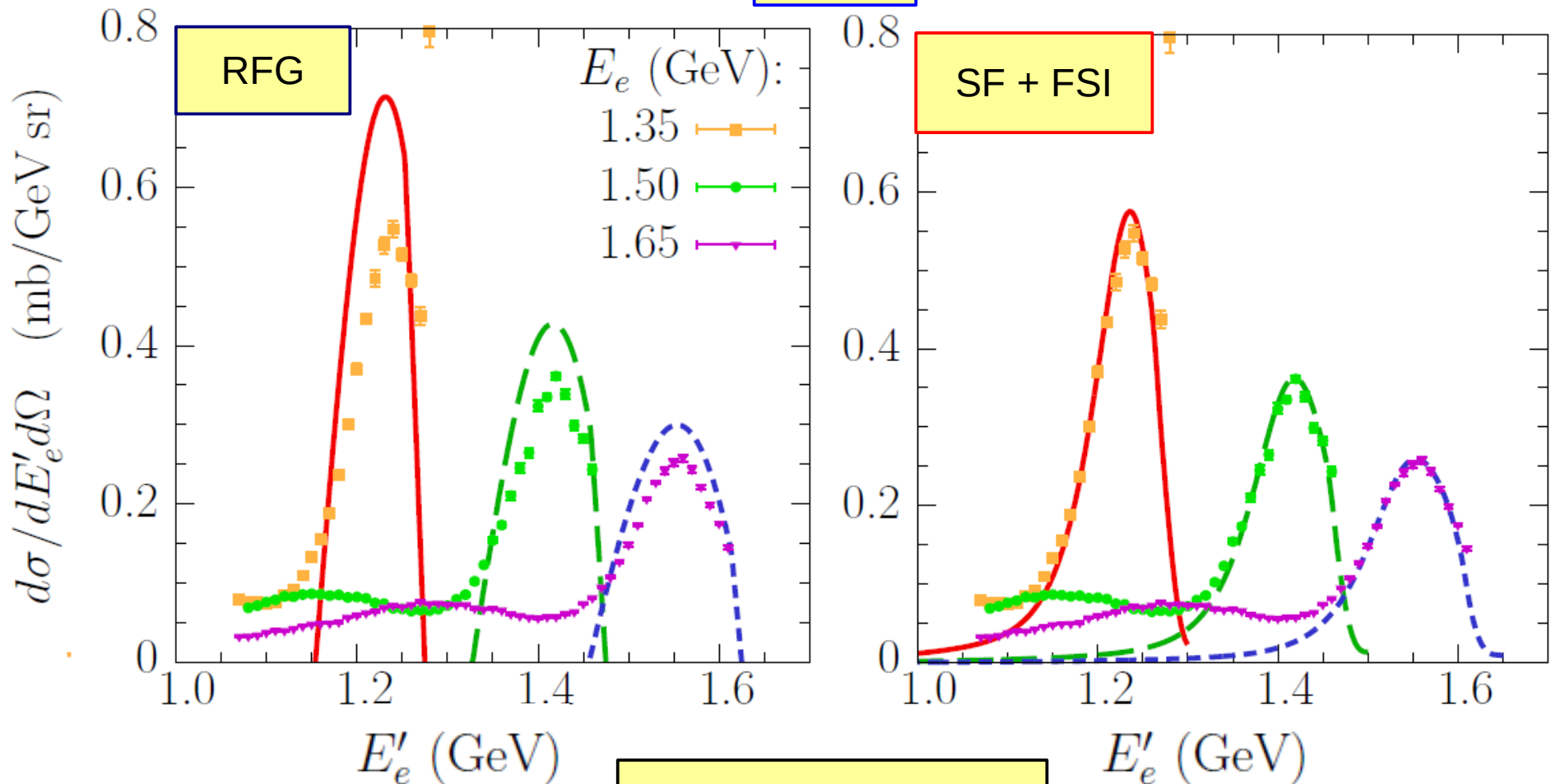
13.5°



data: Baran *et al.*,
PRL 61, 400 (1988)

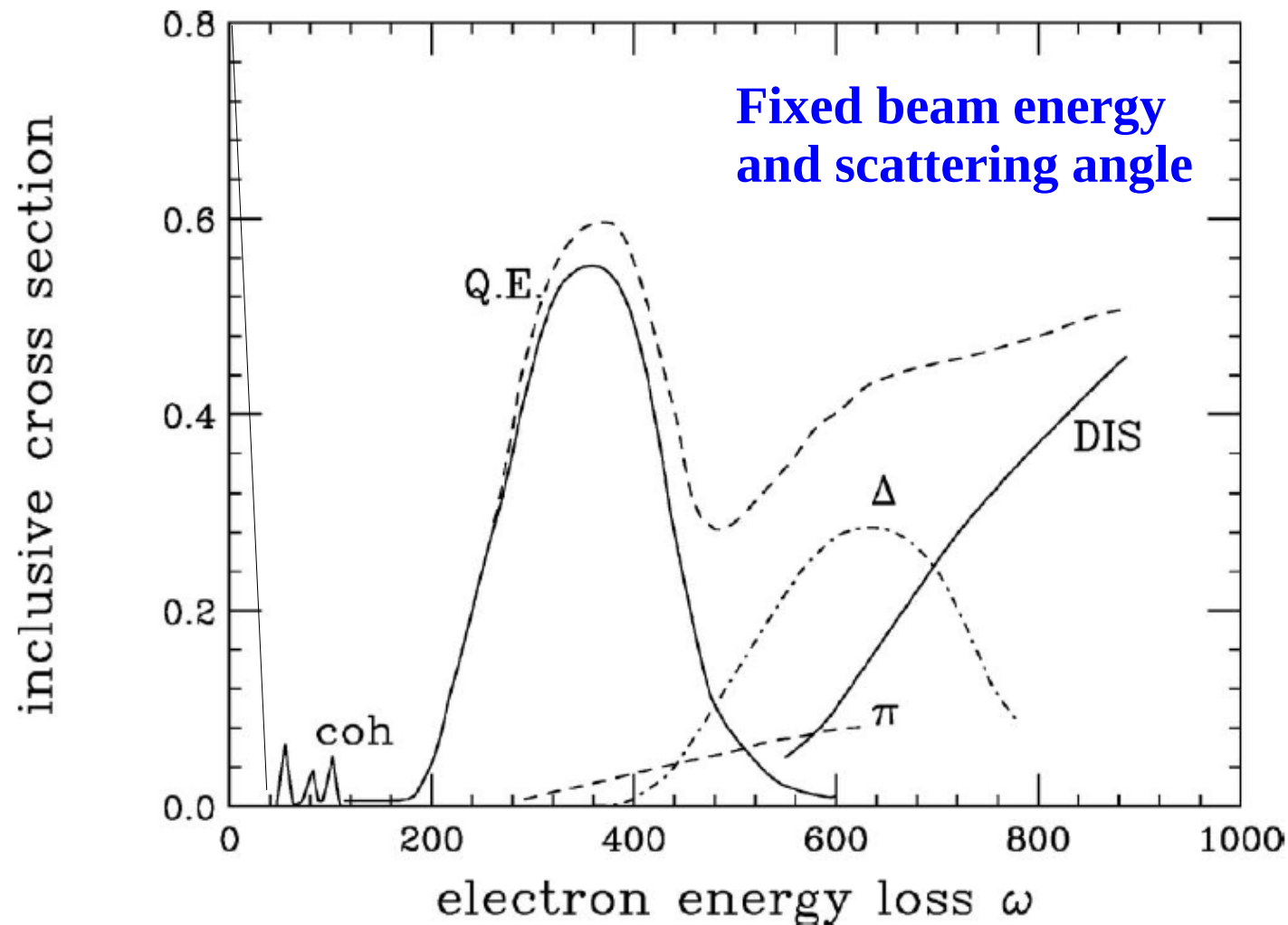
Comparison to $C(e, e')$ data

13.5°



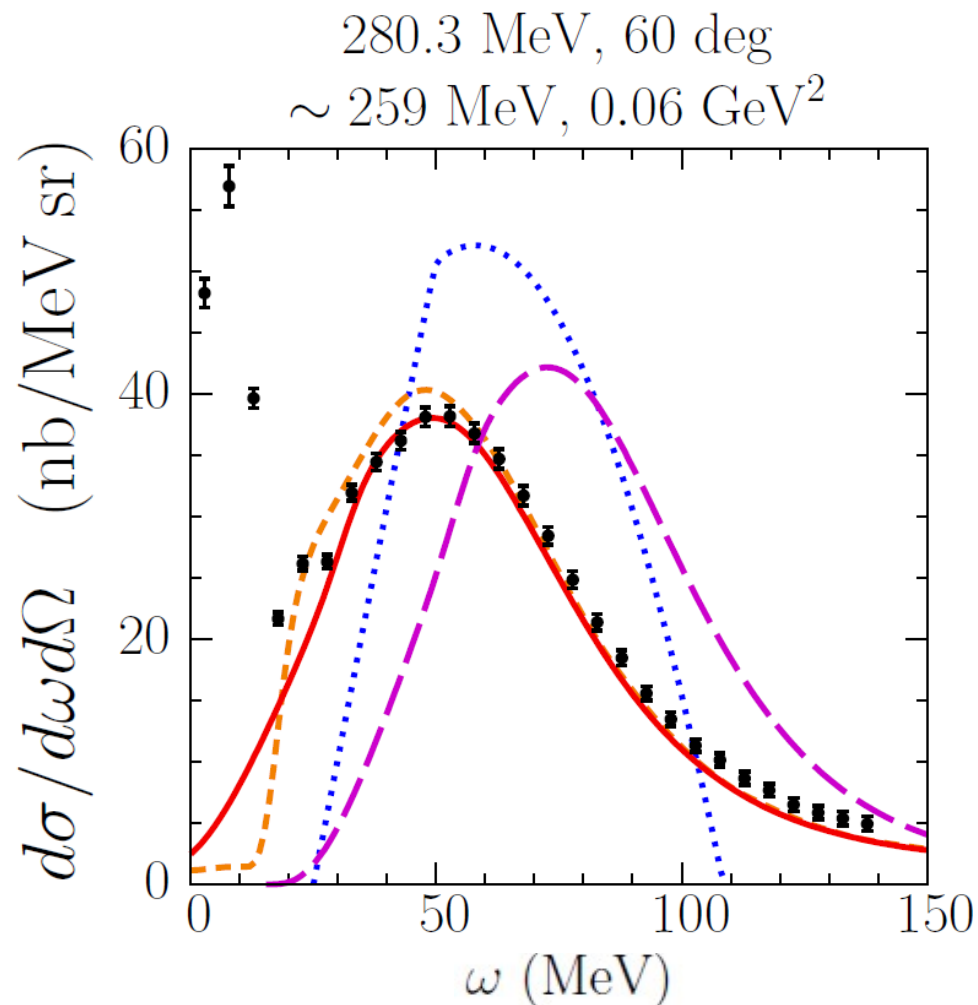
data: Baran *et al.*,
PRL 61, 400 (1988)

Importance of quasielastic scattering



adopted from Benhar *et al.*, RMP 80, 189 (2008)

Compared calculations



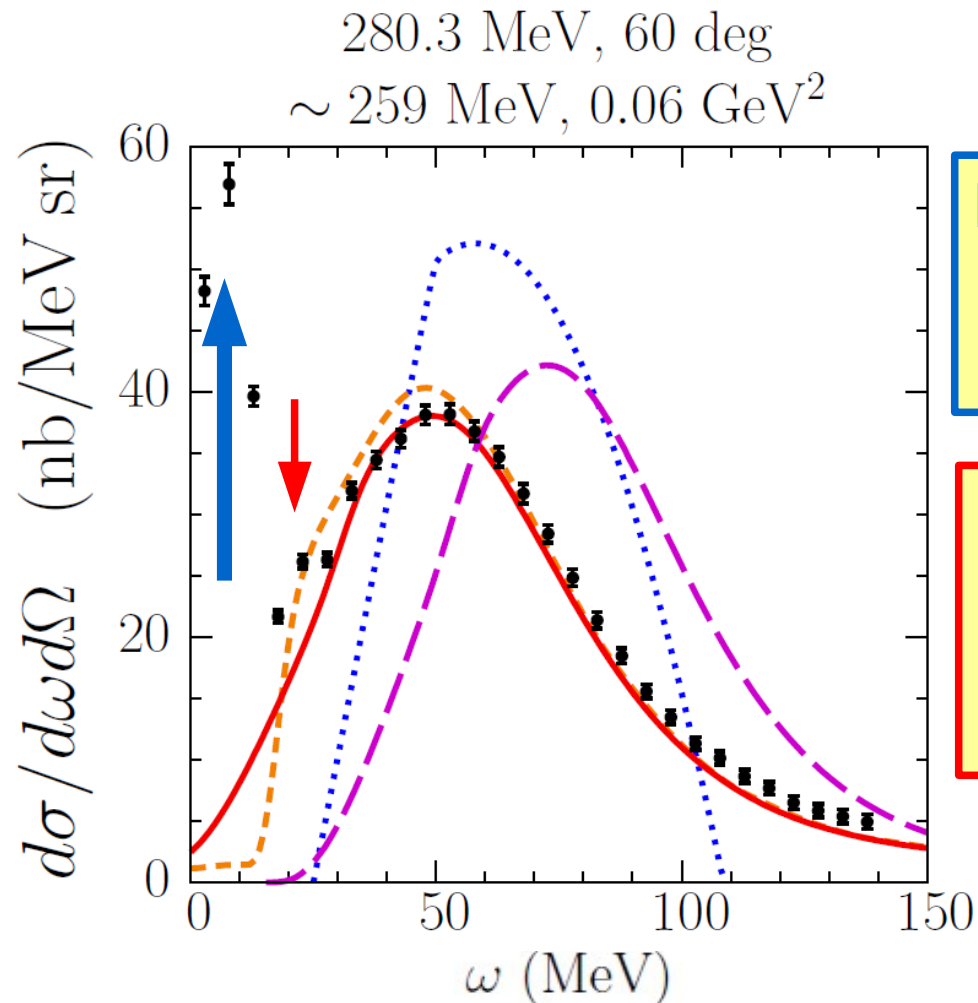
SF calculation,
LDA treatment
of Pauli blocking

SF calculation,
step function

RFG model
 $\varepsilon = 25 \text{ MeV}$
 $p_F = 221 \text{ MeV}$

SF calculation
without FSI

Compared calculations

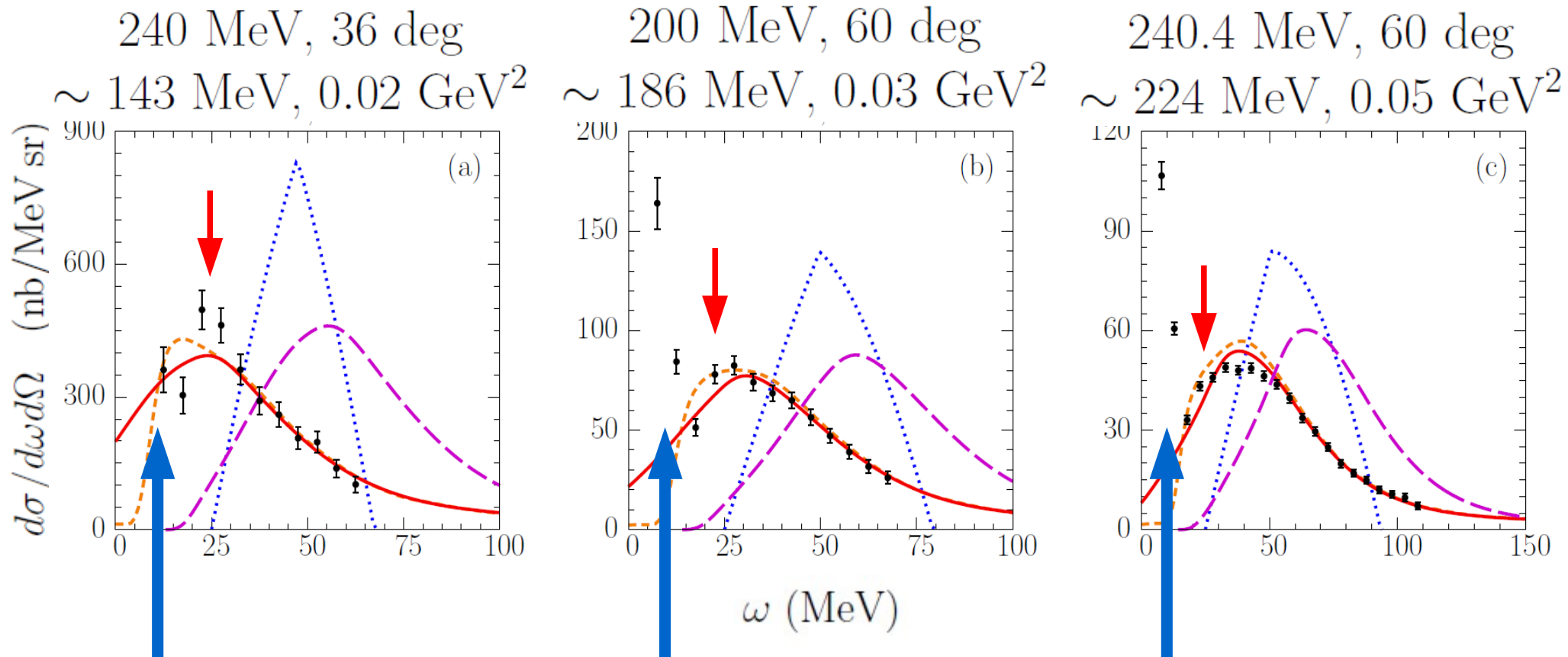


Calcs. include
QE by 1-body
current only

Elastic scattering
and excitation
of low- E_x levels

Giant resonance
 $E_x = 22.6$ MeV,
 $\Gamma = 3.2$ MeV

Comparisons to $C(e,e')$ data



Barreau *et al.*,
 NPA 402, 515 (1983)

Comparisons to $C(e,e')$ data

280.3 MeV, 60 deg

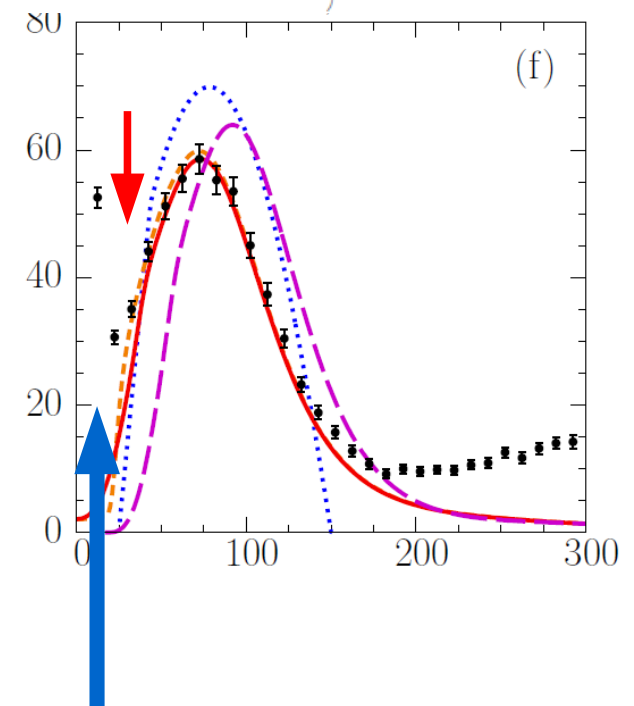
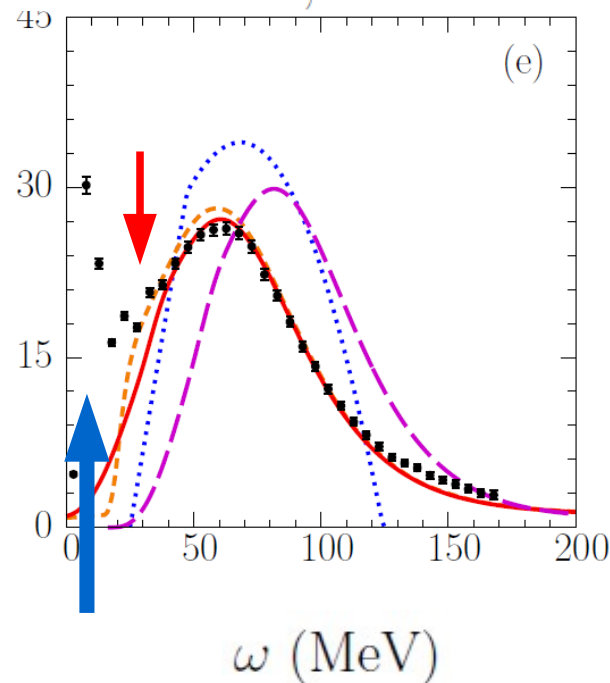
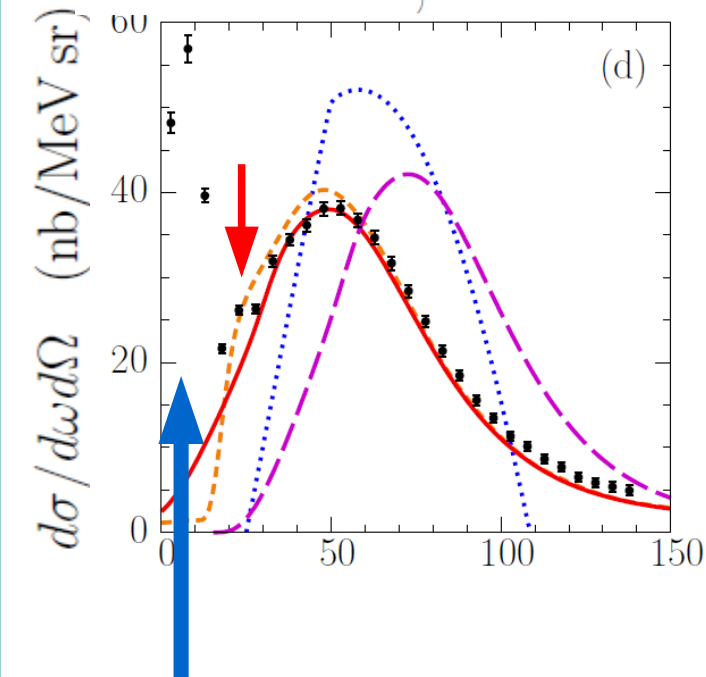
320.3 MeV, 60 deg

560 MeV, 36 deg

$\sim 259 \text{ MeV}, 0.06 \text{ GeV}^2$

$\sim 295 \text{ MeV}, 0.08 \text{ GeV}^2$

$\sim 331 \text{ MeV}, 0.10 \text{ GeV}^2$

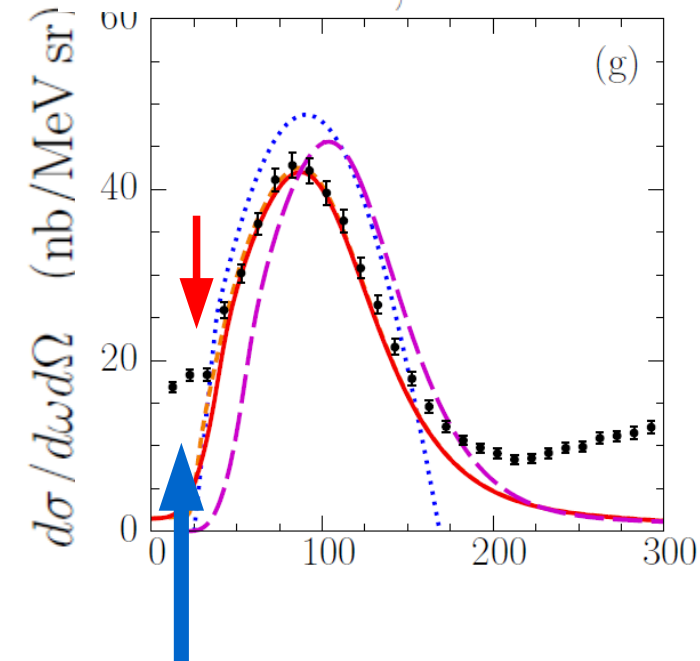


Barreau *et al.*,
NPA 402, 515 (1983)

Comparisons to $C(e,e')$ data

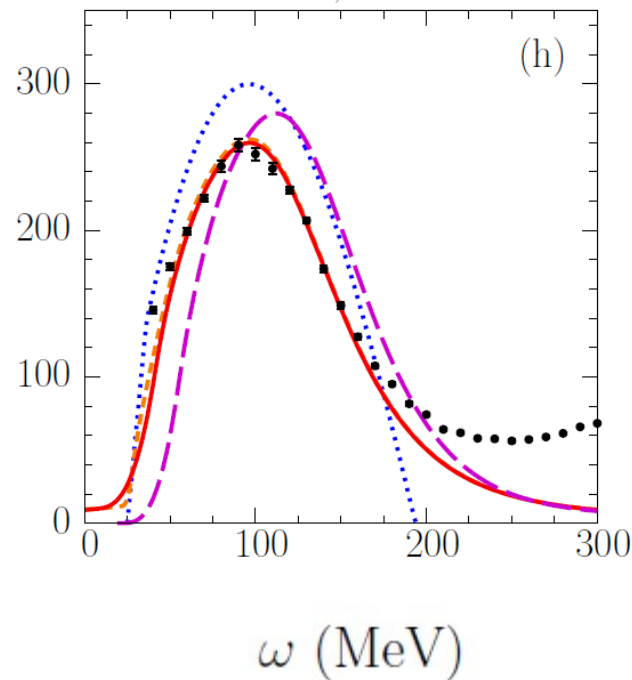
620 MeV, 36 deg

~ 366 MeV, 0.13 GeV^2



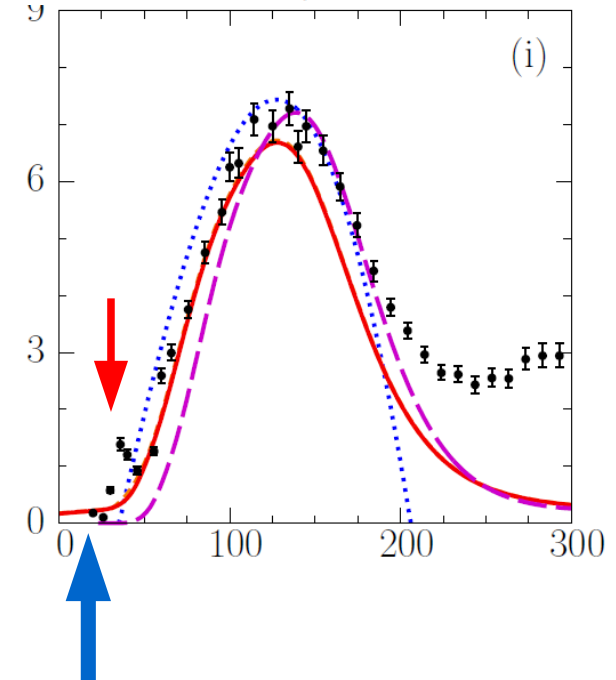
1650 MeV, 13.5 deg

~ 390 MeV, 0.14 GeV^2



500 MeV, 60 deg

~ 450 MeV, 0.19 GeV^2



Barreau *et al.*,
NPA 402, 515 (1983)

Baran *et al.*,
PRL 61, 400 (1988)

Whitney *et al.*,
PRC 9, 2230 (1974)

Comparisons to $C(e,e')$ data

The supplemental material of PRD 91,033005 (2015) shows comparisons to the data sets collected at **54 kinematical setups**

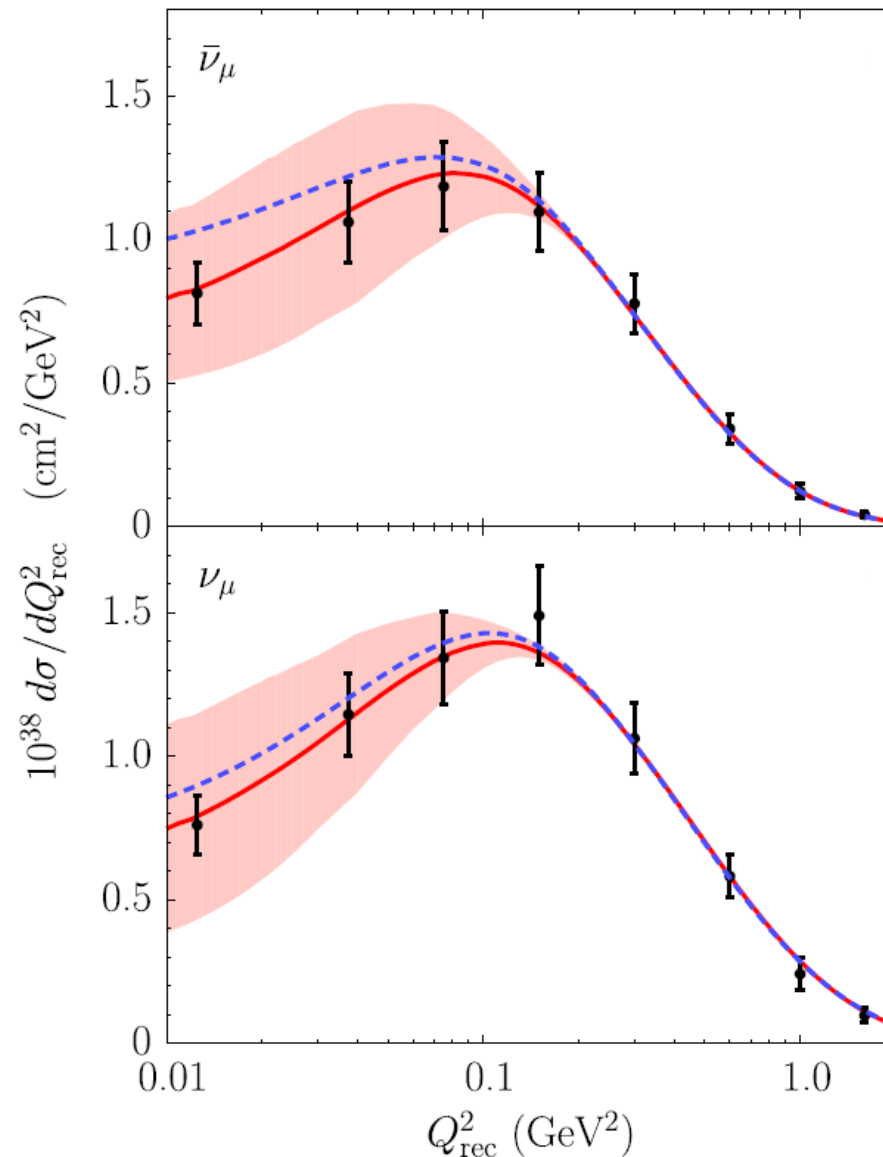
- energies from ~ 160 MeV to ~ 4 GeV,
- angles from 12 to 145 degrees,
- at the QE peak, the values of momentum transfer from ~ 145 to ~ 1060 MeV/c and $0.02 \leq Q^2 \leq 0.86$ (GeV/c) 2 .

CCQE MINERvA data

SF calculations
with FSI

VS.

SF calculation
without FSI



Fields *et al.*,
PRL 111, 022501
(2013)

A. M. A.,
PRD 92, 013007
(2015)

Fiorentini *et al.*,
PRL 111, 022502
(2013)

CCQE MINERvA data

TABLE I. Fit results to the CC QE MINERvA data.

	antineutrino	neutrino	combined fit
	including theoretical uncertainties:		
M_A (GeV)	1.16 ± 0.06	1.17 ± 0.06	1.16 ± 0.06
$\chi^2/\text{d.o.f.}$	0.38	1.33	0.93
	neglecting theoretical uncertainties:		
M_A (GeV)	1.15 ± 0.10	1.15 ± 0.07	1.13 ± 0.06
$\chi^2/\text{d.o.f.}$	0.44	1.38	1.00
	neglecting FSI ($M_A = 1.16$ GeV):		
$\chi^2/\text{d.o.f.}$	2.49	2.45	2.42

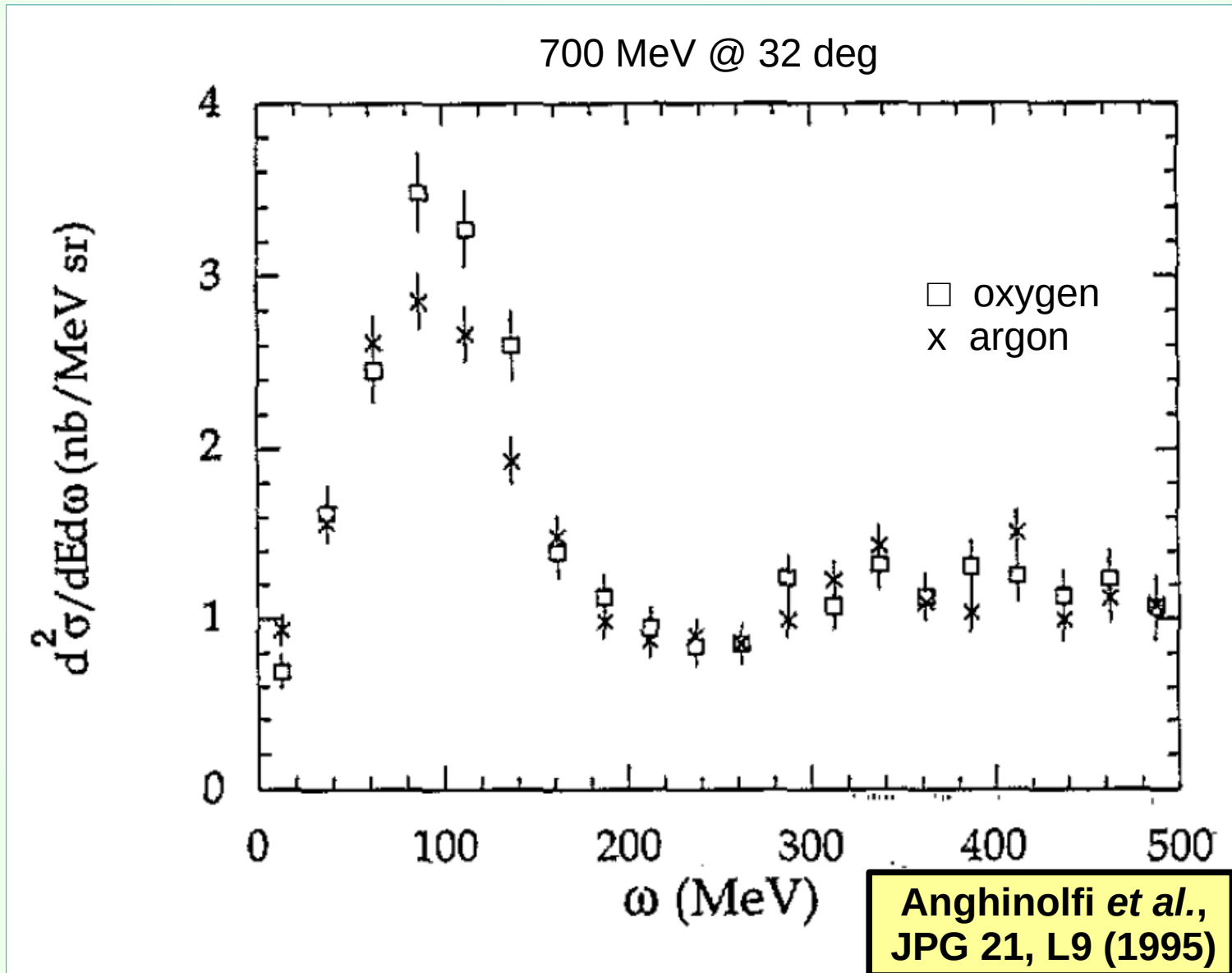
Summary

- An accurate description of nuclear effects, including final-state interactions, is crucial for an **accurate reconstruction of neutrino energy**.
- Theoretical models **must be validated** against (e,e') data to estimate their uncertainties.
- The spectral function formalism can be used in Monte Carlo simulations to **improve the accuracy** of description of nuclear effects.



Measurement of the spectral function of argon in JLab

What do we know about Ar?



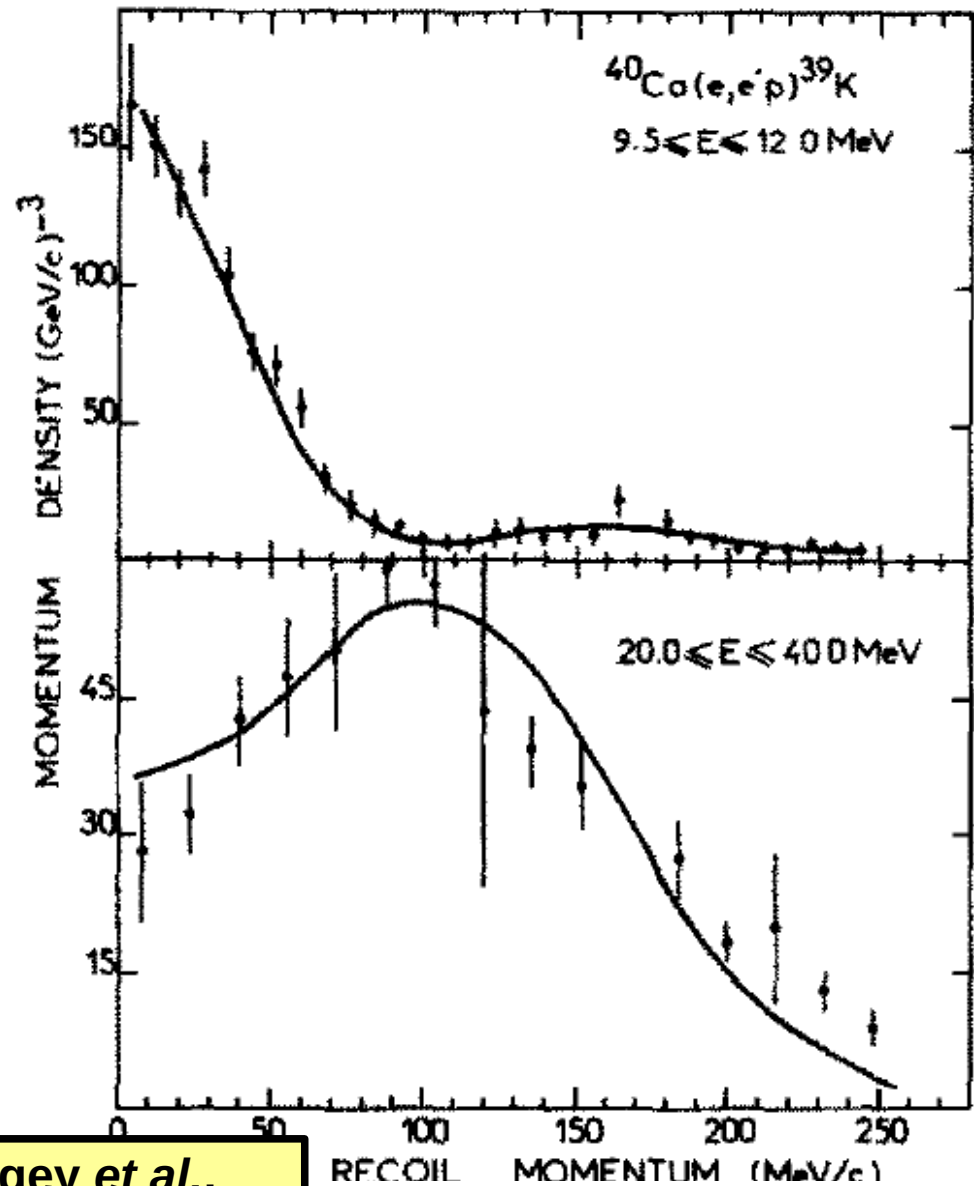
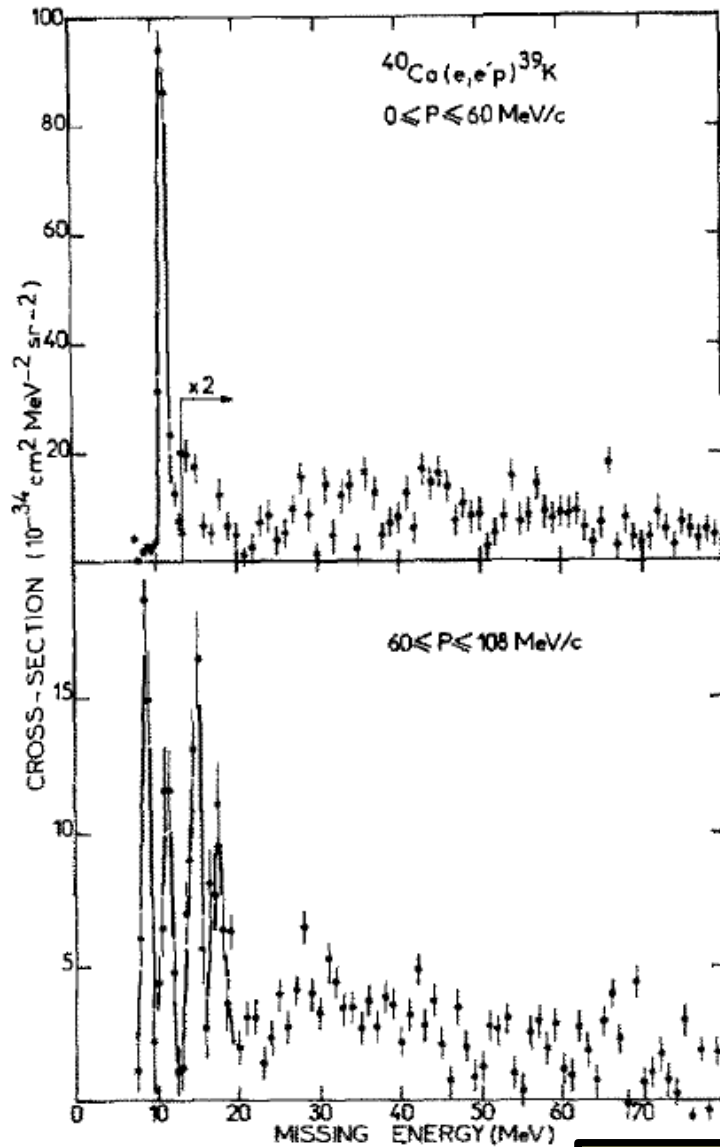
What do we know about Ar?

- nuclear excitations by up to ~ 11 MeV
Cameron & Singh, Nucl. Data Sheets **102**, 293 (2004)
- angular distributions of $^{40}\text{Ar}(p, p')$ for a few excitation lvls.
Fabrici *et al.*, PRC **21**, 830 & 844 (1980); De Leo *et al.*,
PRC **31**, 362 (1985); Blanpied *et al.*, PRC **37**, 1304 (1988)
- angular distributions of $^{40}\text{Ar}(p, d)^{39}\text{Ar}$
Tonn *et al.*, PRC **16**, 1357 (1977)

What do we know about Ar?

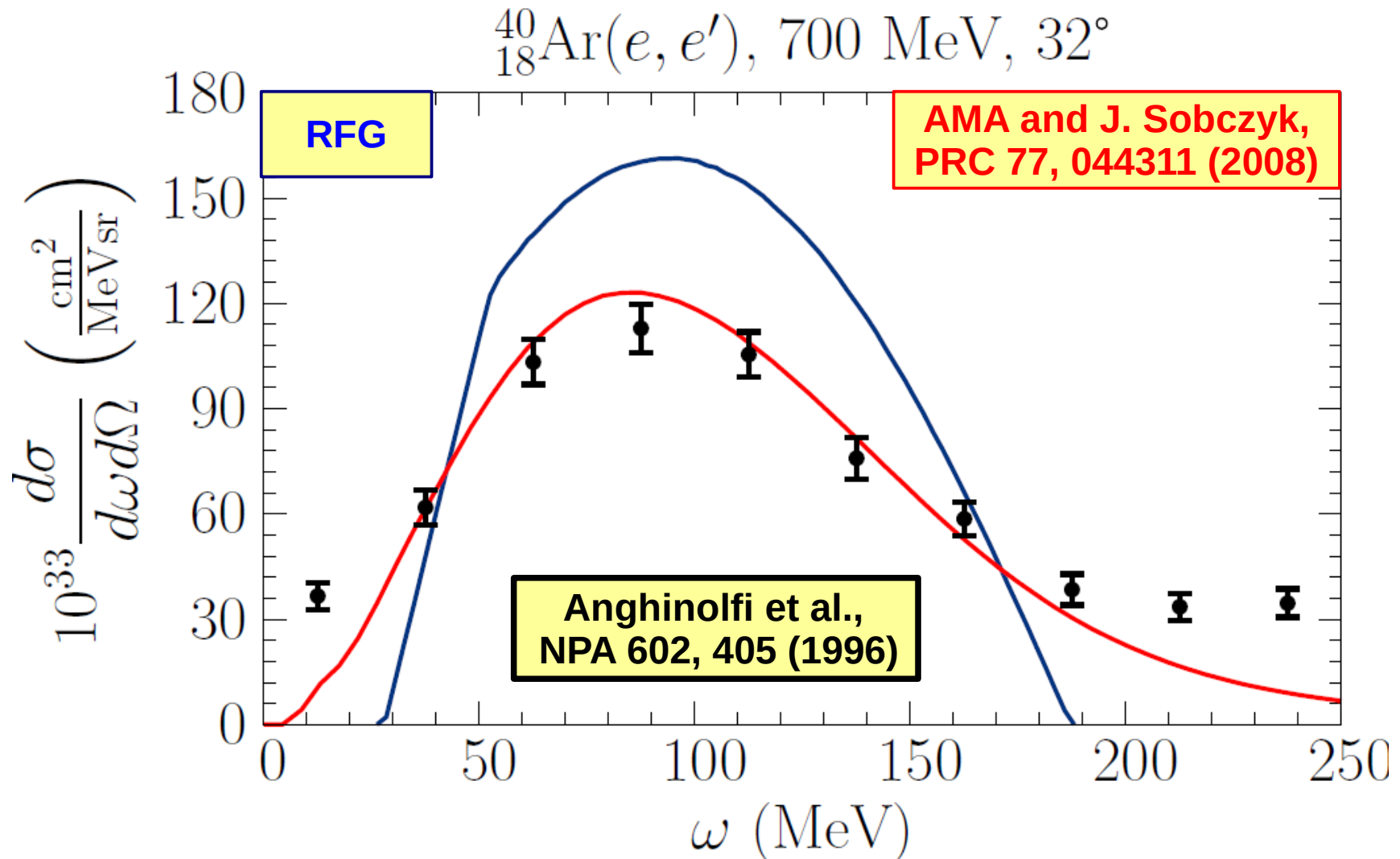
- n -Ar total cross section from energies < 50 MeV
Winters *et al.*, PRC **43**, 492 (1991)
- $^{40}\text{Ar}(\nu_e, e)$ cross section from the mirror $^{40}\text{Ti} \rightarrow ^{40}\text{Sc}$ decay
Bhattacharya *et al.*, PRC **58**, 3677 (1998)
- Gamow-Teller strength distrib. for $^{40}\text{Ar} \rightarrow ^{40}\text{K}$ from $0^\circ(p, n)$
Bhattacharya *et al.*, PRC **80**, 055501 (2009)
- $^{40}\text{Ar}(n, p)^{40}\text{Cl}$ cross section between 9 and 15 MeV
Bhattacharya *et al.*, PRC **86**, 041602(R) (2012)

Spectral function of ^{40}Ca



Mougey *et al.*,
NPA 262, 461 (1976)

Approximated SF of ^{40}Ar



Experiment E12-14-012 at JLab

"We propose a measurement of the coincidence (e,e'p) cross section on argon. This data will provide the experimental input indispensable to construct the argon spectral function, thus paving the way for a reliable estimate of the neutrino cross sections."

**Benhar et al.,
arXiv:1406.4080**

Experiment E12-14-012 at JLab

Primary goal: extraction of the proton shell structure of ^{40}Ar from $(e,e'p)$ scattering

- spectroscopic factors,
- energy distributions,
- momentum distributions.

Secondary goal: improved description of final-state interactions in the argon nucleus.

Relevance for DUNE

- Neutrino oscillations

Reduction of systematic uncertainties from nuclear effects, especially for the 2nd oscillation maximum.

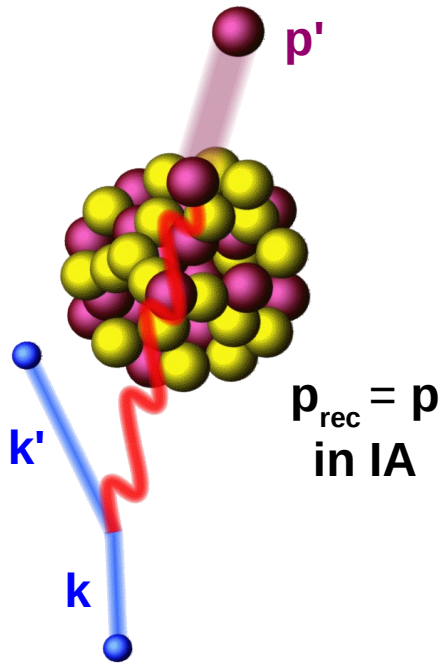
- Proton decay

Probed lifetime affected by the partial depletion of the shell-model states.

- Supernova neutrinos

Information on the valence shells essential for accurate simulations and detector design.

Impulse approximation



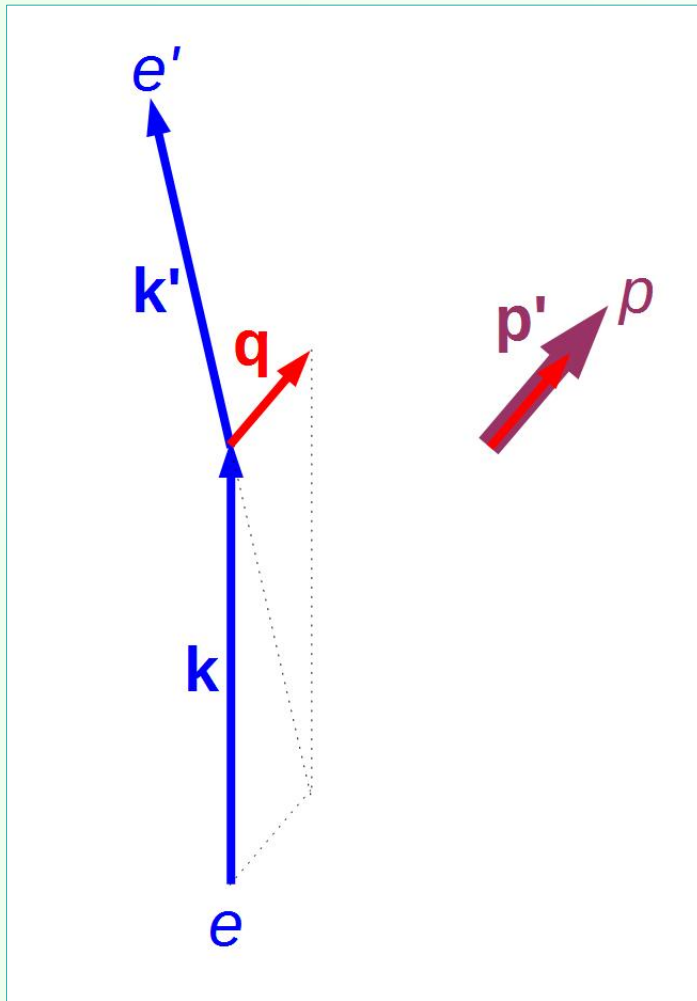
$$\frac{d^6 \sigma_{\text{IA}}}{d\Omega_{k'} dE_{k'} d\Omega_{p'} dE_{p'}} \propto \sigma_{ep} S(\mathbf{p}, E) T_A(E_{p'})$$

σ_{ep} elementary cross section

$S(\mathbf{p}, E)$ spectral function

$T_A(E_{p'})$ nuclear transparency

(Anti)parallel kinematics, $\mathbf{p}' \parallel \mathbf{q}$



Energy conservation

$$E_{\mathbf{k}} + M_A = E_{\mathbf{k}'} + E_{\mathbf{p}'} + \sqrt{(M_A - M + E)^2 + \mathbf{p}_{\text{rec}}^2}$$

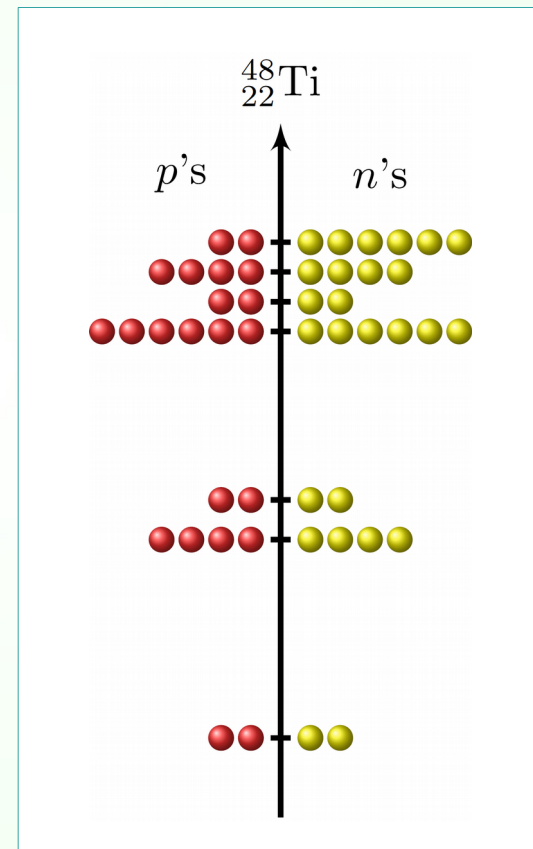
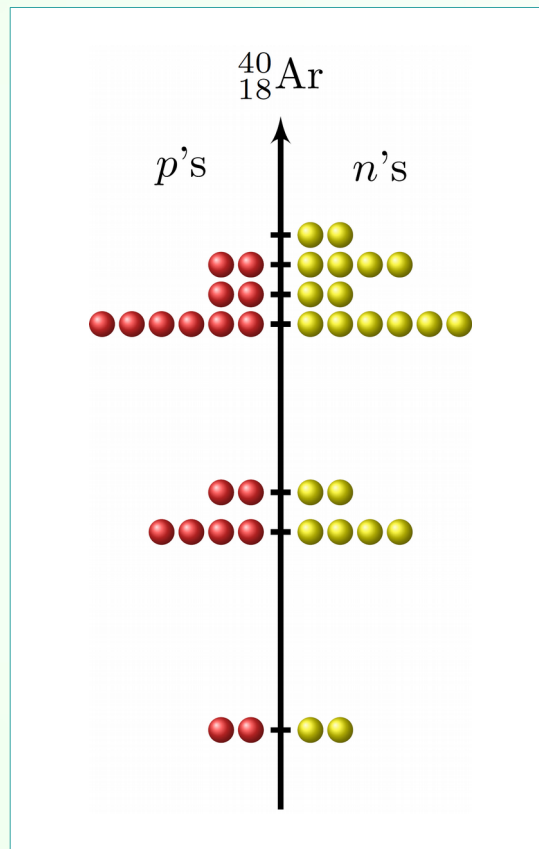
Momentum conservation

$$\mathbf{q} = \mathbf{p}' + \mathbf{p}_{\text{rec}} \rightarrow |\mathbf{q}| = |\mathbf{p}'| + |\mathbf{p}_{\text{rec}}|$$

$$\mathbf{q} = \mathbf{p}' + \mathbf{p}_{\text{rec}} \rightarrow |\mathbf{q}| = |\mathbf{p}'| - |\mathbf{p}_{\text{rec}}|$$

Impulse Approximation, $|\mathbf{p}_{\text{rec}}| = |\mathbf{p}|$

Neutron spectral function of ^{40}Ar

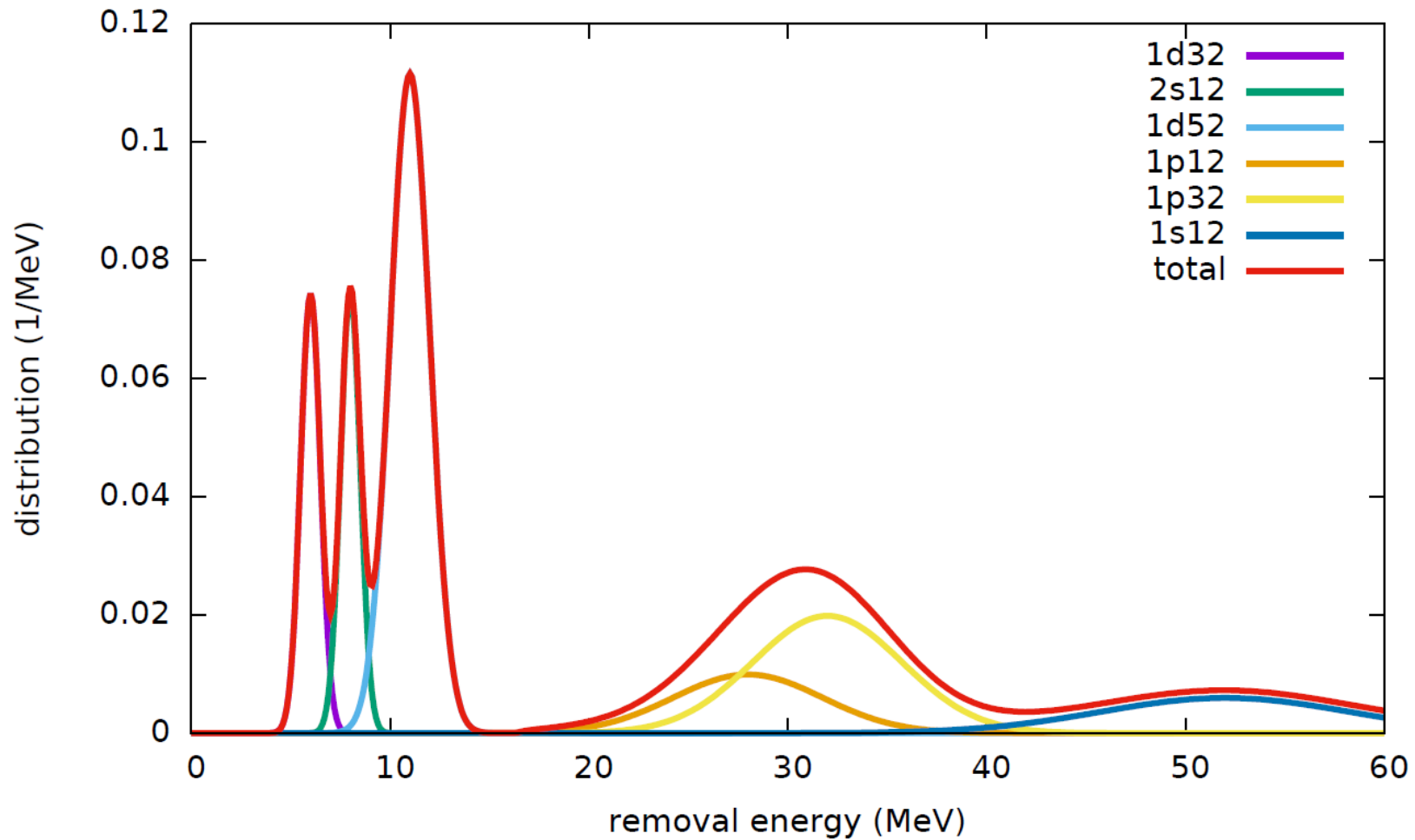


Kinematic settings

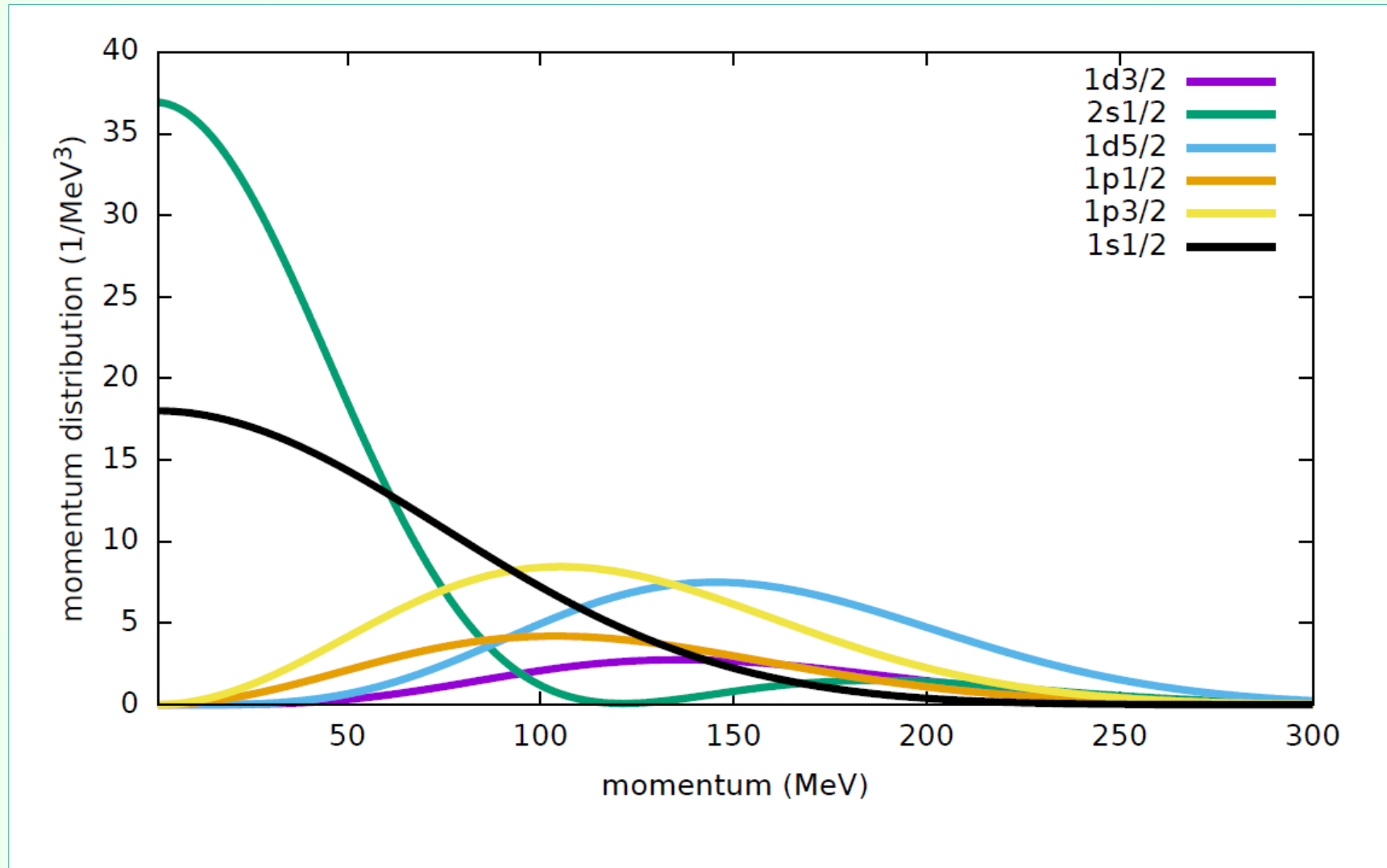
	E_e MeV	$E_{e'}$ MeV	θ_e deg	P_p MeV/ c	θ_p deg	$ \mathbf{q} $ MeV/ c	p_m MeV/ c	Ar events	Ti events
kin1	2222	1799	21.5	915	-50.0	857.5	57.7	44M	13M
kin2	2222	1716	20.0	1030	-44.0	846.1	183.9	63M	21M
kin3	2222	1799	17.5	915	-47.0	740.9	174.1	73M	28M
kin4	2222	1799	15.5	915	-44.5	658.5	229.7	159M	113M
kin5	2222	1716	15.5	1030	-39.0	730.3	299.7	45M	61k
(e, e')	2222		15.5					3M	3M

**Data collected
Feb - Mar 2017**

Expected energy distributions

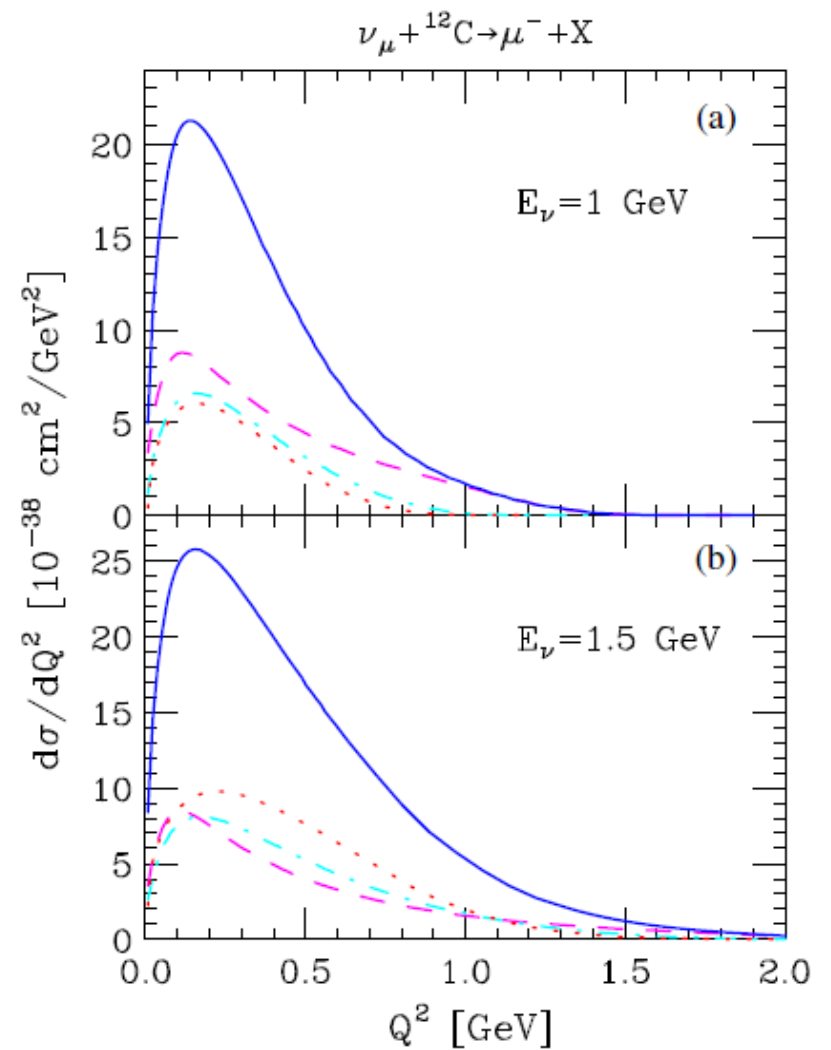
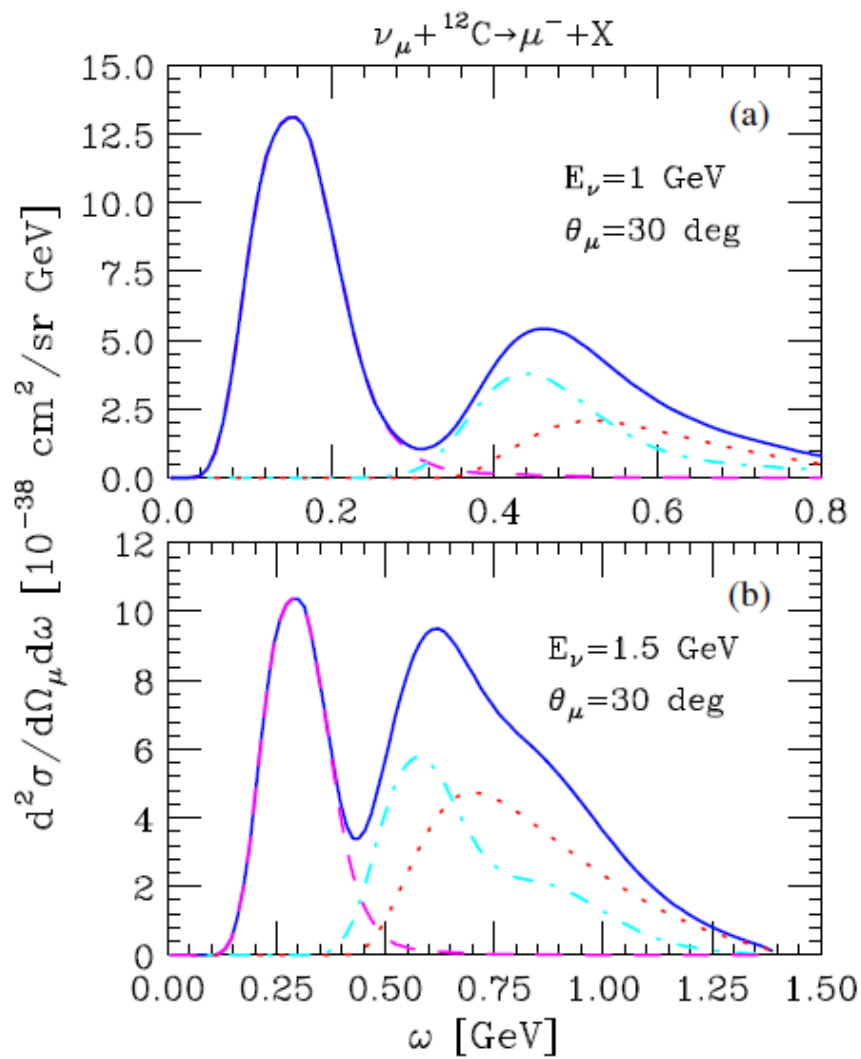


Momentum distributions

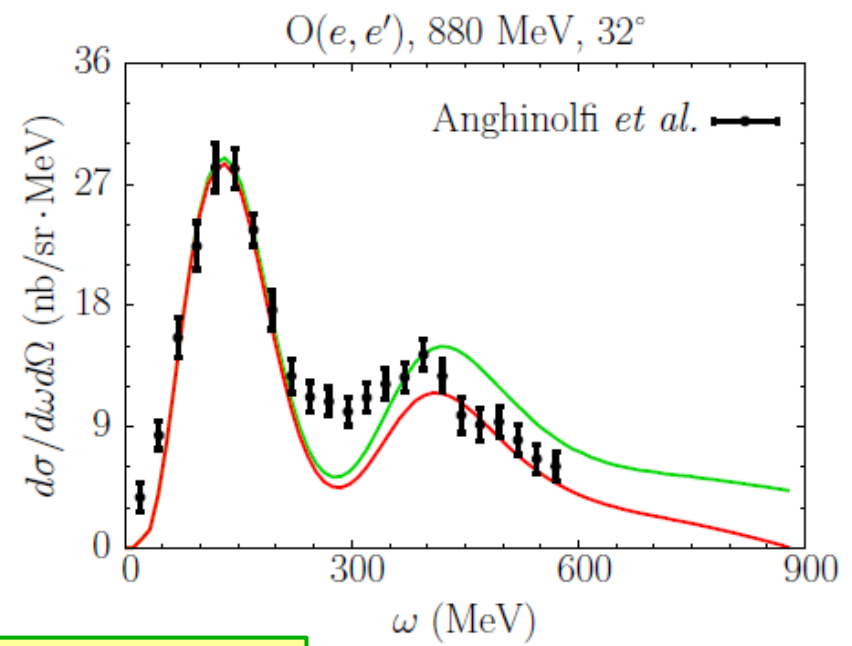
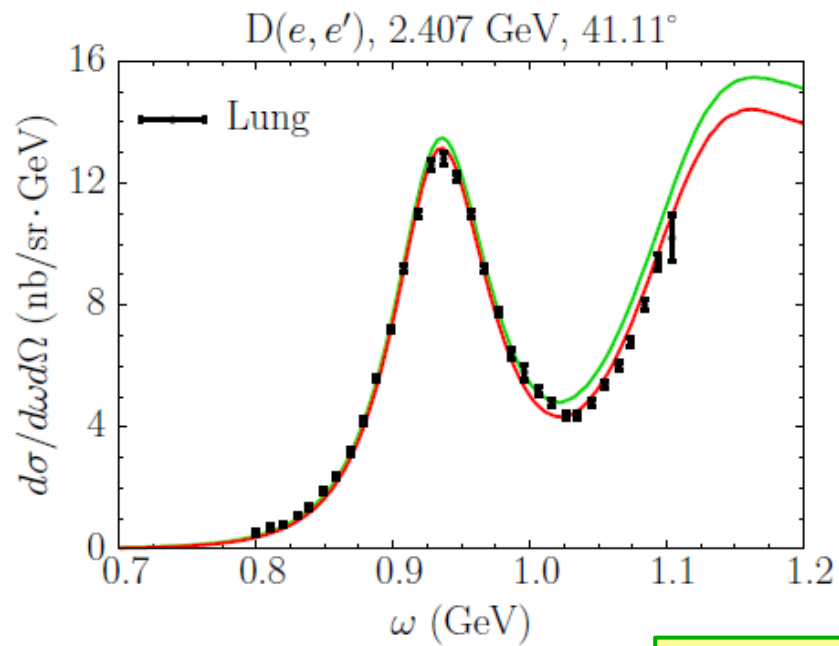




Backup slides

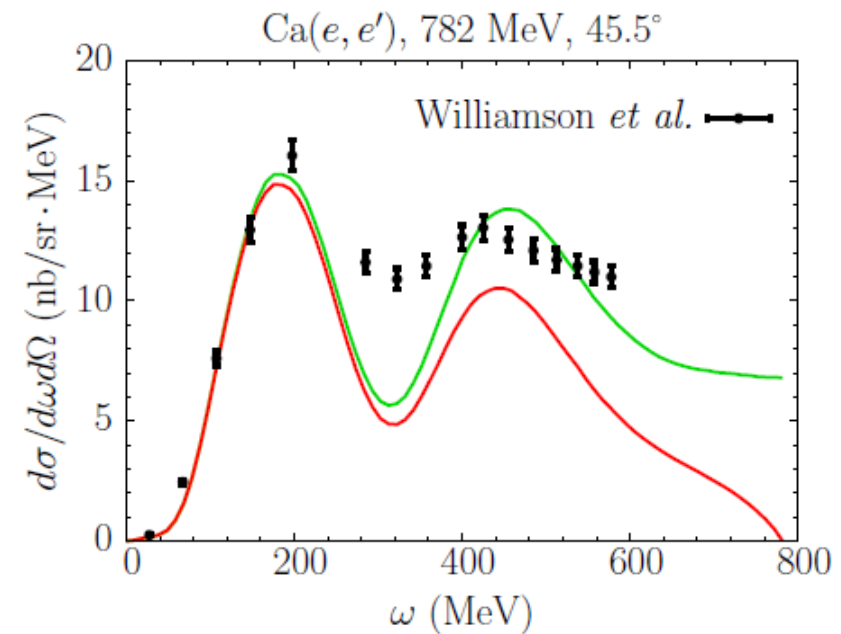
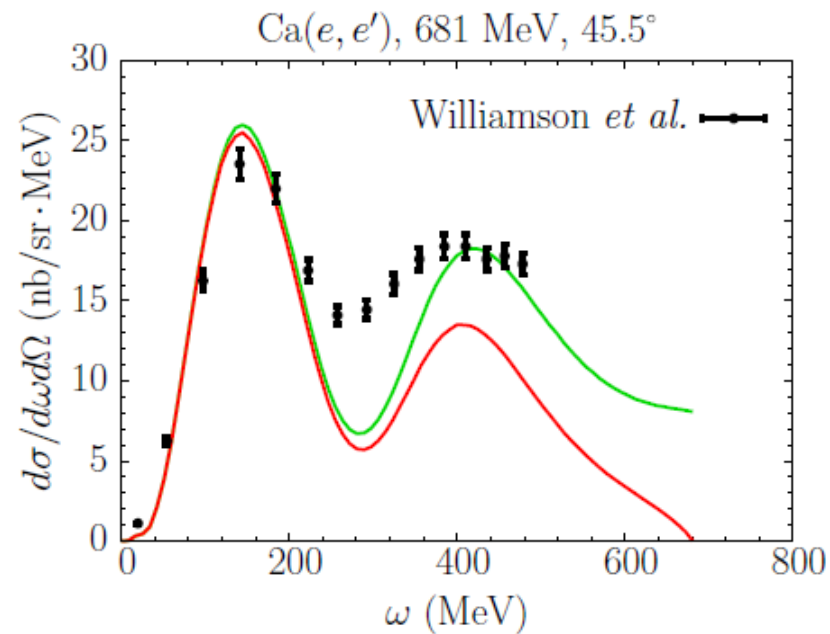


Vagnoni et al., PRL 118, 142502 (2017)



Conserved current

Conserved energy



Other NC and CC QE data

